Functional characterization of HtrA2 in the pathogenesis of Parkinson´s disease

Dissertation

zur Erlangung des Grades eines
Doktors der Naturwissenschaften

der Mathematisch-Naturwissenschaftlichen Fakultät
und
der Medizinischen Fakultät
der Eberhard-Karls-Universität Tübingen

vorgelegt
von

Poonam Sood
aus Dehradun, India

December 2013

Tag der mündlichen Prüfung:	08.04.2014
Dekan der Math.-Nat. Fakultät:	Prof. Dr. W. Rosenstiel
Dekan der Medizinischen Fakultät:	Prof. Dr. I. B. Autenrieth
1. Berichterstatter:	Prof. Dr. Rejko Krüger
2. Berichterstatter:	Prof. Dr. Robert Feil
Prüfungskommission:	Prof. Dr. Rejko Krüger
	Prof. Dr. Olaf Riess
	Prof. Dr. Hartwig Wolburg
	Prof. Dr. Robert Feil

Declaration

I hereby declare that I have produced the work entitled: “**Functional characterization of HtrA2 in the pathogenesis of Parkinson´s disease**”, submitted for the award of a doctorate, on my own (without external help), have used only the sources and aids indicated and have marked passages included from other works, whether verbatim or in content, as such. I swear upon oath that these statements are true and that I have not concealed anything. I am aware that making a false declaration under oath is punishable by a term of imprisonment of up to three years or by a fine.

Tübingen, _____ _____

Date Signature

Publications

Parts of this work have been published in:

Poster presentation

Poster presentation in German Parkinson´s congress , 13-15 March 2013 and NGFN conference, April 18-20, 2013 Poonam Sood[1,2,3], Silke Nuber[5], Nicole Kieper[2], Nicolas Casadei[3,5], Thomas Ott[4], Julia Fitzgerald[2], Olaf Riess[5] , Rejko Krüger[1,2`] (2013) **Characterization of transgenic mice overexpressing wild type and G399S mutant HtrA2/Omi – implications for PD.**

Manuscript in preparation

Scientific paper in preparation

TABLE OF CONTENTS

1 INTRODUCTION

1.1 PARKINSON´S DISEASE (PD)

Although Parkinson´s disease (PD) was already known in ancient India under the Name of "Kampavata", the syndrome was first described and documented in 1817 in an article "essay on the shaking palsy" by the British physician James Parkinson (Kempster et al., 2007). His work was unrecognized for decades, until the neurologist Jean Martin Charcot recognized the importance of Parkinson´s work and named the disorder as "maladie de Parkinson" (Parkinson´s disease).

PD is the second most common neurodegenerative disorder, after Alzheimer´s disease, affecting approximately 1% of the population above the age of 55 years (Nussbaum and Ellis, 2003; Lees et al., 2009). In addition to age gender may also influence the incidence of PD as several studies show evidence of a higher incidence in men compared to women (de Lau and Breteler, 2006). The main characteristics of PD are tremor, rigidity, bradykinesia, and postural instability; though the motor symptoms can be accompanied by nonmotor symptoms such as olfactory deficits, sleep impairments and psychiatric problems. However these motor symptoms do not become apparent until 50-60% of the dopaminergic neurons in the substantia nigra pars compacta (SNc) have undergone degeneration (Fearnley and Lees, 1991). This disease is also characterized by a profound loss of dopamine (DA) in the striatum and the presence of intracytoplasmic protein inclusions called Lewy bodies (LB) which mainly consist of alpha-synuclein and ubiquitin (Forno, 1996).The progression of this disease is irreversible. Presently there is no treatment to arrest or retard the progression of neurodegeneration. The available methods of pharmacological or surgical treatment can alleviate some of the symptoms, but can lead to serious side effects (Schapira, 2007). Because of these reasons, PD has been the subject of intense investigation to understand its

origin and pathophysiology and to develop new therapeutic strategies or preventive measures based on reliable biomarkers.

1.1.1 PD: CLINICAL SIGNS AND SYMPTOMS

Classically, motor dysfunction is used as the clinical diagnosis of PD. PD is characterized by bradykynesia, rigidity, tremor, and postural instability with an asymmetric onset spreading to become bilateral with time. Tremor at rest is one of the most prevalent characteristic of the disease and it occurs in 70% of the PD patients (Hoehn and Yahr, 1967). Rigidity is a motor sign, detected as a resistance to passive movement of the limbs. Bradykinesia refers to a slowness and paucity of movement; examples are loss of facial expression and involuntary movements such as arm swinging when walking. Bradykinesia is not due to limb rigidity and can be observed in the absence of rigidity during treatment. Postural instability is the relevant, because it can lead to falls with resulting injury (Lang and Lozano, 1998).

Other motor features are abnormal gait and posture that manifest as rapid shuffling steps with a forward-flexed posture when walking or freezing (also referred to as motor block, speech and swallowing difficulties, and a mask like facial expression (Jankovic, 2008). But more recently PD has been recognized as a complex disorder with both motor and nonmotor symptoms (NMS), such as depression, sleep disturbance, sensory abnormalities, autonomic dysfunction, and cognitive decline (Langston, 2006). NMS affect all PD patients independent of the disease course and may even precede the motor manifestations (Chaudhuri and Schapira, 2009). Although the causes of motor dysfunctions are quite well understood, the cause of few NMS in PD is known such as nucleus basalis of Meyenrt (NBM) degeneration is correlated with Dementia, smell loss with olfactory bulb pathology, depression with locus coeruleus and raphe nucleus degeneration and constipation is correlated with dorsal nucleus of the vagus and enteric plexus neurons (Tolosa and Pont-Sunyer, 2011).

1.1.2 RISK FACTORS FOR DEVELOPING PD

Age represents the strongest risk factor for PD and the majority of cases develop the illness at late onset. However, it's still unclear whether it is chronological age or the aging process that is responsible for PD (Kempster et al., 2010). There is also evidence for sex being one of the risk factor for PD, since more men have PD compared to women (at an approximate ratio 1.5-2:1). There is also evidence that early menopause, hysterectomy, or removal of the ovaries increases the risk in women and even loss of estrogen production in women with age may remove a protective effect (Ragonese et al., 2004; Popat et al., 2005).

The role of environmental factors in PD came into focus with the discovery that exposure to the neurotoxic ion of the synthetic heroin analogue MPTP (MPP^+) lead to Parkinsonism in humans (Langston et al., 1983). There are some other chemicals which are known to cause Parkinsonism in some animals such as the pesticides paraquat and rotenone (Tanner et al., 2011). Both MPP^+ and paraquat/rotenone are mitochondrial toxins since they inhibit complex I of the respiratory chain (Schapira, 2010). MPTP is converted into the active neurotoxin MPP^+ once it has crossed the blood brain barrier (BBB) by the outer mitochondrial membrane enzyme monoamine oxidase (Heikkila et al., 1990). Other environmental causes include solvent exposure (n-hexane, methanol), carbon monoxide poisoning, hydrogen sulfide intoxication, and perhaps manganese, which lead to striatal cell degeneration (Kenborg et al., 2012).

Genetic factors play an important role in PD and to date account for approximately 15% of all cases – this concept came into focus when many investigators recognized that PD could occasionally be identified in families (Golbe et al., 1990). Genetic causes (discussed in detail later) are coming more into picture as important underlying causes and they collectively account for about 30% of the familial and 3%-5% of the sporadic cases.(Klein and Westenberger, 2012).

1.1.3 PD AND NEUROPATHOLOGY

Neuronal loss in the substantia nigra pars compacta (SNpc) and subsequent loss of striatal dopamine content are considered as being responsible for the classical motor features of PD. The neuropathological diagnosis of PD requires the detection of marked dopaminergic neuronal loss in the SNpc and the appearance of Lewy bodies, eosinophilic inclusions consisting of a dense core surrounded by a pale-staining halo of radiating filaments (Dickson et al., 2009). Though not all PD cases have Lewy bodies for example Parkin mutation cases of PD do not generally reveal Lewy bodies although they show substantial loss of dopaminergic neurons in the substantia nigra pars compacta that underlies their movement disorder (Pramstaller et al., 2005). However, the neuropathological features of PD are known to be more widespread for many decades, with many non-dopaminergic nuclei affected, including the locus coeruleus, reticular formation of the brain stem, raphe nucleus, dorsal motor nucleus of the vagus, basal nucleus of the Meynert and amygdala (Jellinger, 2012). All these nuclei degenerate with Lewy body pathology, suggesting a common pathogenic process as that occurring in the SNpc (Witt et al., 2009). There is also evidence for the presence of Lewy bodies in peripheral tissues that take the pathology associated with PD to another level (Braak et al., 2006; Fujishiro et al., 2008). From the above findings, it has been suggested that pathology in PD may not start in the SNpc, but rather Lewy body pathology and the deposition of alpha-synuclein are proposed to originate in the olfactory bulb and lower brain stem, from where they spread in stages to involve the midbrain and then spreading to cortical regions (Braak et al., 2003). Although it is recognized that not all PD cases exactly follow this pattern of spread (Kalaitzakis et al., 2008), it is widely accepted that spreading of pathology can occur in PD (Dunning et al., 2012).

1.2 MECHANISMS OF NEURODEGENERATION IN PD

1.2.1 OXIDATIVE STRESS IN PD

Since the 1980´s there have been various evidences in the literature that implicate reactive oxygen species (ROS) as a step to causing neuronal cell death. Starting from the concept of free radical production as a result of increased chemical and enzymatic oxidation of DA (Fahn and Cohen, 1992) through the mechanism of action of toxins such as 6-hydroxydopamine (6-OHDA) (Heikkila and Cohen, 1973) to evidence from postmortem and clinical investigations (Dexter et al., 1989b; Spina and Cohen, 1989; Dexter et al., 1994), oxidative stress and the resulting oxidative damage have emerged as the major role player in PD. The source of the oxidative stress is always a matter of debate but one obvious contributor is increased free radical formation originating from mitochondria. Mitochondria are resonsible for the production of energy in the form of adenosine triphosphate (ATP). It involves the transport of protons across the inner mitochondrial membrane by means of an electron transport chain. Electrons are passed through a series of proteins or enzymes with various oxidation-reduction reaction by the production of an electron gradient. At the last step of energy ATP generation oxygen is reduced to water. However in the case of mitochondrial dysfunction, oxygen can be prematurely and incompletely reduced to generate the highly damaging superoxide radical (.O2-) (Li et al., 2013).

1.2.2 MITOCHONDRIAL DYSFUNCTION IN PD

Impairment of mitochondrial function has been implicated in neurodegeneration in PD for a long time (Obeso et al., 2010). Alterations of the electron transport chain enzyme complex I appear to be particularly relevant to PD. In fact mitochondrial dysfunction in relation to PD first came into focus with the discovery of mitochondrial complex I deficiency in the substantia nigra of some PD patients (Schapira et al., 1989). Post-mortem brains of PD

patients showed deficient staining for complex I in the substantia nigra (Schapira et al., 1989) and subsequently this deficiency was also seen in the skeletal muscle and platelets (Mizuno et al., 1989). MPTP and rotenone neurotoxins, used to generate PD models, both disrupt mitochondrial function, inhibiting complex I activity (Shulman et al., 2011). However recently it has been reported that the mitochondrial deficiency is not present in all PD patients, either in the brain, platelets, or other tissues. In average there is a reduction in activity in about 35% of the patient group (Schapira, 2008). It has been reported that the complex I defect in PD patients reduces the threshold of apoptosis mediated by the mitochondria through lowering ATP production and generation of free radicals and render cells to the proapototic protein Bax (Perier et al., 2005).

Mitochondrial dynamics can be affected in several ways, including depolarization as a result of mitochondrial toxins, disturbance in fission-fusion homeostasis, alteration of damaged mitochondrion disposal through mitophagy and reduced functionality as a result of inherited or somatic mutations in the mtDNA (Schapira and Gegg, 2011). The construction of cybrids (hybrid cell lines), obtained from the fusion of cells that lack mtDNA with platelet mtDNA from PD patients has demonstrated an example of a mitochondrial coding defect complex I (Ghosh et al., 1999).

Finally, recently interest in the role of mitochondria in PD has originated from the genetic investigations in familial PD. Mutations in Parkin, Pink1, DJ-1 and LRRK2 are associated with altered mitochondrial function (Schapira, 2008, 2011; Schapira and Jenner, 2011). HtrA2 is a mitochondrial protease and its role in neuroprotection was first known when knock out mouse model of HtrA2 showed behavioral deficits, specifically Parkinsonism with striatal damage (Martins et al., 2004). Later several mutations (discussed in detail later) were found associated with PD (Strauss et al., 2005; Bogaerts et al., 2008; Lin et al., 2011). Mutations in Parkin, the gene encoding for the ubiquitin ligase, have been reported to be the most common cause of PD in people younger than 40 years (Kitada et al., 1998; Lucking et al., 2000), although mutations have been rarely found in Parkin patients with typical late-onset

(Farrer et al., 2001; Lohmann et al., 2003). Parkin KO flies were reported to have muscle pathology, mitochondrial dysfunctions and apoptosis (Greene et al., 2003). Pink1 is another mitochondrial protein localized to the outer mitochondrial membrane (Silvestri et al., 2005), and mutations in Pink1 have been implicated for autosomal recessive PD (Valente et al., 2004). Removal of Drosophila homologue of Pink1 leads to male sterility, defects in mitochondrial morphology and increased sensitivity to multiple stresses (Clark et al., 2006). Pink1 mutants show indirect flight muscle and dopaminergic neuronal loss accompanied by locomotor defects. Transgenic expression of Parkin in Pink1 mutants rescued all Pink1 loss of function phenotypes in Drosophila but Pink1 expression couldn´t rescue Parkin mutant Drosophila phenotypes (Park et al., 2006b). Recently Parkin and Pink1 have also been linked to mitophagy, which is implicated in the pathogenesis of PD (Narendra et al., 2008; Geisler et al., 2010). DJ1 is another mitochondrial protein and mutations in this protein are reported to cause rare autosomal recessive PD (Bonifati et al., 2003). Moreover GWAS, laser-captured human dopaminergic neuron studies and SNpc transcriptome studies have revealed a deficit in the mitochondrial electron transport chain in PD (Elstner et al., 2011).

1.2.3 ALTERED PROTEOLYSIS IN PD – PROTEASOMAL AND LYSOSOMAL

The presence of multiple proteins in Lewy bodies, with alpha-synuclein being the most abundant, led to the idea that the catabolism of waste, damaged or mutated proteins might be disturbed in PD which leads to cellular aggregation and neuronal death (Spillantini et al., 1998; Shashidharan et al., 2000). To investigate this hypothesis, the role of the ubiquitin-proteasome system (UPS) and lysosomes in pathogenesis of PD were well studied. Many studies confirmed an important role of proteins involved in the UPS such as UCHL1 (Gong and Leznik, 2007) and the E3 ligase, Parkin (Shimura et al., 2000). Several studies found that there is a reduction in proteasomal enzyme activity in the SN of PD patients (McNaught et al., 2003) and that there are alterations in the expression of proteasomal subunits and in

their regulatory caps in PD patients (McNaught et al., 2001; McNaught et al., 2002a; McNaught et al., 2002b). Furthermore, depletion of 26S proteasomes in mice leads to neurodegeneration with Lewy body-like inclusions (Bedford et al., 2008). Recently the attention was turned to an alternative degradation pathway and therefore focused on the role of lysosomes and autophagy in neurodegeneration in PD. There are several studies which suggest that dysfunctional lysosomes provide an important link to the pathogenesis in PD and are clearly linked to the events that occur in mitochondria and lead to oxidative stress (Schapira and Jenner, 2011). HtrA2 has been reported to be a positive regulator of autophagy and might be important in the quality control mechanisms involved in neurodegenerative diseases (Li et al., 2010). Pink1 and Parkin have also been functionally linked with the selective autophagy of mitochondria which is implicated in the pathogenesis of PD (Geisler et al., 2010).

1.2.4 INFLAMMATORY CHANGE

There is a role of reactive microgliosis in PD, which leads to inflammatory change. In postmortem studies of ‘PD patients, alterations have been found in the cytokines in both the SN and the CSF (Hirsch and Hunot, 2000; Hunot and Hirsch, 2003) who also showed inducible nitric oxide synthase to be present in activated microglia and that this can be linked to increased 3-nitrotyrosine immunoreactivity, indicative of peroxynitrite attack on proteins (Hirsch et al., 2003). Activated microglia have also been detected in the brain of MPTP-treated monkeys and drug addicts many years after toxin exposure, suggesting that once initiated, glial cells may play a role in progressive neuronal loss over long period of time (Langston et al., 1999; McGeer et al., 2003; Barcia et al., 2004) .

1.2.5 EXCITOTOXIC MECHANISMS

Excitotoxicity is included as a pathogenic mechanism that is thought to contribute to cell death in PD (Dexter and Jenner, 2013). The major contributor is overactivity of the subthalamic nucleus (STN), which releases glutamate and which innervates the SNpc and the internal segment of the globus pallidus (Bevan et al., 2002; Steigerwald et al., 2008). The recent technique deep brain stimulation (DBS) can correct the overactivity of the STN, producing the clinical benefit in PD, Moreover, the recent investigations utilizing DBS in PD have associated it with a lack of progression of motor symptoms (Tagliati et al., 2010).

According to the current view PD is not a single disease but rather a syndrome of multiple causes and manifestations. There are several examples which explain this view – such as the general absence of Lewy bodies in SNpc in PD cases with Parkin and only 30% of sporadic PD patients have complex I defect (Dexter and Jenner, 2013) and iron accumulation is also not seen in all postmortem nigral tissue of PD patients. But it becomes increasingly obvious that pathologic events occurring in SNpc may not originate in the brain but may be a result of peripheral events that propagates itself through synucleinopathy to eventually reach the brain (Dexter and Jenner, 2013).

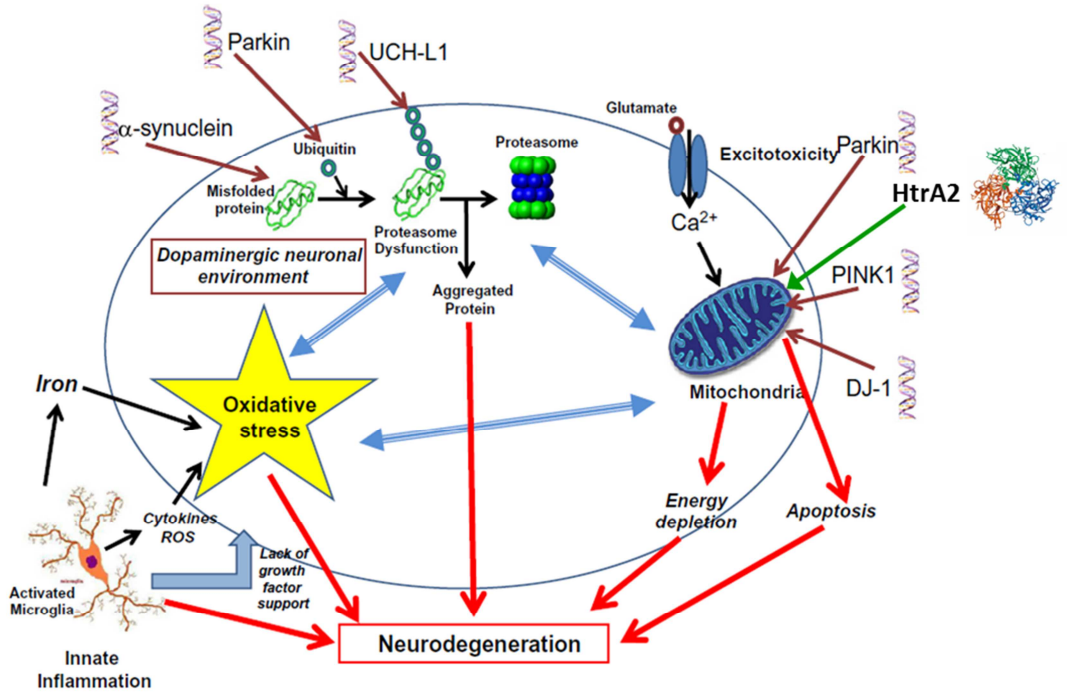

Figure 1.1 Key molecular mechanisms that are widely accepted to contribute to the neurodegenerative process in dopaminergic neurons in the substantia nigra in PD. Blue double-headed arrows indicate molecular mechanisms that may not only be toxic in their own right but importantly may also influence other molecular mechanisms known to be features in PD. Double helix structures identify some of the common gene mutations found in familial PD and brown and green arrows indicate where the altered protein may interfere with cell function and overlap with known mechanisms of cell death in sporadic PD. ROS, reactive oxygen species. Green arrow shows the probable role of protein in PD (adapted from (Dexter and Jenner, 2013).

1.3 PD AND SYNUCLEIN OLIGOMERS

1.3.1 ALPHA-SYNUCLEIN AGGREGATION

Lewy bodies are one of the pathological hallmarks of PD. But not all PD patients have Lewy bodies and in no mouse model Lewy body structures have been noticed to date. These facts have led to the study of alpha-synuclein aggregation in more detail and recently a concept of alpha-synuclein oligomer mediated toxicity has come into focus, though the function of alpha-synuclein in relation to PD is still unclear.

Alpha-synuclein is a 14kD neuronal protein from a family of structurally related proteins that are highly expressed in the brain (Ueda et al., 1993; Jakes et al., 1994). The main physiological form of alpha-synuclein in the brain appears to be an unfolded monomer

(Fauvet et al., 2012). Aggregation of two or more monomers leads to the formation of soluble oligomeric species, which are also called as protofibrils (Walsh et al., 1997). There are evidences for endogenous alpha-synuclein oligomers in brain extracts from rodent models (Mazzulli et al., 2011; Winner et al., 2011). Initially the alpha-synuclein oligomers were detected in the brain extracts from post-mortem samples (Sharon et al., 2003). There are various factors that are thought to promote the cascade of alpha-synuclein aggregation such as missense mutations in the alpha-synuclein gene (SNCA) such as A53T (Polymeropoulos et al., 1997), A30P (Kruger et al., 1998), E46K (Zarranz et al., 2004), G51D (Lesage et al., 2013), and H50Q (Appel-Cresswell et al., 2013; Proukakis et al., 2013) associated with rare familial autosomal dominant forms of PD (Polymeropoulos et al., 1997; Conway et al., 1998; Kruger et al., 1998; Greenbaum et al., 2005), post-translational modifications of alpha-synuclein (Fujiwara et al., 2002; Neumann et al., 2002), and dysfunction of cellular machinery that includes chaperone networks (that regulate protein folding and refolding) and the ubiquitin-proteasomal system (UPS) and autophagy-lysosomal pathway (ALP) which are responsible for elimination of harmful proteins (Tyedmers et al., 2010; Hartl et al., 2011). Examination of human postmortem tissue has demonstrated that components of UPS and its activity, as well as the ALP constituents, are reduced in the substantia nigra of PD patients compared to controls (Chu et al., 2009).

It could not be proven until now that the insoluble alpha-synuclein-containing inclusions alone are responsible for the PD. Lewy bodies are also observed at autopsy of aged individuals without clinical features of PD, constituting approximately 12 % of a series of >1,200 consecutive autopsy cases (Saito et al., 2004). Mice expressing human A53T mutant alpha-synuclein under the control of the prion-related protein promotor is one of the PD transgenic animal models with one of the most severe phenotypes to date and displays neurodegeneration with fibrillary alpha-synuclein inclusions but also shows a range of alpha-synuclein species, including insoluble aggregates and soluble oligomeric forms (Giasson et al., 2002; Lee et al., 2002). All the above findings demonstrate that Lewy pathology alone

cannot be responsible for alpha-synuclein mediated neuronal cell death. There must be a different form of oligomeric alpha-synuclein that leads to toxicity and leading to cell death.

1.3.2 ALPHA-SYNUCLEIN OLIGOMER TOXICITY

An emerging hypothesis proposes that there are toxic oligomeric species of alpha-synuclein (Kalia et al., 2013). Studies using protein-fragment complementation assays have shown that alpha-synuclein oligomers are associated with increased toxicity in cell culture models as measured by release of adenylate kinase from damaged cells, adenosine triphosphate levels or caspase 3/7 activity (Outeiro et al., 2008; Danzer et al., 2011). Various studies have also been conducted in animal models to examine the role alpha-synuclein oligomers to cell toxicity. Various alpha-synuclein mutants have been designed to show different aggregation properties. Addition of one or more missense mutations that involve specific alanine residues (for example A56P or triple mutant A30P/A56P/A76P) that participate in alpha-synuclein amyloid fibril formation produces mutant forms of alpha-synuclein with decreased capacity to form fibrils but increased propensity to form soluble oligomers (Karpinar et al., 2009). These designed mutants were expressed in Drosophila melanogaster and Caenorhabditis elegans (nematode worm). In both the models it was observed that there was increased loss of not only dopaminergic neurons but also other neuronal populations. The loss of non-dopaminergic neurons along with dopaminergic neurons in these models once again supported the hypotheses that PD is a multisystem disorder affecting many non-dopaminergic neurons systems (Winner et al., 2011). These findings support a role for alpha-synuclein oligomers in mediating both dopaminergic and non-dopaminergic neurons. Further there are findings in which there is the observation that higher oligomer levels are associated with disease. The amount of alpha-synuclein oligomers were found higher in transgenic mice expressing A53T mutant alpha-synuclein compared to transgenic mice expressing wild type alpha-synuclein and in mouse models of Gaucher disease versus wild-type mice (Tsika et al., 2010). Moreover the levels of alpha-synuclein oligomers are increased in the cerebral

cortex of patients with idiopathic PD, compared to age-matched normal controls (Paleologou et al., 2009) . All the above findings point at a link between endogenous alpha-synuclein oligomers and neurodegeneration of PD.

1.4 PD GENETICS

Although most patients with idiopathic or late-onset PD do not appear to have inherited the disease, a positive family history is associated with a high risk of having PD. Through the study of rare large families with clearly inherited Parkinsonism, several genes have been identified and implicated for the disease. Our understanding of the underlying mechanisms for the initiation and progression of PD began with the identification of mutations in the gene encoding alpha-synuclein (SNCA) and by the demonstration that alpha-synuclein is the major component of Lewy bodies (Polymeropoulos et al., 1997; Spillantini et al., 1997). Since then, 18 loci, named as PARK1 to PARK18, and 11 genes have been associated with inherited forms of Parkinsonism (TABLE 1.1). Genetic research during the last decade, has revealed that PD is not a single clinical entity, but rather a heterogenous group of clinical manifestations and symptoms (Corti et al., 2011). Some familial forms carry atypical clinical features, such as young-onset with dystonia, or the early occurrence of dementia or dysautonomia. Around 5-10% of patients with clinical signs of PD carry a mutation in one of the known genes that cause autosomal dominant recessive forms of the disease (Corti et al., 2011). Although this percentage is less, there is evidence that the same genes may play a prominent role in common sporadic form of the disease (for example the presence of mutations in LRRK2 gene both in the familial form and with late-onset autosomal dominant Parkinsonism) (Paisan-Ruiz et al., 2004).

Locus	Chr.	Inheritance	Gene	Mutation	First described by
PARK1	4q21-23	Dominant	**α-Synuclein**	A30P, E46K, A53 point mutations	Polymeropoulos et al., 1997
PARK2	6q25.2-27	Recessive	**Parkin**	Point mutations, deletions, duplications, insertions	Kitada *et al.*, 1998
PARK3	2p13	Dominant	**-**	Not identified-	Gasser *et al.*, 1998
PARK4	4q21-23	Dominant	**α-Synuclein**	A30P, E46K, A53 genomic duplications/triplications	Singleton *et al.*, 2003
PARK5	4p14	Dominant	**UCH-L1**	1 mutation in a single PD sibling pair	Leroy *et al.*, 1998
PARK6	1p35-36	Recessive	**PINK-1**	Appr. 50 point mutations, rare large deletions	Valente *et al.*, 2004
PARK7	1p36	Recessive	**DJ-1**	Appr. 50 point mutations and large deletions	Bonifati *et al.*, 2002
PARK8	12cen	Dominant	**LRRK2**	>80 Missense variants, >7 of them pathogenic	Zimprich *et al.*, 2004
PARK9	1p36	Recessive	**ATP13A2**	>5 Point mutations	Ramirez *et al.*, 2006
PARK10	1p32	Dominant	**-**	Not identified-	Hicks *et al.*, 2001
PARK11	2q36-37	Dominant	**GIGYF2**	7 Missense variants	Lautier *et al.*, 2008
PARK12	Xq21-25	Unclear	**-**	Not identified-	Pankratz *et al.*, 2003
PARK13	**2p12**	**Unclear**	**Omi/HtrA2**	**3 Missense variants**	**Strauss *et al.*, 2005**
PARK14	22q13	Recessive	**PLA2G6**	2 Missense variants	Gregory *et al.*, 2008
PARK15	22q12-13	Recessive	**FBXO7**	3 Point mutations	Di Fonzo *et al.*, 2008
PARK16	1q32	Recessive	**-**	Not identified	Satake *et al.*, 2009
PARK17	16q13	Dominant	**VPS35**	Not identified	Zimprich *et al.*, 2011
PARK18	3q27.1	Dominant	**EIF4G**	Point mutation	Chartrier-Harlin *et al.*, 2011

Table 1.1 Parkinson´s genes (Corti et al., 2011)

The lack of a clear family history in monogenic PD forms can result from recessive inheritance, reduced penetrance, or either the disorder may be the result of genetic predisposition to environmental toxins or to a combination of several genes that each increases the risk of the disease to a limited extent (Corti et al., 2011). Genes involved in PD can be inherited in an autosomal dominant or recessive way. Dominant genes are usually identified by positioning large number of members from the generations. Disease causing mutations in these genes are mostly missense variations, whose pathogenicity can be supported by several lines of evidence: the mutation clearly segregates with the disease in family studies; the mutation is located in an important domain of the encoded protein; the mutation is highly conserved across different species; and there is in-vitro and in-vivo proof that the mutation causes dysfunction or increases cell death (Hampe et al., 2006). Though

these dominant mutations may be found in clinically unaffected individuals, a phenomenon referred to as reduced penetrance (Sharma et al., 2012). Dominant mutations can act either through toxic gain of function or a loss of function mechanism (Kobayashi et al., 2003). To date, only three genes, alpha-synuclein, VPS35 and LRRK2, have been clearly shown to cause autosomal dominant PD.

Recessive genes are identified by linkage studies in nuclear families in which the same chromosomal segments inherited from a common ancestor are transmitted through both maternal and paternal lineages. Most of these recessive alleles lead to absence of encoded protein or an inactive protein and hence resulting in the loss of function (Wang et al., 2009). Mutations in the recessive genes Parkin, Pink1 and DJ1 are undoubtedly associated with heritable and early onset Parkinsonism. However penetrance can be reduced in rare cases as observed in 56-year old unaffected carrier with heterozygous mutations in Parkin (Deng et al., 2006).

Though the pathogenicity of several loci and genes associated with PD has not been confirmed, the mitochondrial serine protease HtrA2 is one such candidate whose role in the pathogenesis of PD has been supported by in-vitro and in vivo studies, but there are several studies which have given conflicting results. G399S and A141S mutations identified in PD patients in some studies but also found in controls in some other studies (Simon-Sanchez and Singleton, 2008). So the firm evidence for the causative role of HtrA2 mutations is still debated. This is discussed in detail in the next section.

1.5 HTRA2 – A MITOCHONDRIAL PROTEIN

1.5.1 GENERAL INTRODUCTION

HtrA2 is a mitochondrial serine protease with a great extent of homology to bacterial high temperature requirement A protease (HtrA) (Faccio et al., 2000). The bacterial HtrA family members are characterized by the combined presence of a trypsin-like protease domain and one or two C-terminal PDZ domains and they have been implicated in stress tolerance and

pathogenicity (Pallen and Wren, 1997). Bacterial HtrA acts as a chaperone at normal temperature while at increased temperatures it acts as a protease to remove denatured proteins and allows for cell survival after heat shock or stress (Pallen and Wren, 1997). There are four paralogues of HtrA present in humans and mice identified to date namely HtrA1 (Zumbrunn and Trueb, 1996), HtrA2 (Faccio et al., 2000), HtrA3 (Nie et al., 2003), and HtrA4 (Clausen et al., 2002). HtrA2 resides in the mitochondrial intermembrane space (IMS), while its paralogues HtrA1, 3 and 4 are targeted to the secretory pathway (Vande Walle et al., 2008). While HtrA2 is the most well studied member of this protease family (discussed in detail later), much less information is available on HtrA1 which has been found to be associated with several diseases such as arthritis, cancer, and Alzheimers´s disease (Grau et al., 2005; Milner et al., 2008; Chien et al., 2009; Hara et al., 2009). However, even less information on HtrA3 and very little on HtrA4 are currently available (Bhuiyan and Fukunaga, 2009). HtrA3 is the closest homologue of human HtrA1 and is correlated with ovarian cancer and is implicated to play a role as a tumor suppressor (Bowden et al., 2010).

1.5.2 STRUCTURE

Human HtrA2 is derived from an eight-exon gene located on chromosome 2q13, has an open reading frame encoding 458 amino acids and is ubiquitously expressed in human tissues (Gray et al., 2000). It is expressed as a 49-kDa proenzyme that is targeted to the mitochondrial intermembrane space (IMS) (Gray et al., 2000), although a fraction of endogenous HtrA2 is also found in the nucleus (Kuninaka et al., 2007). HtrA2 protein has a transmembrane domain (TM), a trypsin-like catalytic domain, and a PDZ domain, located among amino acids 105-121, 182-330 and 390-445, respectively (Fig 1.2). The IAP binding motif binds to IAPs and relieves its inhibitory effect on caspases (Faccio et al., 2000). The PDZ and protease domain play important roles in HtrA2 activation and specificity. The TM domain anchor behind the N-terminal mitochondrial localising sequence (MLS) most likely attaches the precursor protein into the mitochondrial inner membrane, where it undergoes

proteolytic maturation (Martins et al., 2002). During maturation, the first 133 aminoacids from N-terminus are cleaved thus exposing an inhibitor of apoptosis protein (IAP)-binding motif (IBM) (Lin et al., 2011).

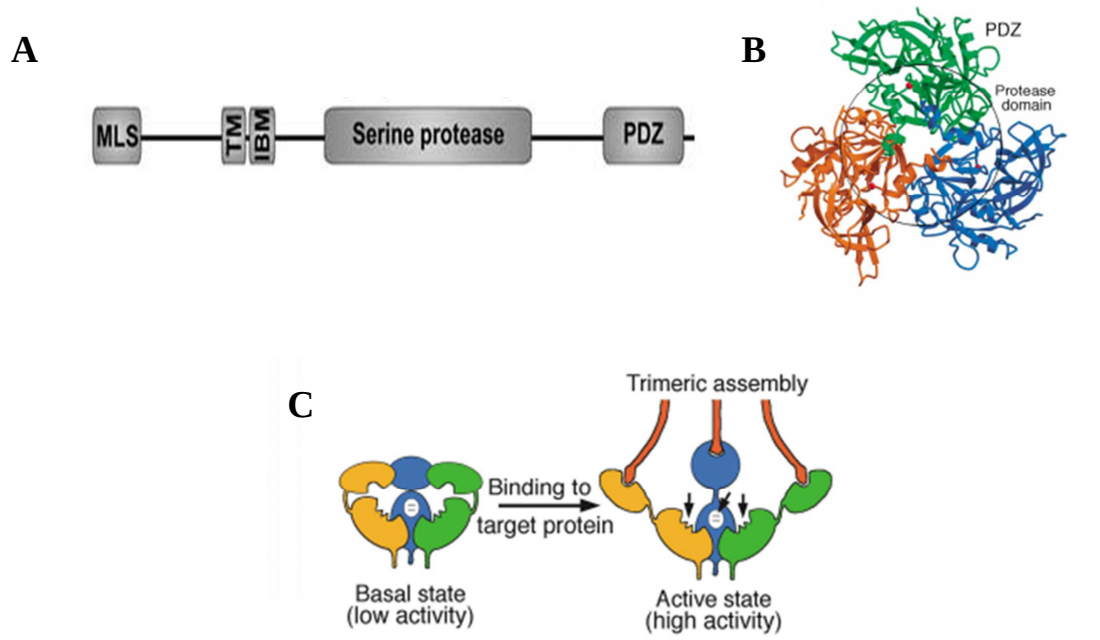

Figure 1.2 Structure of HtrA2 (A) schematic view of HtrA2 domains.- Mitochondrial localising sequence (MLS), transmembrane (TM), inhibitor of apoptosis protein (IAP)-binding motif (IBM), serine protease and PDZ domain **(B)** Tertiary structure of HtrA2(Lin et al., 2011) **C)** Proposed working model for HtrA2 (Yun et al., 2008)

Thus the fully processed protein which is 36-kDa having a short N-terminal domain, well defined serine protease and PDZ domains (van Loo et al., 2002).

HtrA2 exists as a trimer (See Fig.1.2B). Trimerization creates a pyramid-shaped structure, with the N-terminal IAP-binding sequences on top and the PDZ domains at the bottom. The access to the active site of the serine protease is restricted by the C-terminal PDZ domain, which packs against the protease domain through van der Waals contacts (Yun et al., 2008)

In the basal state, the PDZ domains keep the protease activity of HtrA2 in check. Upon binding to the substrate, the PDZ domain open up to expose the substrate-binding site of the protease domains, resulting in the cleavage of specific substrates (Yun et al., 2008).

1.5.3 FUNCTION

It is well known that human HtrA2 executes essential roles in the mitochondria and contributes to apoptosis (Zhang et al., 2007). HtrA2 has been found to be involved in both caspase-dependent and independent apoptosis. On receiving apoptotic stimuli, HtrA2 is released in the cytosol, where it interacts with IAP´s through its N-terminal tetrapeptide motif and relieves inhibition on upstream caspase-9 (Martins et al., 2002).

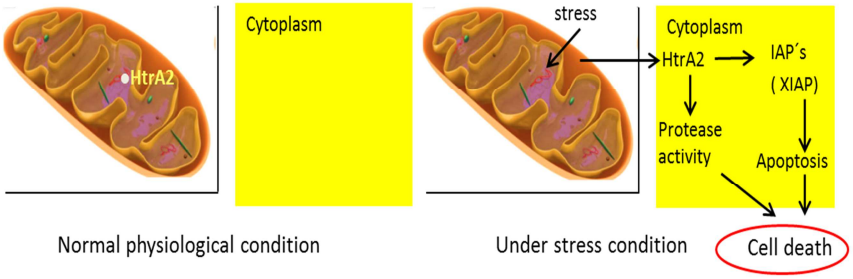

Figure 1.3 HtrA2 mediated apoptosis

Furthermore, it cleaves several anti-apoptotic proteins such as XIAP, Pea-15 and Hax-1 in a caspase-independent manner (Cilenti et al., 2004; Trencia et al., 2004). The other known HtrA2 substrates include WARTS (Kuninaka et al., 2007), APP (Park et al., 2006a) and cIAP1 and cIAP (Srinivasula et al., 2003). Three more mitochondrial substrates of HtrA2 have been discovered namely PDHB, IDH3A and HSPA8, which implicated HtrA2 in a novel mechanism relating to mitochondrial metabolism (van Loo et al., 2002).

Besides from its proapototic functions, HtrA2 has been implicated in neurodegenerative disorders such as Parkinson's and Alzheimer's disease (Jones et al., 2003) because of its neuroprotective role inside mitochondria. Recently HtrA2 has also been implicated as a positive regulator of autophagy facilitating the degradation of mutant proteins involved in neurodegenerative diseases (Li et al., 2010). Here it has been reported that HtrA2 activates autophagy through digestion of Hax-1, which suppresses autophagy in a Beclin-1-dependent pathway. Moreover, HtrA2 induced autophagy also lead to degradation of p62, which assemble the autophagic machinery for efficient degradation of impaired mitochondria (van Loo et al., 2002). The proteolytic activity of HtrA2/Omi is also markedly up-regulated in

response to heat shock or stress (Gray et al., 2000). Whether HtrA2 is a mitochondrial chaperone it is contradictory (Vande Walle et al., 2008). Although the literature suggests that HtrA2 might be upregulated in the case of unfolded protein response (Papa and Germain, 2011) further studies are needed to confirm its role as a mitochondrial chaperone.

1.5.4 PD AND HTRA2

The mitochondrial protease HtrA2 is localized in the mitochondrial intermembrane space and is an ATP-dependent enzyme structurally and functionally related to the bacterial quality control proteases DegP and DegS (Clausen et al., 2011). Its loss leads to accumulation of unfolded proteins in the mitochondria, oxidative stress, and defective mitochondrial respiration which suggests that like its bacterial homologs HtrA2 also functions as a quality control protease (Moisoi et al., 2009).

Mice lacking HtrA2 function (protease activity) or expression (HtrA2 knockout mice) exhibit early onset neurodegeneration and motor impairments similar to PD (Martins et al., 2004) (Jones et al., 2003). Through these studies, first time HtrA2 was thought to have protective role in neurons that requires its protease activity and was correlated with the homologous bacterial stress-adaptive proteins DegP and DegS (Martins et al., 2004). The importance of HtrA2 mouse models is discussed in detail in section 1.7. XIAP is a well-known substrate of HtrA2 and inhibits active caspases, and the characterization of XIAP-deficient mice showed no phenotype giving a clue for neuroprotective role of HtrA2 (Harlin et al., 2001). Further it has been shown that the neurodegeneration and early death in mnd2 mice is rescued by a neuron targeted human HtrA2 transgene which further explains the neuroprotective role of HtrA2 (Kang et al., 2013). HtrA2 has been found to be one of the constituent of alpha-synuclein containing inclusions in the brains of patients with PD, dementia or multiple-system atrophy (Strauss et al., 2005; Kawamoto et al., 2008). Moreover some mutations and polymorphisms in HtrA2 have been associated with sporadic cases of PD (Strauss et al., 2005; Bogaerts et al., 2008; Lin et al., 2011) in German, Belgian and Taiwanese population

respectively (Fig 1.5). Though most of these sites of mutations are conserved sites, but one of these nucleotide positions where the mutation has been found – position 399, G is highly conserved.

Figure 1.4.Schematic view of the HtrA2 protein indicating the localization of mutations in HtrA2 associated with PD.

However some of these mutations were also found in the control patients in the later studies, though the mutation carriers in controls (not clinically investigated) were younger than the expected age at onset (Simon-Sanchez and Singleton, 2008), but soon after this study Bogaerts published one more HtrA2 mutation, Arg404Trp in PD patients predicted to freeze HtrA2 in an inactive form (Bogaerts et al., 2008). And recently another missense mutation Pro143ala in HtrA2 was identified in Taiwanese PD patients. So the mutations in HtrA2 are inconsistently associated with a risk of PD and so still debated.

Interestingly the mutations in HtrA2 which are associated with PD lie next to p38 and CDK5 phosphorylation sites (Plun-Favreau et al., 2007; Fitzgerald et al., 2012). Mutations in the serine protease domain - A141S (Strauss et al., 2005), P143A (Lin et al., 2011) and the PDZ domain - G399S (Strauss et al., 2005) and R404 (Bogaerts et al., 2008) are shown in figure 1.5 and along with that the phosphorylation sites are also indicated.

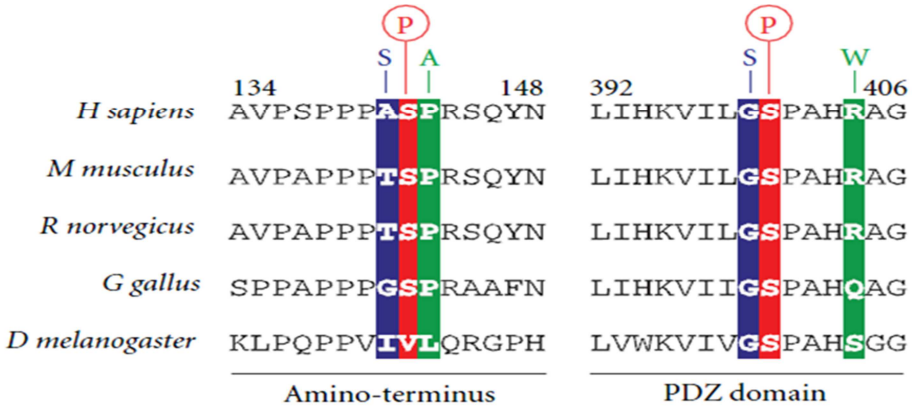

Figure 1.5 Phosphorylation sites adjacent to S141 polymorpghism and G399 mutation in HtrA2 (Desideri and Martins, 2012)

Except the R404W mutation, all other mutations lie exactly just one position next to the phosphorylation sites. Both A141S (Strauss et al., 2005), P143A (Lin et al., 2011) are adjacent to Serine 142 and G399S (Strauss et al., 2005) and R404 (Bogaerts et al., 2008) are adjacent to and near to the Serine 400 phosphorylation site (Fig 1.5) respectively.

The function of HtrA2 has also been linked to Pink1 in relation to PD. It was found that HtrA2 was phosphorylated upon activation of the p38 pathway in a Pink1-dependent manner, and there was an increase in phosphorylated HtrA2 in the brains of sporadic PD patients and decreased in Pink1 mutated patients (Plun-Favreau et al., 2007). It is also reported that HtrA2 is phosphorylated at S400 by Cyclin-dependent kinase-5 (Cdk5) in a p38-dependent manner (Fitzgerald et al., 2012). Here it's also reported that phosphorylation of HtrA2 at S400 is involved in maintaining mitochondrial membrane potential under stress conditions and hence important for mitochondrial function. Activation of similar pathway is also involved in the phosphorylation of another site, S142, which is also located adjacent to the site of mutation, found in PD patients and is phosphorylated in a p38 and Pink1-dependent manner (Plun-Favreau et al., 2007). HtrA2 is also reported to be phosphorylated at S212 by Akt which reduces its protease activity (Yang et al., 2007).

Recently PARL and HtrA2 interaction has been linked to intricate ischemic neuronal apoptotic process starting within mitochondria (Hsu, 2013). It has also been shown that down regulation of PARL after ischemia is an important step in ischemic neuronal injury and it

increases neuronal vulnerability by decreasing HtrA2 processing (Yoshioka et al., 2013). Goo et al showed that mitochondrial DNA conformational stability is related to HtrA2 and its deficiency causes mtDNA damage through reactive oxygen species and mutation, which may lead mitochondrial dysfunction and trigger cell death in ageing cells. All the above studies show the importance HtrA2 in maintenance of mitochondrial homeostasis and regulation of cellular apoptosis in relation to PD.

1.5.5 ANIMAL MODELS OF HTRA2 IN RELATION TO PD

The HtrA2 came into focus in relation to PD, when mnd2 (motor neuron degeneration 2) mutation found in mouse was identified as a homozygous missense mutation (Ser276Cys) in the protease domain of the nuclear-encoded mitochondrial serine protease HtrA2 (Yacobi-Sharon et al., 2013). The mnd2 was identified in 1990 as a spontaneous, recessively inherited mutation that arose on the C57BL/6J inbred background (Jones et al., 1993). The earliest symptoms observed in these mice were altered gait and cessation of normal weight gain, followed by ataxia, repetitive movements and akinesis. Striatal neurons were most susceptible in these mice, but other neurons in the central nervous system, brain stem and spinal cord, including motor neurons were affected at later stages (Rathke-Hartlieb et al., 2002). Both the features of necrosis and apoptosis were observed in these mice. Early degeneration of mitochondria was also noted (Rathke-Hartlieb et al., 2002; Jones et al., 2003). This finding about mnd2 mice was followed by another important finding in which homozygous deletion of HtrA2 gene lead to similar phenotype as mnd2 mice with early death resulting from the loss of striatal neurons. These mice die within 30 days due to a Parkinsonian phenotype. These mice did not show degeneration of TH-positive dopaminergic neurons in the substantia nigra though the loss of neurons as well as TH-positive fibers was observed. The exact nature of cell death in these mouse lines is unclear, however, the reduced mitochondrial membrane potential and abnormal shape of mitochondria in electron microscopy certainly points towards mitochondrial dysfunction mediated cell death in these

mice. This suggested that while the serine protease activity of HtrA2 knockout mice have a protective function, the IAP binding motif does not have an obvious nonredundant proapoptotic role (Martins et al., 2004).

To address this issue XIAP (a well-known substrate of HtrA2) knock out model has also been generated which showed no phenotype (Harlin et al., 2001). So, though it can´t be proved clearly, since HtrA2 might have some important substrates which are unknown still, but from the above models and results one can speculate a significant protective function of HtrA2 that requires its protease activity. More recently it has been shown that transgenic expression of human HtrA2 in the central nervous system of mnd2 mice rescues them from neurodegeneration and prevents their premature death (Kang et al., 2013), which confirmed the neuroprotective role of HtrA2. In addition Liu and colleagues (2007) as an attempt to examine the biological relevance of wild type HtrA2 overexpression in mice, investigated the phenomenological data of organ weights, hair phenotype or pregnancy abnormalities, but found no defect. No cell death or behavioral evaluation was performed in this study. So with this limited approach the acquired results did not show an effect on overall phenotype.

A neuroprotective role of HtrA2 has also been shown in Drosophila HtrA2 mutant model (Tain et al., 2009). Tain and colleagues showed in this study that Drosophila HtrA2 null mutants are viable but exhibit mild mitochondrial defects, loss of flight and climbing ability, male infertility and sensitivity to oxidative stress and mitochondrial toxins. These data were consistent with findings in mice and humans and suggest that HtrA2 is indispensable for mitochondrial integrity. It was also confirmed that HtrA2 is not required for developmental or stress-induced apoptosis in Drosophila. But similar studies on Drosophila could not replicate previous findings (Yun et al., 2008). The loss of function study by Yun and colleagues suggested that HtrA2 does not play an essential role in regulating mitochondrial integrity in the Pink1/Parkin pathway in Drosophila. Recent studies in mice also showed similar results where neurodegeneration in the HtrA2 mutant mice could not be rescued by overexpression of Parkin (Yoshida et al., 2010).

From the above findings it can be concluded that the role of HtrA2 in relation to PD is still not clear and established. Hence further studies need to be conducted to explain the role of HtrA2 in PD.

1.6 AIMS

Neurological disorders can be modeled in animals so as to generate specific pathogenic events and behavioral phenotypes. PD is the second most common neurodegenerative disease, affecting 1 % of the population above the age of 55 years (Lees et al., 2009). There are several proteins and mutations in these proteins which have been implicated to play role in PD but much of this process still remains a mystery. The mitochondrial protease, HtrA2/Omi is localized to the mitochondrial intermembrane space and has a pro-apoptotic function when released in the cytosol. Its role in neuroprotection was initially demonstrated by neurodegeneration and mitochondrial dysfunction in the mice lacking HtrA2/Omi expression or function (Jones et al., 2003; Martins et al., 2004) Furthermore PD - associated variants in the HtrA2/Omi has been discovered in German, Belgian and Taiwanese PD patients (Strauss et al., 2005; Bogaerts et al., 2008; Lin et al., 2011). Although several studies have pointed to the importance of a mitochondrial role for HtrA2/Omi, the mechanism of neuroprotection and the relevance of mutations in relation to PD are still not clear.

Therefore we sought to further understand the relevance of HtrA2/Omi and HtrA2/Omi mutations by generating transgenic (TG) mice overexpressing human wild type (TG HtrA2 WT) and G399S (TG HtrA2 G399S) mutant HtrA2. Transgenic mouse lines overexpressing human HtrA2 WT and human HtrA2 G399S mutant were generated in our laboratory.

The data obtained will be presented according to the following specific aims:

Firstly to assess the expression of transgenic HtrA2 in the different brain regions of mice, using biochemical methods and then confirming it by immunohistochemical methods. Second aim was to determine the implications of overexpressing human WT and G399S HtrA2 in mice in relation to PD. As PD is characterized by motor and learning impairments and in some cases also by anxiety levels, we analyzed our HtrA2 mouse lines using behavioral assays such as rotarod, challenging beam walk and OF to assess PD phenotype. And then

finally investigate the mechanism underlying any behavioral or pathological phenotype observed in these mouse lines. This was also assessed by using various biochemical and immunohistochemical methods.

2 MATERIALS AND METHODS

2.1 MATERIALS

2.1.1 REAGENTS

Unless mentioned otherwise, general chemicals were purchased from: Roche (Basel, Switzerland), Sigma (Steinheim, Germany), Invitrogen Life Technologies (Karlsruhe, Germany), Merck (Darmstdt, Germany).

Specialized reagents	**Source**
1 Kb DNA ladder plus (#SM 1331/2/3)	Fermentas
PageRuler Plus pre-stained protein ladder (#26619)	Invitrogen
ECL Western blotting detection reagent (#RPN2109)	GE Healthcare
Complete protease inhibitor cocktail tablets (#04693116001)	Roche
Phosphatase inhibitor cocktail tablet (#04906845001)	Roche
Zeocin (#R250)	Invitrogen
GoTaq DNA Polymerase (#M8305)	Promega
Vectashield mounting medium for fluorescence (#H-1000)	Vector laboratories
Effectene transfection reagent (#301425)	Qiagen
Hoechst stains (#62249)	Thermo Scientific
Mitotracker Green (#M-7514)	Molecular Probes, Invitrogen
Jung tissue freezing medium® (#020108926)	Leica microsystems Nussloch GmbH
Acetyl-Asp-Glu-Val-Asp-7-amido methyl coumarin (#A 1086)	Sigma

Table 2.1 Specialized reagents

2.1.2 BUFFERS AND SOLUTIONS

All buffers and solutions were prepared in distilled water unless otherwise stated.

Buffer/Solution name	Ingredients
Phosphate buffered saline (PBS) 10X	1370 mM NaCl, 27mM KCL, 81mM Na_2HPO4 and 14.7mM KH_2PO4 in dH_2O, pH 7.4
TENS buffer	100mM Tris pH 8.5, 5mM EDTA, 0.2%SDS (w/v), 200mM NaCl
Proteinase K	20µg/ml water
Homogenising buffer	50mM Tris, 150mM NaCl, 5mM EDTA
Tris buffered saline 10X (TBS)	0.5M Tris-HCl, 1.5M NaCl, pH7.2
Tris buffered saline –Tween (TBS + Tween)	1x TBS, 0.05% TWEEN 20 (v/v)
4% Paraformaldehyde	Paraformaldehyde (w/v) in PBS was dissolved by boiling. The solution was cooled down on ice and filtered using filter paper
Running buffer	124 mM Tris, 960mM Glycin, 0.005% SDS (w/v)
Transfer buffer	2.5mM Tris, 19.2 mM Glycin , 20 % Methanol(v/v)
5X- Laemmli-buffer	62.5 mM Tris-HCl pH 6.8, 5% ß-Mercaptomethanol (v/v), 2% SDS (w/v), 10% Glycin (w/v), 0.05% Bromophenolblue (v/v)
Blocking solution	5% non-fat milk (w/v) in TBS for Western Blot (WB) 5% normal goat serum in PBS for histology
Complete protease inhibitor cocktail tablets solution	1 tablet was dissolved in 2 ml of water.
Phosphatase inhibitor cocktail tablet solution	1 tablet was dissolved in 2 ml of water
TAE buffer	40mM Tris, 0.05% acetic acid (v/v), 1mM EDTA in water, pH.

	7.5-8.0
Permeabilisation solution	0.2 % Triton-X-100 in PBS
Assay buffer for caspase 3 activity	20mM HEPES, 0.1% (w/v) CHAPS, 5mM DTT and 2mM EDTA, pH 7.4
Lysis buffer for caspase 3 activity	50mM HEPES, 5mM CHAPS, 5mM DTT, pH 7.4

Table 2.2 Buffers and solutions

2.1.3 KITS

Kit	Purpose	Source
Genopure plasmid midi kit	Plasmid isolation	Roche
Quick change site directed mutagenesis kit	Mutagenesis	Strategene,
FD NeuroSilver™ Kit II	Silver staining for protein aggregates	FD Neurotechnologies,inc, USA
In Situ cell death detection kit, TMR red /TUNNEL KIT	Apoptotic cell death	Roche diagnostics, Basel, Switzerland
LightCycler 480 SYBR Green I Master	Quantitative real time pcr (qRT-PCR)	Roche

Table 2.3 Kits used

2.1.4 ANTIBODIES

For Western blotting (WB) primary antibodies were diluted to the desired concentration in 5% milk (w/v) in 5 ml TBS-T. The mixture was stored at 4°. Primary Antibodies used for immunofluorescence were diluted in 5% (w/v) BSA.

2.1.4.1 PRIMARY ANTIBODIES

Antibody	Species	Dilution		Source	Special conditions
		WB	IH/IF		
HtrA2/Omi (#AF1458)	Rabbit	1:3000	1:500	R & D systems,	
Actin (#A5316)	Mouse	1:5000		Sigma	
FLAG M2 - peroxidase (HRP) clone M2 (#A8592)	mouse	1:1000		Sigma	
LC3B (#2775)	Rabbit	1:1000		Cell signaling laboratories	PVDF membrane, wet blotting, antibody dilution in 5% BSA
Complex IV (#MS404)	Mouse	1:1000		Millipore	Loading samples heated at 37℃
VDAC (#AB10527)	Mouse	1:10,000		Millipore	
PhosphoS400 HtrA2 Generous gift from Dr. Helene Plun-Favreau (UCL Institute of Neurology, London, UK)	Rabbit		1:500		
α-Synuclein (#S5566)	Mouse		1:100	Sigma	
XIAP (#AF8221)	Goat	1:1000		R & D	

				systems	
Trap1 (#612344)	Mouse	1:1000		BD Transduction laboratories	Loading samples heated at 37℃
FLAG M2 monoclonal antibody (#F1804)	Mouse		1:100	Sigma	
Cleaved caspase-3 (D175) (#9661)	Rabbit	1:1000	1:200	Cell signaling laboratories	
Cleaved caspase 9 (#9509)	Rabbit	1:1000		Cell signaling laboratories	
Ubiquitin (# MAB1510)	Mouse	1:4000		Millipore	

Table 2.4 Primary Antibodies

2.1.4.2 SECONDARY ANTIBODIES

Antibody	**Dilution**		**Source**
	WB	**IH/IF**	
Anti-mouse HRP	1:5000		GE Healthcare
Anti-rabbit HRP	1:10,000		GE Healthcare
Anti-goat HRP	1:5000		GE Healthcare
Anti-Mouse Alexa Fluor 488		1:1000	Invitrogen
Anti-Rabbit Alexa Fluor 546		1:1000	Invitrogen
Anti-Mouse Alexa Flour 546		1:1000	Invitrogen

Table 2.5 Secondary Antibodies

2.1.5 SPECIALIZED INSTRUMENTS

Instrument	Source
Fluorescence Microscope	Zeiss
Live Cell MicroscopeAxiovert 2000 plus Zeiss incubator XL	Zeiss
Leica VT1000S vibrating Blade Microtom	Leica
Cryostat	Leica
iBlot system	Invitrogen
Light Cycler	Roche
Perfusion pump	ISMATEC
NanoDrop	Nanodrop
T10 basic ULTRA TURREX homogeniser	IKA®-Werke GmbH & Co. KG, Staufen

Table 2.6 Instruments used

2.1.6 MOUSE LINES USED

I. C57BL/6 — Black 6 wild-type mice used for breeding and maintenance of transgenic lines (Charles River, Germany)

II. Transgenic (TG) HtrA2 WT — Black 6 mice overexpressing human wild type (WT) HtrA2

III. Transgenic (TG) HtrA2 G399S — Black 6 mice overexpressing human HtrA2 with G399S mutation

2.2 METHODS

2.2.1 MODELS

2.2.1.1 MICE

2.2.1.1.1 BACKGROUND ABOUT MOUSE LINES

The TG HtrA2 WT and TG HtrA2 G399S DNA constructs were created by Nicole Kieper and Dr. Mira Lang (previous PhD students in our laboratory) and the mouse lines were generated by standard pronuclear injection (Dr. Thomas Ott, IZKF-Service Transgene Tiere). Subsequent breeding and husbandry were carried out in the animal facility of the Hertie - Institute.

I. GENETICS

Full length FLAG-tagged WT HtrA2 cDNA was cloned into a pCMV-Tag4A vector (cloning and description in Strauss et al., 2005). Then the pCMV-Tag4A vector was digested with EcoRV and KpnI and cloned into the pBluescript II KS (-) vector (Agilent Technologies, #212208). The mouse Prp promoter was a kind gift from Kathrin Grundmann (University of Tubingen) and was also cloned into the pBluescript vector in front of the HtrA2 cDNA. A poly A tail was finally cloned after the HtrA2 DNA (Fig. 2.1)

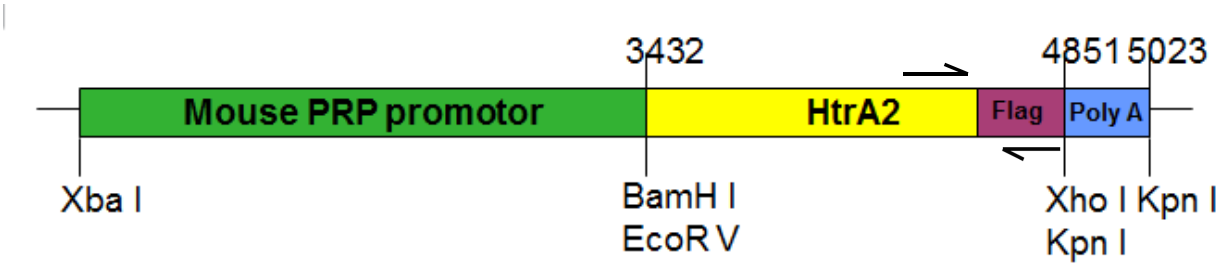

Figure 2.1 Cloning sites in pBluescript II KS (-) vector used to generate TG mouse lines. Arrows represent PCR primers.

II. SELECTION

Potential transgenic founder mice were identified by using conventional PCR. DNA from ear skin was isolated by isopropanol precipitation and a PCR was performed. The following primers for HtrA2 were used: 5'-GTTAGCTCTGCTCAGCGTTCCAG-3' as forward primer in the HtrA2 cDNA and 5'CGTCGTCATCCTTGTAATCCTCG-3' as reverse primer starting in the FLAG-tag sequence. If the transgenic construct is present, a 576 bp PCR product can be detected. Positive male founders F1 were bred with 8 week old C57BL/6N females (Charles River, Germany). Animals from the F2 generation were used for analysis of the organ specific expression of the recombinant protein.

2.2.1.1.2 BREEDING STRATEGY FOR MICE

Heterozygous (Het´) mice were crossed with each other and the resulting homozygous (Hom´) mice were identified by quantitative RT PCR (qRT-PCR). These homozygous mice were crossed with C57BL/6 (NonTG) mice to generate heterozygous mice.

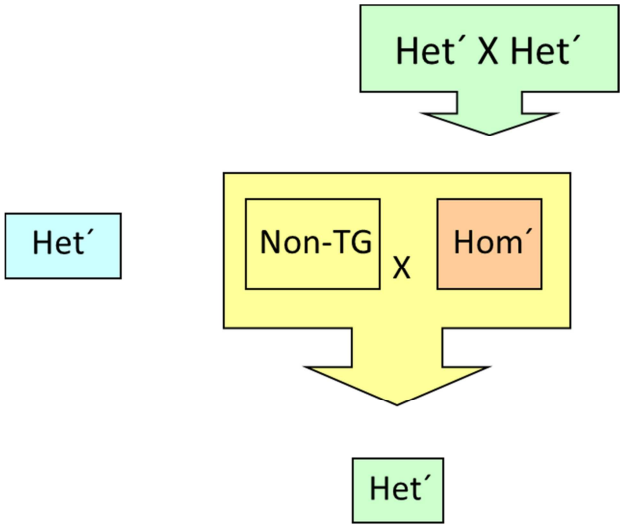

Figure 2.2 Breeding strategy where Het´ '= heterozygous mice, Hom´= homozygous mice and Non-TG= non-transgenic mice.

2.2.1.1.3 NOMENCLATURE USED OF MICE BRAIN REGIONS:

For WB and immunohistochemical studies the different brain regions were assigned the following names.

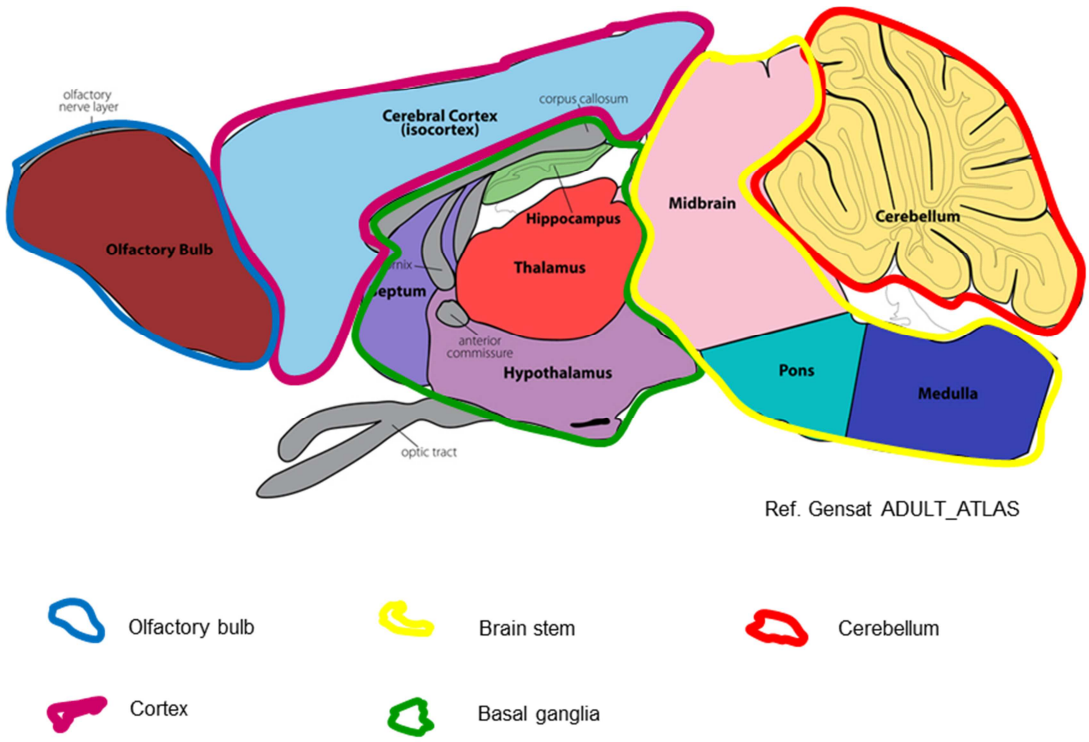

Figure 2.3 Assigned regions of mice brain used for WB and immunohistochemical studies (image adapted from Gensat ADULT_ATLAS; http://www.gensat.org/atlas/ADULT_ATLAS_09.jpg)

2.2.1.2 CELLS

- SH-SYSY
- MEF's

2.2.1.2.1 CELL CULTURE

I. Thawing of SH-SY5Y cells and MEF cells

Cell culture of SH-SYSY cells and MEF cells involved similar media and procedures. Cells stored in liquid nitrogen were thawed quickly in a 37℃ pre-warmed water bath and transferred into 5 ml of pre-warmed medium. After centrifugation for 5 min at 1000 rpm, the cell pellet was resuspended in 10 ml of pre-warmed medium and added to 75 cm^2 flasks.

II. Cell culture routine

Cells were split every 2-3 days according to their confluency. For this, cell culture medium was removed and cells were washed once with 7 ml PBS. To detach cells from the flask, 2ml of pre-warmed trypsin was added and incubated at 37° for 3-5 min. After adding 10 ml pre-warmed medium, all the cells were tried to be retrieved into the medium and in order to break clusters the media was pipetted up and down for 3-4 times. Later the whole cell suspension was spun down for 5 min at 1000 rpm and the resulting cell pellet resuspended in 10 ml culture medium. Cells were split 1:4 in a new flask to a final volume of 10 ml.

2.2.1.2.2 TRANSFECTION OF CELLS

MEF cells and SH-SYSY cells were transfected with effectene transfection reagent, using the protocol provided by the company. On the day before transfection, cells were plated at an adequate density to give 60% confluency on the following day (200,000 cells per well of a 6-well plate). For each well 1 µg/µl concentrated DNA was used for transfection using the

protocol. Cells were harvested for protein lysates or used for immuncytochemistry after two days of incubation at 37℃ and 5% $CO_{2.}$

2.2.1.2.3 LIVE CELL IMAGING MICROSCOPY IN MEF CELLS

Live cell imaging was assessed to study colocalisation of mitochondria with lysosomes in MEF cells. Cells were cultured in Lab-TekHII chambered coverglasses (#155382; Nalge Nunc International). Analysis of the colocalisation of mitochondria with lysosomes was carried out for MEF cells by staining mitochondria with 100 nM Mito Tracker Green FM (Invitrogen, USA) and 100 nM Lysotracker Red DND-99 (Invitrogen, USA) for 15 minutes. Hoechst 33342 was used to stain nuclei.

Live cell imaging analysis was performed using an inverted Zeiss Axiovert microscope (Zeiss Plan-Apochromat 63x/1.4) with an incubation chamber temperature at 37℃, a humidified atmosphere, and 5% $CO_{2.}$ Stacks of the images were taken with an AxioCamMRm camera (Zeiss, Germany) with distances 0.240 µm per stack. For each image, three to five stacks were taken. The series of images were saved uncompressed and analysed with AxioVision software (Zeiss, Germany).

2.2.2 MOLECULAR BIOLOGICAL EXPERIMENTS

2.2.2.1 GENOTYPING

In order to isolate DNA, skin of mice was used. For this an ear biopsy was performed from each mouse. This skin was then used for DNA isolation.

2.2.2.1.1 DNA ISOLATION

200µl TENS buffer and 10µl of proteinase K was added to the skin and then left overnight at 55° C on a shaker. To this 87 µl of 5M NaCl was add ed and left on ice for 10 minutes. Then the mixture was centrifuged at 14000 rpm for 20 minutes at room temperature (RT). The

supernatant was aspirated and the pellet was discarded. Then 200µl of 100 % isopropanol was added to this supernatant and left at RT for 10 minutes. The mixture was centrifuged again at 14000 rpm for 20 minutes and the supernatant was discarded and the pellet was stored. The pellet was washed with 70% (v/v) ethanol solution for 10 minutes at 14000 rpm. Then the supernatant was discarded and the DNA pellet was left for drying for two hours at RT. The DNA pellet was then mixed with 30 µl of water and used for Polymerase Chain Reaction (PCR).

2.2.2.1.2 QUANTITATIVE RT–PCR (QRT-PCR)

In order to identify homozygous mice from the mixed population of mice, qRT-PCR was used. A LightCycler I and SyberGreen (both provided by Roche) were used for the qRT-PCR. The amount of produced PCR product was detectable with SyberGreen. This dye intercalates in the DNA and gives fluorescence which is then read by the light cycler and gives a reading in the form of arbitrary values. A standard curve was made for a house-keeping gene (mouse ß-actin) and for the gene of interest (hHtrA2) of a heterozygous animal. The results of the PCR with unknown samples were compared with the standard curve. In each run a negative control (DNA of non-transgenic animal) and a positive control (DNA of heterozygous animal) was included. The ΔCt value of the positive control was set to 1. The ΔCt value of qRT-PCR with unknown samples was compared to the values of positive control.

<u>qRT-PCR Conditions:</u>

95°C – 10´

95°C – 30´´ ⎫
65°C – 10´´ ⎬ 45X cycles
72°C – 20´´ ⎭

72°C – 3´

8°C- infinity ∞

- Acquisition of data at every cycle + melting curve.

ß-Actin was used as a house keeping gene.

Gene	Forward primer	Reverse
HtrA2	5´CCAAGCTTTCCCGATGTTCAGCA3´	5´-CGTCGTCATCCTTGTAATCCTCG-3´
ß-Actin	5´GATCTGGCACCACACCTTCT	5´TCTTCTCCCGGTTAGCTTTG3´

Table 2.7 Primer combination used for qRT PCR

2.2.2.1.3 CONVENTIONAL PCR

In order to determine the expression of transgenic human HtrA2 gene in mice, the HtrA2 gene was amplified using conventional PCR and was run on a 1% agarose gel. For this the primers flanking the exogenous gene were used and if the exogenous gene was present in a particular sample it was amplified, while in case of the absence of exogenous gene (Non-TG mice) there was no amplification.

Conventional PCR conditions:

95°C 5´

95℃……..30´´

55℃ 30´´ } 25X Cycles

72℃……45´´

72℃ 3´

8℃ infinity ∞

Gene	Forward primer	Reverse
HtrA2	5´ GTTAGCTCTGCTCAGCGTTCCAG-3´	5´-CGTCGTCATCCTTGTAATCCTCG-3´

Table 2.8 Primer combination used for conventional PCR

Components	Amount
DNA	2-3µl of ear biopsy lysate
Reaction buffer (5X)	5µl
dNTP´s (2mM)	1,0µl
Primer forward (10mM)	2,0µl
Primer reverse (10mM)	2,0µl
Betaine (1M)	0,5µl
GoTaq polymerase	0,3µl
Water	13,0µl

Table 2.9 Components of typical PCR reaction

2.2.2.1.4 AGAROSE GEL ELECTROPHORESIS

Agarose gel electrophoresis was performed to separate and analyze DNA: The DNA was visualized by adding 0.2 µg/ml ethidium bromide to the molten agarose before casting it. DNA strongly binds to ethidium bromide by intercalating between the bases and is fluorescent, absorbing UV light and transmitting the energy as visible light. Samples were diluted in 5X loading dye before loading and 1 kb molecular weight ladders were used to analyze the size of the DNA. Gels were run at 100 V in TAE buffer.

2.2.2.2 PREPARATION OF PLASMID-DNA FROM BACTERIA

Bacteria having the plasmid of interest were grown in 2 ml of antibiotic-free LB-medium at 37°. On the next day 200 µl of the bacterial culture was inoculated into 200 ml LB-medium containing an appropriate antibiotic and grown to an OD_{600} of 0.5. The culture was centrifuged at 3500 rpm for ten minutes, the resulting pellet was resuspended in the buffer provided in the Genopure plasmid midi kit and the proceeding plasmid-DNA purification

procedure was performed using the Genopure plasmid midi kit protocol. DNA concentration was measured using NanoDrop.

2.2.2.3. IN-VITRO MUTAGENESIS

In-vitro mutagenesis was performed using Quick change site directed mutagenesis kit according to the protocol stated by the company was followed except that instead of PfuTurbo DNA polymerase that was provided with the kit, GoTaq polymerase was used for the PCR reaction. For designing the primers for mutagenesis Stratagene´s web based QuickChange primer design program available online at http://www.stratagene.com/qcprimerdesign was used.

2.2.2.4 TRANSFORMATION OF COMPETENT BACTERIA

For transformation of competent bacteria, these were slowly thawed on ice. Meanwhile 2µl DNA was added to the bacterial aliquot (100µl) and incubated on ice for 20 minutes. After this bacteria were given heatshock at 42℃ followed by 2 min. incubation on ice. To this bacterial suspension, 250-500µl of prewarmed LB-medium was added and the mixture was incubated for 1 hour at 37° C under continuous shak ing (300 RPM).Bacteria were then spun down for 2 min at 1000 rpm and the resulting pellet was resuspended in 100µl LB-medium. 10µl and 90µl of the bacterial solution were plated on LB agar plates with the corresponding antibiotics. Incubation was performed in inverted position at 37°. On the next day, single bacteria clones were picked and inoculated in 2ml LB-medium. After 8-10 hours growth at 37° and 250 rpm, 200µl of this culture was inoculat ed in 200 ml LB-medium with antibiotics and grown at 37°.

2.2.2.5 PREPARATION OF GLYCEROL STOCKS

One colony of bacteria was picked up from the agar plate by a pipette tip and put into 2 ml of LB broth media with the respective antibiotic. And the bacteria were allowed to grow in this media overnight. Next day, out of the bacterial suspension obtained, 700 µl was added in the freezing tube containing 500 µl of autoclaved 50 % glycerol (v/v) and the aliquot was frozen.

2.2.3 BIOCHEMICAL METHODS

2.2.3.1 PREPARATION OF PROTEIN LYSATES FROM MOUSE TISSUE

Organs and different regions of brain were dissected from mice in ice-cold conditions and transferred into 1.5 ml reaction tube and washed with PBS, and then transferred immediately into liquid nitrogen. After preparation of all tissue samples, these were lysed by adding homogenizing buffer containing 4% complete protease inhibitor cocktail solution (v/v) and a 4 % phosphatase inhibitor cocktail solution (v/v) in each 1.5 ml reaction tube and then homogenized using a T10 basic ULTRA TURREX homogenizer. The resulting homogenate was centrifuged at 14000 rpm for 30 min at 4℃ and the supernatant was transferred into a new ice-cold reaction tube. The same step was followed two times in order to remove the impurities. Next 10% (v/v) of Igepal® CA-630 was added to each supernatant and vortexed and left on ice for 10 minutes. Again the mixture was centrifuged at 14000 rpm for 30 min. at 4℃. The protein lysate achieved as a supernatant was then transferred into a new 1.5 ml reaction tube and was frozen.

2.2.3.2 PREPARATION OF PROTEIN LYSATES FROM CELL CULTURE

Cells cultivated on 6-well plates, were washed once with ice-cold PBS. PBS was removed completely and 200 µl lysis buffer (1% triton in PBS) was added to each well. This was followed by 5 min incubation on ice and scrapping off the cells using a cell-scrapper. Cell lysates were transferred into a reaction tube on ice and homogenized manually and then centrifuged for 30 min at 4° C at 14000 rpm. The su pernatant obtained was stored and the pellet was discarded. And then the protein was estimated using a Bradford method described in section 2.2.5.2.

2.2.3.3 PROTEIN ESTIMATION (BRADFORD METHOD)

In order to load equal amounts of proteins on gel, protein lysates were estimated by Bradford method. Seven protein standards were used for the standard curve 0, 2, 4, 6, 8, 10, 12µg/µl. From each standard 50µl was added to a 96 well plate in triplicates. Similarly 1µl of unknown lysate plus 49 µl of water was added in triplicates to this similar plate. Now to this 150 µl Bradford solution (1:5 Bradford in water) was added and the protein estimation was done using protmr program in the Elisa reader.

2.2.3.4 WESTERN BLOT (WB)

2.2.3.4.1 SDS-POLYACRYLAMIDE-GEL ELECTROPHORESIS (SDS PAGE)

This method is used to separate proteins based on their size. Therefore SDS, which has a negative charge, binds to all the proteins and converts the charge of each individual protein to a negative charge. The separation of proteins then depends only on their molecular weights. Composition of the separating and the stacking gel is given in the tables below. 50µg of protein was used for loading on the gel after adding 5X Laemmli buffer to a final concentration of 1X and boiling at 95° or 37° for 7 minutes. As a standard, 6µl marker was

used for loading. Electrophoresis was started with 80 V, and after 30 minutes was increased to 120 V.

2.2.3.4.2 ELECTRO BLOTTING

Unless otherwise stated in results section, after the SDS-PAGE proteins were transferred on a nitrocellulose membrane in case of semidry blotting for which iblot apparatus was used following the user manual.

In case of wet blotting polyvinylidenfluorid (PVDF) membrane was used. Therefore PVDF membrane was activated for 1 min in 100% methanol and equilibrated in transfer buffer together with the gel, 6 Whatman papers and the sponges. The blotting apparatus was assembled in the following sequence:

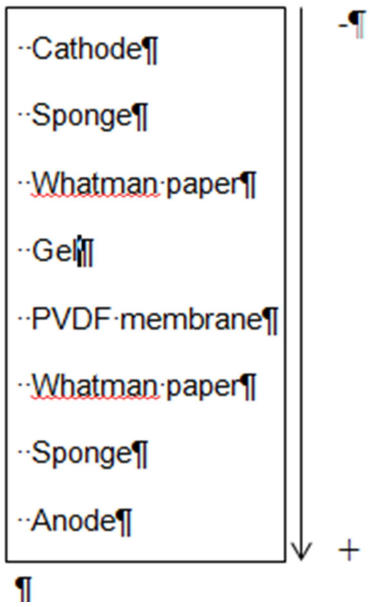

Transfer was performed in a 4° room for overnight at 15 volts. Then the membrane was incubated in a blocking solution for 1 hour at room temperature on the shaker. After that the membrane was incubated with the primary antibody for overnight at 4°. Next day membrane was washed for 3 X 6 min with the TBS-T and then incubated in secondary antibody for 1 hour followed by 3 X 6 min washing steps with TBS-T. Detection was performed with a chemiluminescent hyperfilms (Amersham).

2.2.3.4.3 COMPOSITION OF POLYACRYLAMIDE GELS

Stacking gel	4%
Acrylamide	0.33 ml
ddH2O	1.15 ml
0.5M Tris (pH=)	0.5 ml
10% (w/v) SDS	0.02 ml
TEMED	0.002 ml
10% (w/v) APS	0.02 ml

Table 2.10 Stacking gel

Separating gel	7.5%	10%	12%
Acrylamide	2.5 ml	1.7 ml	2 ml
ddH2O	4.85 ml	2 ml	1.7 ml
1.5M Tris (pH=)	2.5 ml	1.3 ml	1.3 ml
10% SDS	0.10 ml	0.05 ml	0.05 ml
TEMED	0.003 ml	0.002 ml	0.002 ml
10% APS	0.05 ml	0.05 ml	0.05 ml

Table 2.11 Separating gel

2.2.3.5 CASPASE-3 FLUOROGENIC ASSAY

Caspase-3 activity was assessed in the different regions of brain using a fluorescence-based assay. For this Ac-DEVD-AMC was used as a substrate for cleaved caspase 3. Different brain regions of mice (cortex, basal ganglia and cerebellum) were isolated and homogenized using lysis buffer (1ml for cortex region, 500µl for cerebellum and basal ganglia). The homogenized samples were left on ice for 20 minutes and then centrifuged at 200g at 4℃ for 5 minutes to remove tissue and cell debris. The assay was prepared in triplicate. 30 µl of lysate was transferred to a black 96-well plate and made up to 80µl with assay buffer.

Reaction was initiated by adding Ac-DEVD-AMC to a final concentration of 400 µM in a total reaction volume of 100µl. Fluorescence was measured (excitation 360 nm and emission 450 nm) every 5 min for 3 h at 37℃. Data was normalize d for protein content, which was measured by Bradford method and expressed as Δ fluorescence units/min/µg total protein.

2.2.4 BEHAVIORAL EXPERIMENTS

The three mouse lines were characterized using different behavioral methods for motor and coordination effects and anxiety effects. 12 females from each mouse line were used for behavioral studies.

2.2.4.1 ROTAROD

Figure 2.4 Rotarod apparatus

Rotarod is a motor impairment test for the rodents. It consists of wheels rotating with an increasing acceleration from 4 to 40 rpm for seven minutes. The length of time that a given mice stays on this rotating wheel is a measure of their balance, coordination and motor impairment (Jones and Roberts, 1968). The mouse which rides on the wheel for a shorter time is assessed as motorically impaired.

Mice were trained in one day by three trials, each separated by 30 minutes minimum.

1 Training day:

First trial: 3 minutes at 8 rpm

Second trial: 3 minutes at 16 rpm

Third trial: 3 minutes at 20 rpm)

Mice falling before 30 seconds are brought on the rotarod again (3 times maximum)

4 Testing days:

First trial: 7 minutes acceleration 4 to 40 rpm

Second trial: 7 minutes acceleration 4 to 40 rpm

Third trial: 7 minutes acceleration 4 to 40 rpm

The test was done in the dark phase and was repeated every 8 weeks starting from 6 months until the age of 14 months. The weight of the mice was taken at every time point, before the test in order to monitor the health of the mice and to assess if the phenotype observed is not the result of weight gain.

2.2.4.2 CHALLENGING BEAM TRAVERSAL (MOTOR PERFORMANCE AND COORDINATION TEST)

Figure 2.5 Challenging beam walk apparatus

Motor performance was measured with a novel beam test adapted from the traditional beam-walking test (Carter et al., 2001; Fleming et al., 2004). The beam was constructed from Plexiglas (Plastics Zone, Woodland Hills, CA) and consisted of four sections (25 cm each, 1 m total length), each section having a different width. The beam started at a width of 3.5 cm and gradually narrowed to 0.5 to 1 cm increments. Underhanging ledges (1 cm width) were placed 1.0 cm below the upper surface of the beam. Animals were trained to traverse the length of the beam starting at the widest section and ending at the narrowest, most difficult section. The narrow end of the beam led directly into the animal's home cage.

Animals were given two days of training before testing, and all training was performed without the mesh grid. On the first day, animals were given two assisted trials, which involved placing the animal on the beam and positioning the home cage in close proximity to the animal. This encouraged forward movement of mice along the beam. After two assisted trials, animals were able to traverse the entire length of the beam unassisted. Day one of training ended after all animals completed one unassisted run across the entire length of the beam. On the second day of training, animals were required to run two trials.

To make the test more difficult for mice, on the day of the test, a mesh grid (1 cm squares) of corresponding width was placed over the beam surface leaving a 1 cm space between the grid and the beam surface. The underhanging ledges provided a support or “crutch” for the animal to use when a limb slipped on the grid (Hua et al., 2002) and permits assessment of a deficit chronically so that the mice do not need to use compensatory motor strategies to complete the task (Hua et al., 2002) Animals were then videotaped while traversing the grid-surfaced beam for a total of three trials.

Videotapes were viewed and rated in slow motion for errors in steps made by each animal, and time to traverse across 3 trials. An error was counted when, during a forward movement, a limb (forelimb or hindlimb) slipped through the grid and was visible between the grid and the beam surface. An individual animal could make a maximum of four slips per step. Slips or time of movement was not counted if the animal was not making a forward movement or when the animal’s head was oriented to the left or right of the beam. Errors per trial and time to traverse the whole beam were calculated for Non TG and TG HtrA2 mice across all three trials and averaged.

2.2.4.3 OPENFIELD

The Openfield (OF) test was developed by Calvin S. Hall to test emotionality of rodents (Hall CS et al. 1932). It is a commonly used qualitative and quantitative measure of general locomotor activity and exploratory behavior in rodents (Stanford, 2007). It is also used to assess anxiety by including additional measures of time taken to reach the center (latency) of the field, defecation and the first five minutes of activity (Prut and Belzung, 2003)

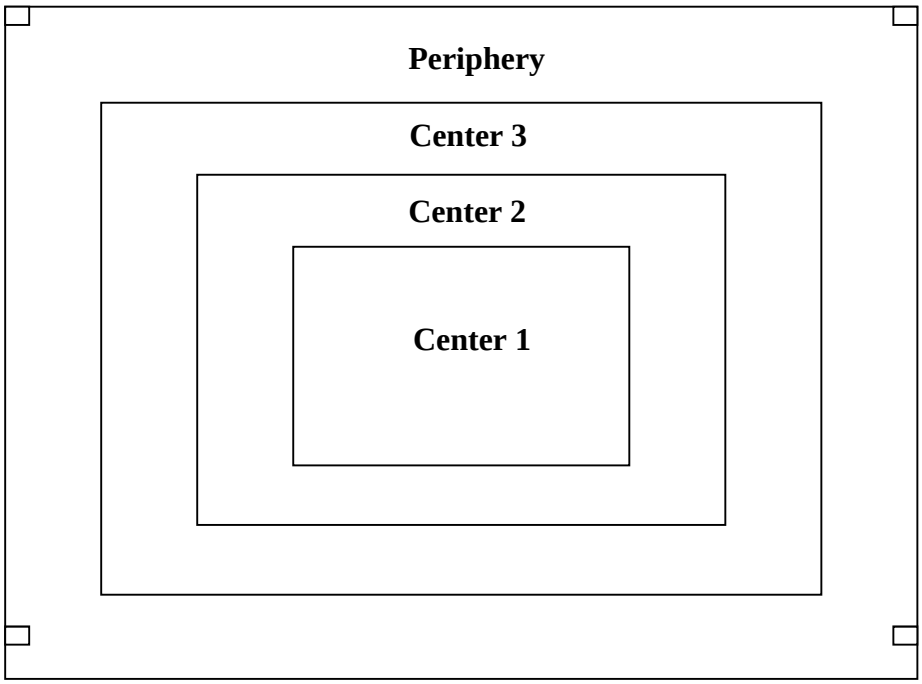

Figure 2.6 Field of OF test

OF consists of a table with surrounding walls. The field is marked in a grid and square crossings as shown in the figure. The mouse is deposited at one corner of the table and left alone in the room and the movement of the mice is traced for 10 minutes by the camera attached to the computer which consists of OF software. The results obtained by OF software were converted into the excel sheets and then these results are used to assess different parameters for example - total time of movement of mice, time taken by each mice to come to the center from periphery and the speed of mice.

2.2.5 HISTOLOGY

2.2.5.1 IMMUNOCYTOCHEMISTRY

For Immunocytochemical staining of cells, culture medium was removed completely and cells were washed once with pre-warmed PBS. Cells were fixed in 100 % ice-cold methanol for 10 min followed by three times washing with PBS and permeabilization for 10 min in 0.2% Triton-X-100/PBS.

After three times washing with PBS, cells were blocked for 30 min in 5% BSA (v/v) and primary antibodies applied for 2 hours at RT. Afterwards, cells were washed three times with PBS and were incubated in secondary antibody solutions for 1 hour. Cells were washed three times again in PBS and stained for nuclei with Hoechst for 5 min at RT. Finally, cells were washed once in PBS and then the coverslips containing cells were mounted on the slides using a mounting medium.

2.2.5.2 PREPARATION OF TISSUE SAMPLES FOR HISTOLOGY

2.2.5.2.1 PERFUSION OF MICE:

Since the blood vessels present in the brain could interfere with the staining procedures, animal was perfused and fixed before the brain was used for stainings.

The following equipment and chemicals were prepared in advance before starting the perfusion procedure:

Equipment	**Chemicals**
Peristaltic pump	1X PBS
1 large needle	**For EM analysis**: 2.5% (w/v) Glutaraldehyde in 4 %
4 small needles	(w/v) paraformaldehyde solution.
Scissors	For fluorescence stainings: 4 % (w/v)
Scalpel	paraformaldehyde solution

Forceps Isofluorene

Container for mouse

Butterfly needle

The heavily anesthetized animal was placed on its back on a rack or paraffin block over a sink. To ensure the mouse is properly sedated after lethal anesthesia, the toes were punched to judge its level of response to painful stimulus. Once the mouse was sedated, the abdomen was made wet with Ethanol. The mouse was placed on a corked surface with abdomen facing up. Using the small needles, the four paws were secured to the surface spreading them as wide as possible. Then the skin was grabbed with forceps at the level of the diaphragm, and was cut to expose the liver. The skin was cut laterally and then up, cutting through the ribs. Flap was lifted and the cutting was continued until the heart was easily accessible. The chest flap was secured to a corked surface with larger needle. The butterfly needle was injected into the left ventricle, and the pump was turned on with a flow no higher than 0.8 ml/min of PBS. Then immediately the right atrium was cut. Pumping was continued in buffer until the liver became a light coffee color and the skin turns white instead of red. At this point, pumping was started by using a fixative for 15 mins. The tail flexibility was tested as an indication for the animal being fixed. The pump was turned off and again switched on to pump buffer. Pump was allowed to flow until air bubbles were expelled out and that only buffer is in the line. After this the pump was turned off.

Now the brain was isolated from the perfused mice and kept overnight in 4% (w/v) PFA solution followed by 2-3 days incubation in 30% (w/v) sucrose solution. And then was kept at frozen conditions.

2.2.5.2.2 CRYOSECTIONING:

The freezed brains were kept at minus 80 for least 48 hours before preparing cryosections. The brain was cut half and then from this half brain, sequential sagittal sections of 6 µm thickness were prepared using a cryostat. Three consecutive sections were mounted onto

the SuperFrost Plus slides (Fisher Scientific) and were freezed after drying at room temperature for 2 hours.

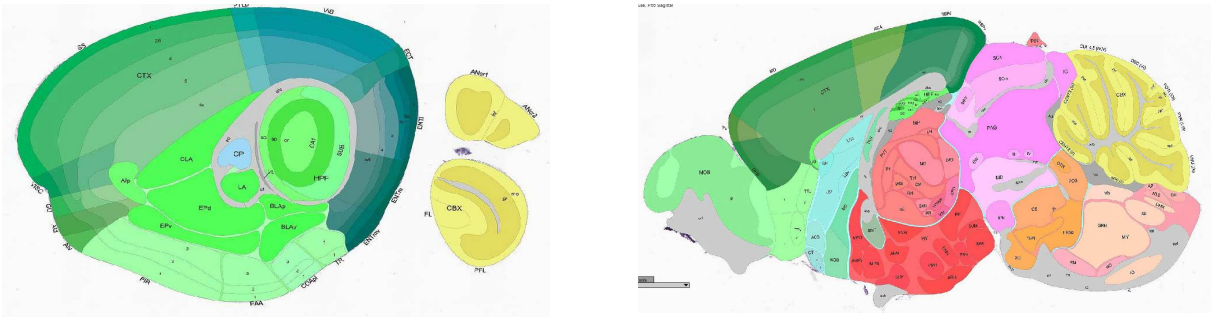

Figure 2.7 Examples of sagittal sections from Allen mouse brain atlas

2.2.5.3 IMMUNOHISTOCHEMICAL METHODS

Unless otherwise stated, immunohistochemistry on cryosections was performed using the following procedure:

The cryosections were kept at 37° C for 30 min. and then washed with water and PBS for 10 min. respectively. For detection of proteinase K (PK) resistant alpha-synuclein, an extra-step including digestion of sections for 30 min (10mM tris/HCL pH 7.8, 100 mM NaCl, 0.1% Nonidet p-40, 20µg/ml PK, 37℃) was incorporated. T he sections were then washed with PBS for 3 times 10 min each. The sections were then covered with the blocking solution (5 % BSA) and incubated for 1 hour at RT. Then the sections were incubated overnight in the primary antibody solution in blocking solution. Next day the slides were washed 3 times with PBS each 10 min and then incubated in 1:1000 secondary antibody solutions for 1-2 hours at RT followed by 3 washings with PBS each 10 min. In order to stain nuclei Hoechst 33342 was used in 1:5000 dilutions in PBS and the sections were incubated in this solution for 10 min. followed by washing in PBS for 10 min. The sections were mounted using Vectashield mounting medium for fluorescence and kept at 4° C t ill the pictures were taken with the fluorescence microscope.

The TUNNEL staining and silver staining was performed according to user manual provided with the TUNNEL KIT and FD NeuroSilver™ Kit II respectively.

2.2.6 DATA ANALYSES AND STATISTICS

All the behavioral was analyzed using GraphPad Prism 5. For statistical analyses a one-way analysis of variance (ANOVA) was performed. Statistical significance was determined by a following "Tukey's Multiple Comparison Test" with *, ** and *** indicating p≤0.05, 0.01 and 0.001, respectively. In bar charts, calculated with Excel, error bars show standard deviation.
All Immunohistochemical pictures were taken using axion software. For colocalisation studies ImageJ software was used. Counting in TUNEL staining was done manually. Statistics were done using Microsoft excel and statistical significance was determined by paired t test with *, ** and *** indicating p≤0.05, 0.01 and 0.001, respectively
All densitometry analysis of WB was done using ImageJ software (Burbulla et al., 2010).

3 RESULTS

3.1 MICE EXPERIMENTS

3.1.1 BIOCHEMICAL & IMMUNOHISTOCHEMICAL CHARACTERIZATION OF HUMAN HTRA2 TRANSGENIC MOUSE LINES

The G399S mutation in HtrA2 has been found in some PD patients (Strauss et al., 2005) but its role in this disease is unknown. To determine the relevance of the G399S mutation in PD we engineered mice overexpressing either human wild type HtrA2 (referred to as TG HtrA2 WT line for this thesis) or human G399S mutant HtrA2 (referred to as TG HtrA2 G399S line for this thesis). C57BL/6 mice from the same genetic background were used as non-transgenic controls (referred to as Non-TG line for this thesis).

The mice were firstly characterized in terms of expression of the transgenic HtrA2 through several biochemical and immunohistochemical methods. In this section, the expression of the transgenic WT HtrA2 and G399S HtrA2 in the transgenic lines at mRNA, and protein level are presented.

3.1.1.1 GENOTYPING

Homozygous mice were generated by crossing two heterozygous mice from each line. qRT PCR was carried out to identify homozygous mice from the mixed population which were then further used for breeding with Non-TG mice to obtain large numbers of transgenic heterozygous mice to be used for the planned behavioral (12 mice from each line), biochemical (20 mice from each line) and immunohistochemical characterization experiments (20 mice from each line).

qRT-PCR was performed, as described in the materials and methods section (chapter 2). In each PCR, a negative control (DNA from a non-transgenic animal) and a positive control (DNA from a heterozygous animal) were included. The ΔCt values of the heterozygous positive controls ranged from 0.8 to 1 in the case of the TG HtrA2 WT line and from 2.5 to 3 for the TG HtrA2 G399S line. The ΔCt values of the unknown samples were compared to the values of heterozygous controls of the corresponding lines. The ΔCt values of homozygous mice were double that of the heterozygous controls i.e. 2 and 6 for TG HtrA2 WT and TG HtrA2 G399S line respectively.

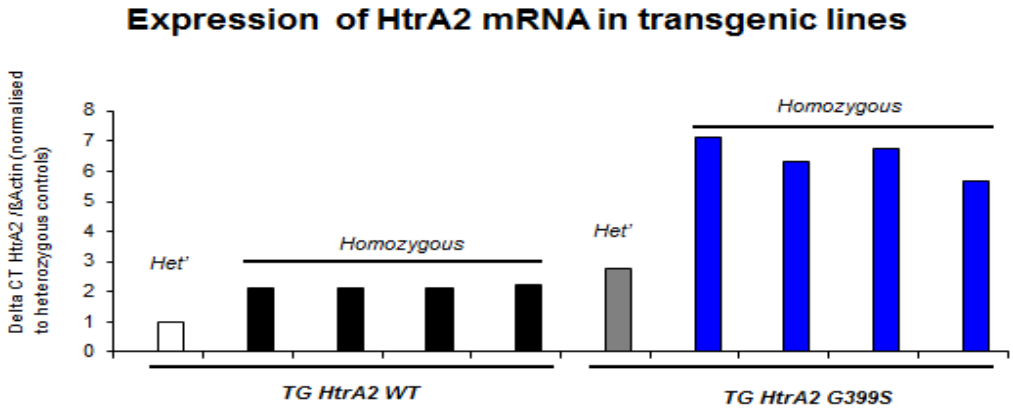

Figure 3.1qRT PCR identification of homozygous mice from the mixed population of transgenic mice. DNA was isolated from the ear skin biopsies and used as template for qRT PCR. The reference for homozygous mice was DNA from heterozygous mice for the house-keeping gene (mouse ß-actin) and for the gene of interest (hHtrA2). Ct values of the samples were compared with a standard curve made from the different concentrations of DNA ranging from 0 to 20ng from 5 combined samples of heterozygous mice to calculate ΔCt. The ΔCt value of the mean average heterozygous positive controls was set to 1. 5-6 homozygous mice were recognized for each line from approximately 60 mice in total. Here are shown in the graph the group of homozygous mice found in each line along with the heterozygous controls.

Identified homozygous mice were then bred with Non-TG mice to generate heterozygous mice. The heterozygous mice were subsequently identified using conventional PCR followed by agarose gel electrophoresis. Owing to the high homology (95%) of the mouse and human cDNA sequence, only primer pairs mapping to the C-terminal end and FLAG-tag were unique to transgenic animals. As a result the 576 bp DNA product could be seen on the agarose gel only in the case of transgenic mice. No band could be seen in the case of Non-TG mice. Heterozygous animals were identified by the presence of a 576bp band on the agarose gel.

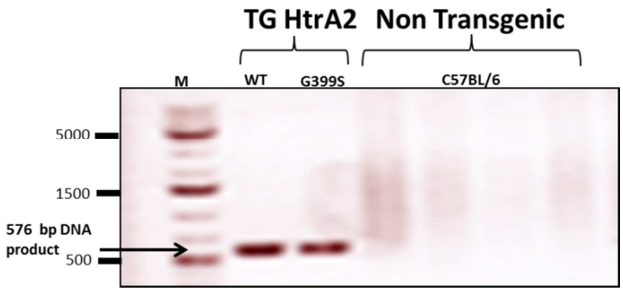

Figure 3.2Conventional PCR identification of transgenic mice. Integration of the insert (576bp) detected in the isolated DNA by conventional PCR using forward primer in the upstream region of the insertion and a reverse primer in the HtrA2-FLAG cDNA sequence downstream of the insertion. DNA was isolated from the ear skin biopsies. The arrow indicates the 576bp DNA PCR product on 1% agarose gel (M= DNA marker).

3.1.1.2 EXPRESSION OF THE HUMAN HTRA2 TRANSGENE IN DIFFERENT BRAIN REGIONS OF TG HTRA2 WT AND TG HTRA2 G399S MICE

Lysates were prepared from five different brain regions of non-transgenic and both transgenic mouse lines. Lysates were prepared from tissue of cortex (CTX), basal ganglia (BG), cerebellum (CBM), brain stem (BS) and olfactory bulb (OB). Several Western blots from different mice, for each line were probed with a rabbit HtrA2 antibody which recognizes both the endogenous and the transgenic HtrA2. Fig. 3.3 below shows examples of HtrA2 protein expression in Non-TG and transgenic mice. Since the expressed transgenic human HtrA2 was tagged with FLAG, it resolves very slightly higher (the FLAG sequence consists of 8 amino acids and has a predicted weight of ˜1 kDa.

The same blots were probed for ß-actin or GAPDH as a loading control. The Human HtrA2 WT and G399S constructs were overexpressed in the mice under the Proline-rich-protein (Prp) promoter. As expected, the transgenic HtrA2 was overexpressed in different brain regions in both the mouse lines as seen in figure 3.3A, with most pronounced expression levels in the cerebellum for the HtrA2 WT overexpressing mice. The expression looked similar in cortex, basal ganglia and olfactory bulb region of two transgenic mouse lines in the figure 3.3 (A). In the cerebellum the expression was more pronounced in TG HtrA2 WT mice, compared to TG HtrA2 G399S mice (Fig 3.3A-B). But at the same time we see that the loading control is not equal in figure 3.3A. In order to quantify and compare expression levels

in two transgenic mouse lines densitometry was performed on the three individual mice from each line for cortex, basal ganglia and cerebellum which confirmed that the HtrA2 overexpression is greater in TG HtrA2 WT mice compared to TG HtrA2 G399S mice in cerebellum, basal ganglia and cortex. In the cerebellum, the expression of total HtrA2 in TG HtrA2 WT mice is almost three times more than TG HtrA2 G399S mice and five times more than Non-TG mice, while in the cortex and basal ganglia the expression of total HtrA2 in TG HtrA2 WT mice is ˜ 30% more than Non-TG and around ˜ 10 % more than TG HtrA2 G399S mice, though the expression of HtrA2 in the basal ganglia of TG HtrA2 G399S mice varied. Overall both WT HtrA2 and the G399S mutant HtrA2 were overexpressed compared to NT controls but the overexpression of WT HtrA2 was greater than that of the G399S mutant HtrA2.

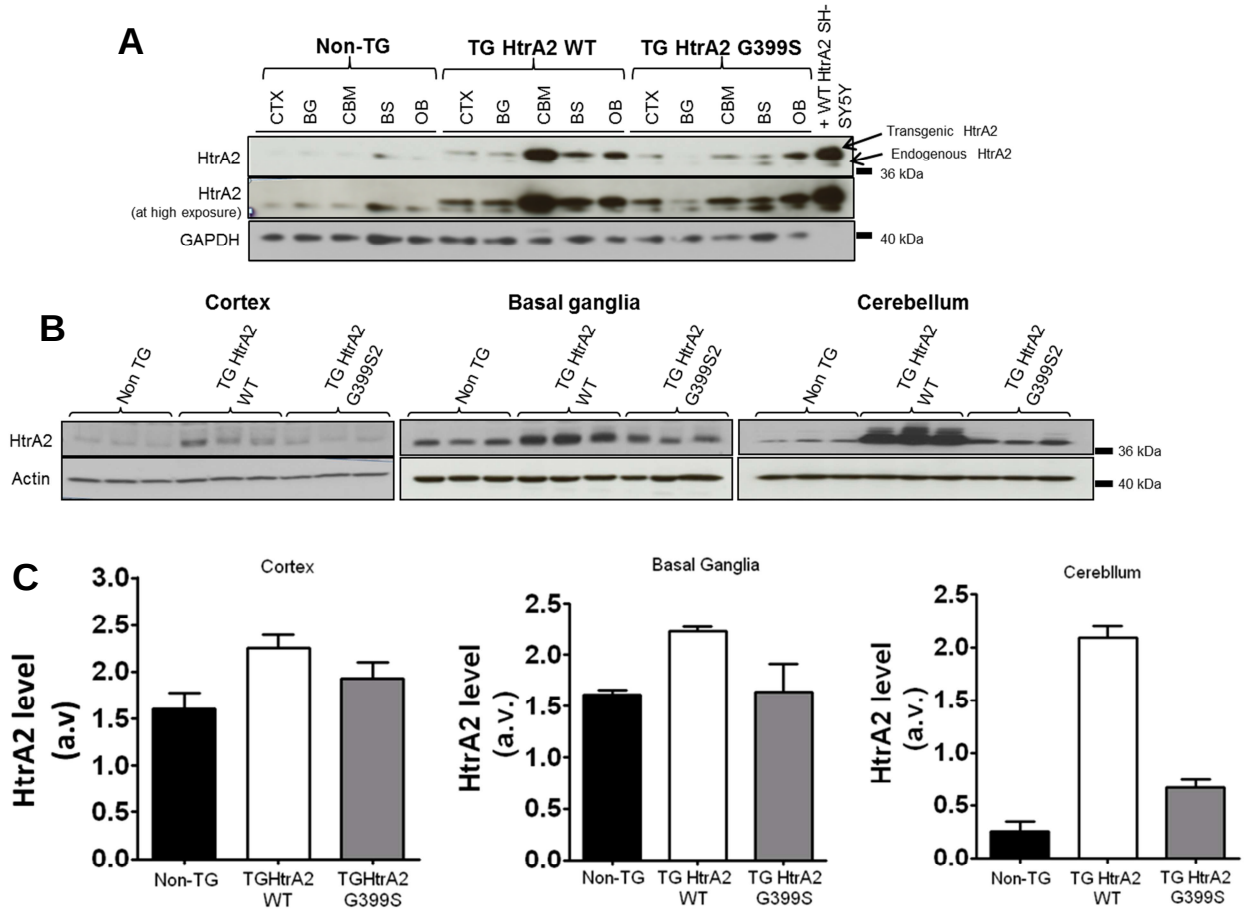

Figure 3.3 Identification of brain region specific HtrA2 overexpression in TG HtrA2 WT and TG HtrA2 G399S mice: (A) Western blot analysis with HtrA2 antibody showing HtrA2 overexpression in different brain regions of two transgenic mouse lines **(B)** Western blot analysis in cortex, basal ganglia and cortex regions with HtrA2

antibody in triplicate mice from transgenic and non-transgenic mouse lines. HtrA2 antibody detects both the endogenous and transgenic HtrA2. 50µg of protein was loaded from lysates of each region. Arrows indicate both endogenous HtrA2 and transgenic HtrA2 respectively; CTX= Cortex, BG=Basal ganglia, CBM= Cerebellum, BS= Brain stem, OB= Olfactory bulb. **(C)** Densitometry analysis from individual triplicate mice from each mouse line for three different regions – cortex, basal ganglia and cerebellum. a.v. = Absolute value.

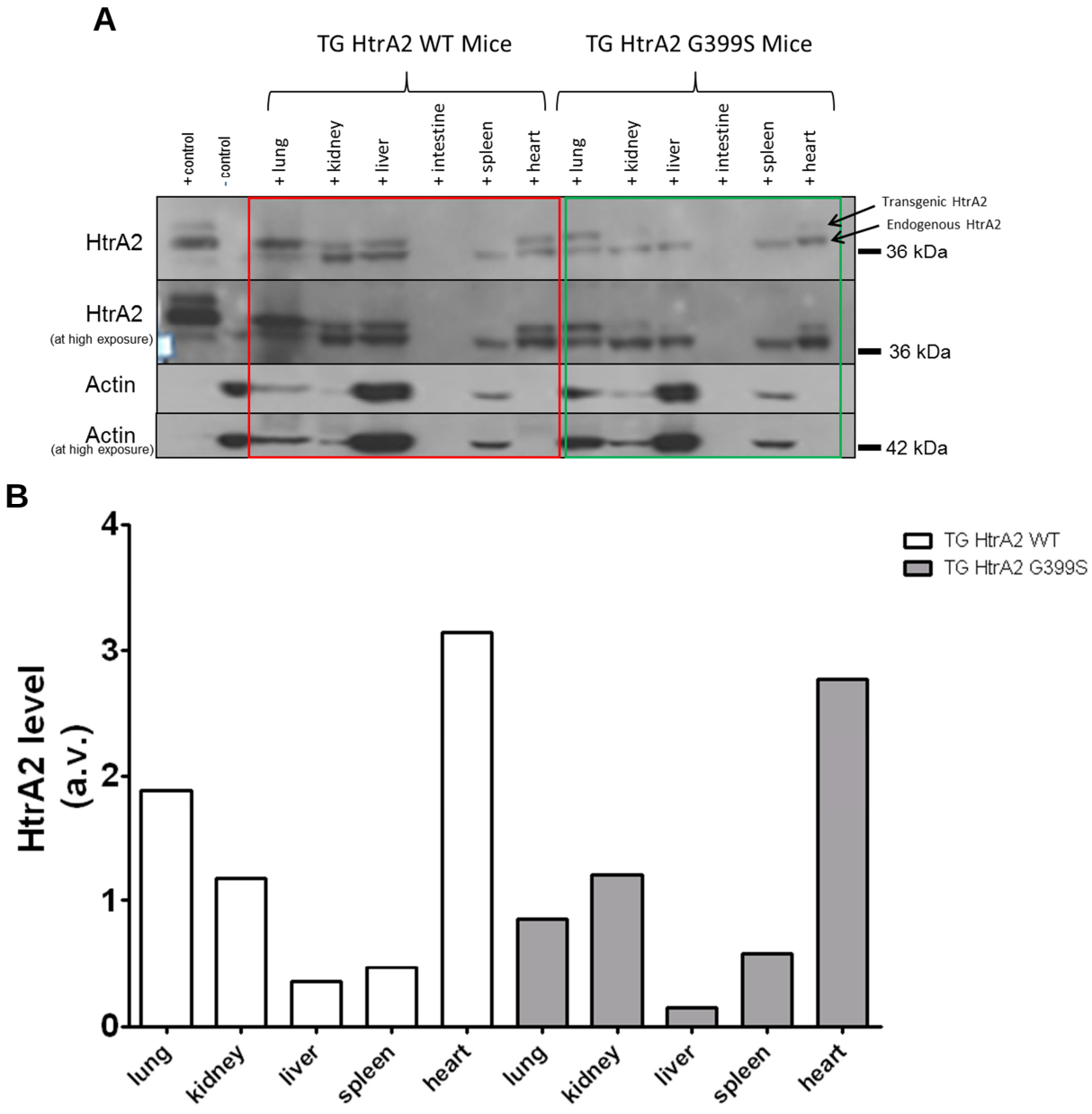

Figure 3.4 Identification of organ specific human (h) HtrA2 overexpression in TG HtrA2 WT and TG HtrA2 G399S mice: (A) Western blot analysis with HtrA2 antibody showing HtrA2 overexpression in different organs of two transgenic mouse lines. HtrA2 antibody detects both the endogenous mouse and transgenic human HtrA2. ß-actin antibody was used as a loading control. 50µg of protein was loaded from lysates of each region. Arrows indicate both endogenous HtrA2 and transgenic HtrA2 respectively; + Control = SH-SY5Y cells overexpressing HtrA2 WT; - Control= Non-TG cortex. **(B)** Quantification of total HtrA2 overexpression in different organs of TG HtrA2 WT and TG HtrA2 G399S mice from the blot shown in Fig.3.4A. The total HtrA2 band intensity was calculated in relation to ß-actin level. a.v. = absolute value.

Figure 3.4A shows the expression of transgenic HtrA2 in different organs from both transgenic mouse lines. The transgenic HtrA2 is overexpressed in lung, kidney, liver and heart but not in spleen. The figure 3.4B shows the densitometry analysis of total HtrA2 protein normalized to ß-actin. The total HtrA2 levels in kidney, spleen and heart of two transgenic mouse lines was almost similar though it was half in lung and liver of TG HtrA2 G399S mice compared to TG HtrA2 WT mice. HtrA2 could not be detected in intestine but at the same time ß-actin band is also absent, so no conclusions can be drawn on expression levels in this region.

3.1.1.3 IMMUNOHISTOCHEMICAL INVESTIGATION OF HUMAN HTRA2 IN THE BRAIN OF TG HTRA2 WT AND TG HTRA2 G399S MICE

To complement the Western blot analysis of HtrA2 protein levels in the brains of our transgenic lines, immunohistochemical stainings on 6 µm cryosections were performed. The sections were co-stained with an anti-FLAG antibody to detect the transgenic HtrA2 and an anti-HtrA2 antibody to detect the total endogenous and transgenic HtrA2. Fluorescent images were acquired using a Zeiss Axio Imager Z1 microscope. As seen in the figures (Fig. 3.5 A-C) the green signal represents FLAG-HtrA2 (transgenic HtrA2), the red signal depicts total HtrA2 (both endogenous and transgenic HtrA2) while the blue staining represents the nucleus stained with DAPI. The merged red and green signal in yellow illustrates the colocalisation of endogenous and transgenic HtrA2. Images were acquired from three different brain regions – cerebellum (A), cortex (B) and basal ganglia (C). All regions showed expression of transgenic human WT and G399S HtrA2 respectively.

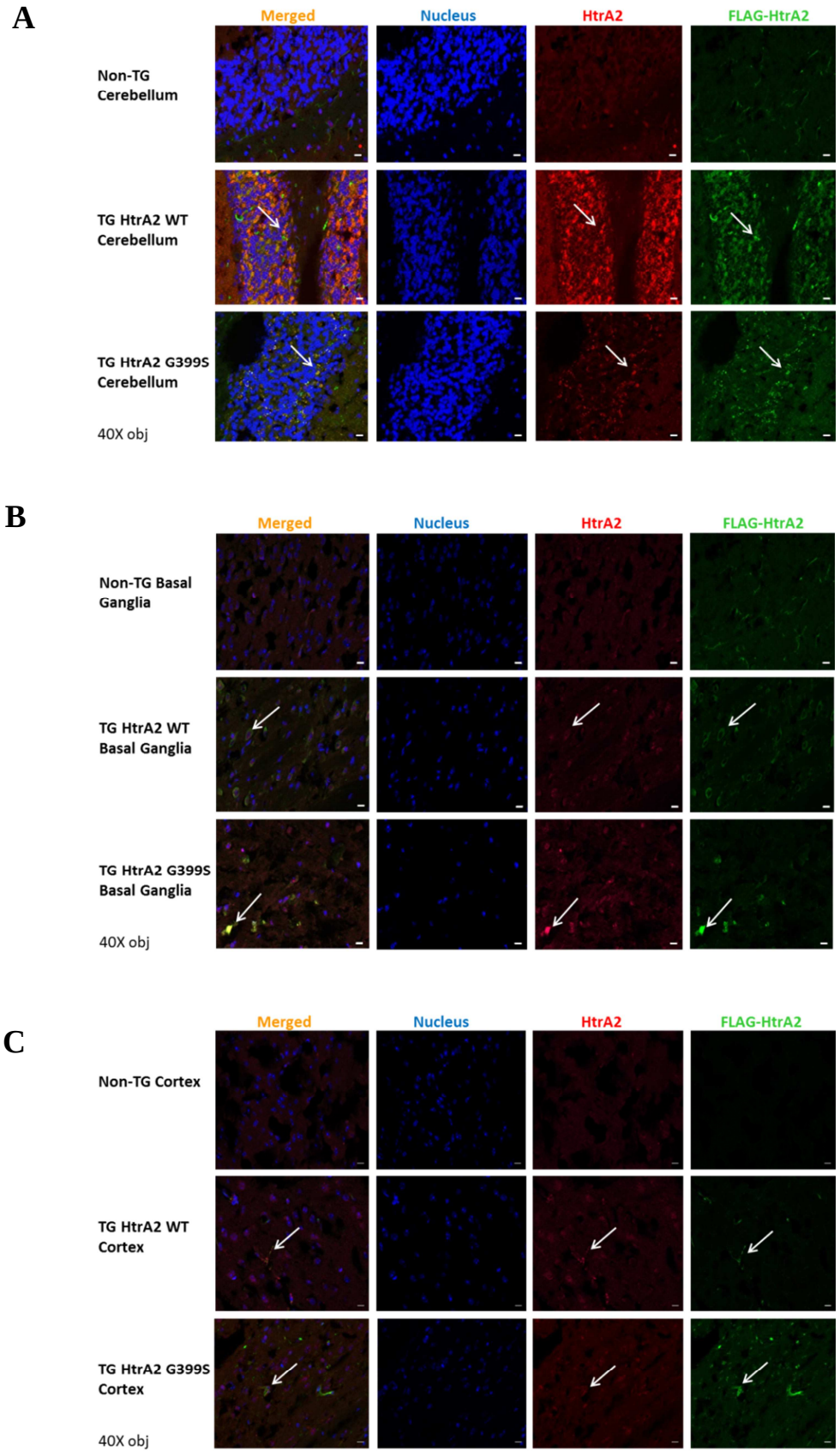
A
Merged
Nucleus
HtrA2
FLAG-HtrA2
Non-TG Cerebellum
TG HtrA2 WT Cerebellum
TG HtrA2 G399S Cerebellum
40X obj
B
Merged
Nucleus
HtrA2
FLAG-HtrA2
Non-TG Basal Ganglia
TG HtrA2 WT Basal Ganglia
TG HtrA2 G399S Basal Ganglia
40X obj
C
Merged
Nucleus
HtrA2
FLAG-HtrA2
Non-TG Cortex
TG HtrA2 WT Cortex
TG HtrA2 G399S Cortex
40X obj

Figure 3.5 Immunohistochemical analysis of HtrA2 expression by HtrA2 or FLAG staining in different brain regions. Degree of HtrA2 and FLAG colocalisation and FLAG signal alone represents the level of overexpression. **(A)** In the **cerebellum** region high degree of FLAG and HtrA2 colocalisation and high level of FLAG signal was observed in TG HtrA2 mice compared to TG HtrA2 G399S mice. **(B)** In the **basal ganglia** region similar degree of FLAG and HtrA2 colocalisation and similar level of FLAG signal was found in both the transgenic mouse lines **(C)** In **cortex** region similar degree of FLAG and HtrA2 colocalisation and similar level of FLAG signal was found in both the transgenic mouse lines. Except of few unspecific dots and green background in FLAG staining there is ninety percent colocalisation of FLAG signal with HtrA2 staining in each region. Stainings were performed in the 12 months old female mice in 6 µm sagittal cryosections. Sections were incubated in HtrA2 and FLAG antibody solution at 1:500 dilutions in 2% BSA solution overnight, after 1 hour of incubation in 8% BSA solution. Blue staining represents nuclei, red staining represents both endogenous and transgenic HtrA2 and the green staining represents FLAG or transgenic HtrA2. Arrows indicate the colocalisation of HtrA2 and FLAG staining. Scale bar =10µm.

The expression of transgenic HtrA2 seemed similar in the cortex and basal ganglia region of both the transgenic mouse lines from the immunohistochemical analyses. This is evident from the green (FLAG) and red (endogenous and transgenic HtrA2) co-localization signal (Fig. 3.5 A-B). The FLAG signal alone provides an evidence for overexpression of HtrA2 in both the transgenic mouse lines. Corresponding to the WB analyses the expression appeared higher in cerebellum region of TG HtrA2 WT mouse line compared to TG HtrA2 G399S as is visible from the representative images (Fig.3.5 A) of transgenic and non-transgenic mouse lines.

In order to confirm the reliability of the antibodies to detect recombinant human HtrA2 in immunohistochemistry the colocalisation of total HtrA2 with the ectopic human FLAG-tagged HtrA2 was revisited in SH-SH5Y cells transiently transfected with FLAG-tagged HtrA2. As seen in figure 3.5D red signal (total HtrA2) colocalises with the green signal (FLAG-HtrA2).

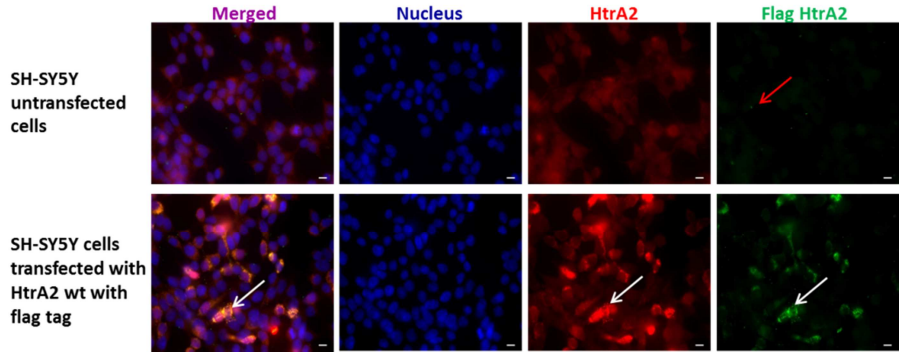

Figure 3.5D Cytochemical staining using HtrA2 and FLAG antibody. HtrA2 /FLAG co-staining was performed on fixed SH SH-5Y cells. SH-SH5Y cells were transfected with FLAG-HtrA2, using the Effectene (Qiagen) transfection reagent according to the manufacturer's instructions and left 48h before fixation with formaldehyde. These cells along with the control cells (without transfection) were co-stained with total HtrA2 and FLAG antibodies. Blue signal represents nuclei, where cells were stained with DAPI. Red signal represents both the endogenous and transgenic HtrA2 and the green signal represents the transgenic FLAG-HtrA2. White arrows indicate examples of colocalisation of HtrA2 and FLAG-HtrA2 staining. Scale bar =10µm.

The next step was to check specifically the expression of the transgene in neurons of the HtrA2 transgenic mice. For this, cryosections of brains from the Non-TG, TG HtrA2 WT and TG HtrA2 G399S were co-stained with FLAG antibody (transgenic HtrA2) and NeuN (neurons). Images were acquired from the cortex, basal ganglia and cerebellum region. As seen in the figures 3.6 A-D, red FLAG signal colocalises with green neuronal signal, illustrating that transgenic HtrA2 is expressed in neurons in these three brain regions. But since the FLAG-GFAP co-staining was not reliable for technical reasons. The expression in glial cells cannot be confirmed.

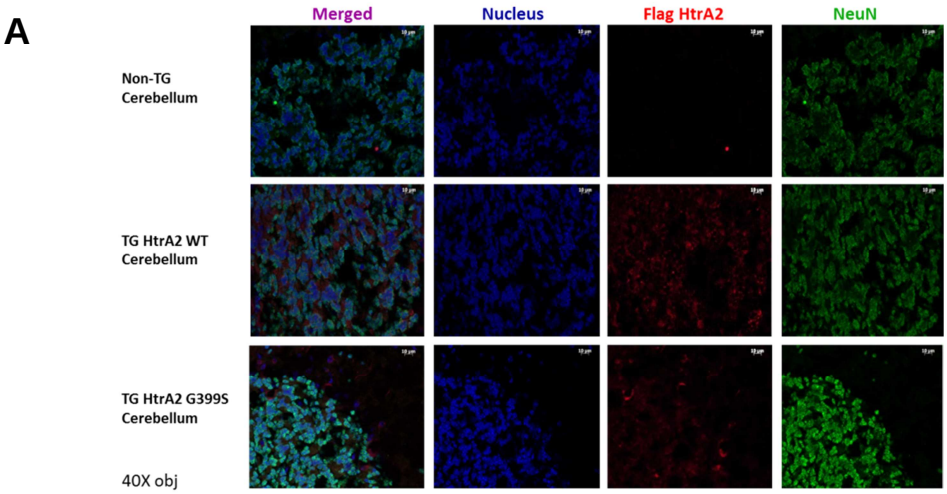

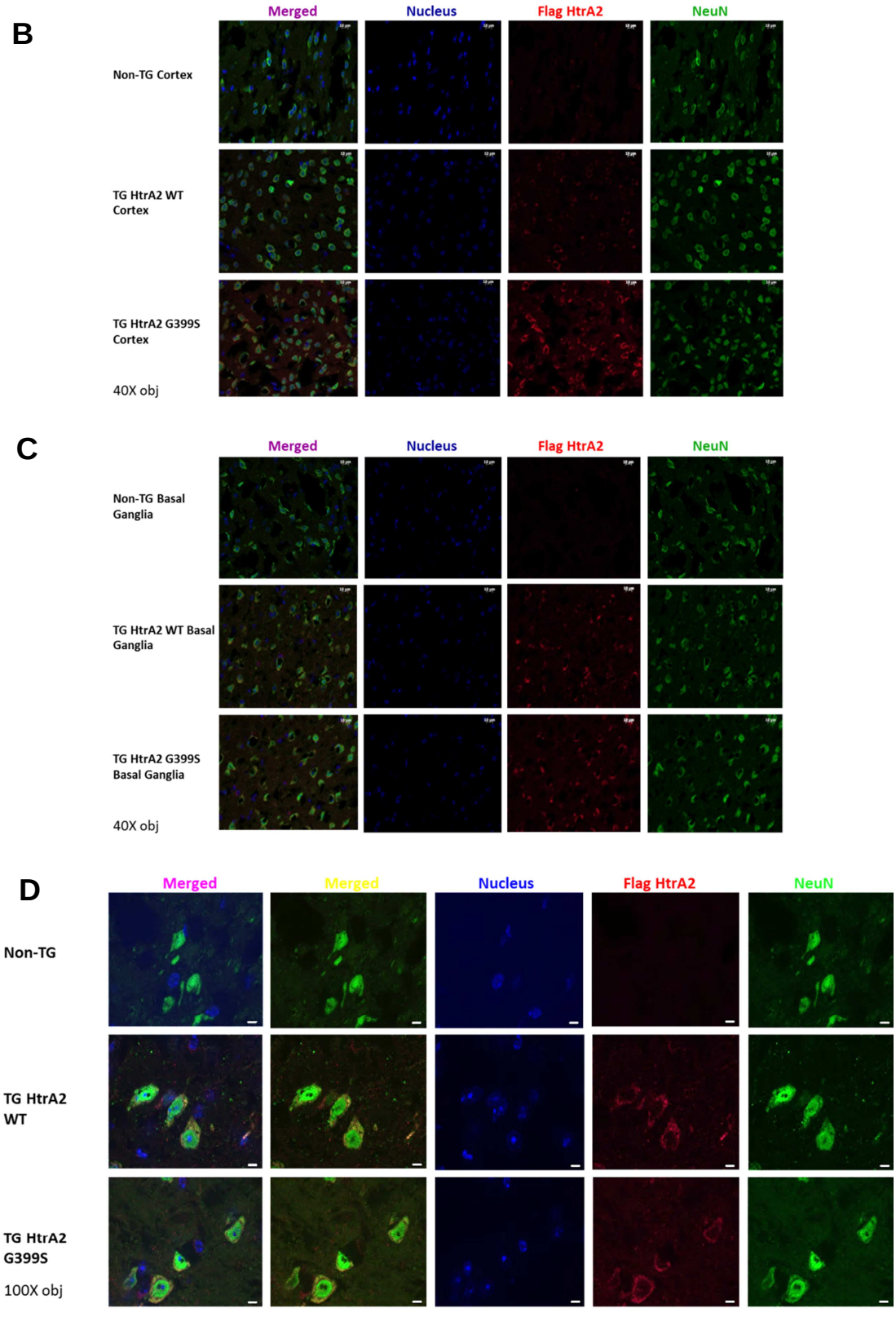

Figure 3.6 Immunohistochemical staining using FLAG and NeuN antibodies in (A) cerebellum **(B)** Cortex **(C)** Basal ganglia region**. (D)** Representative image at higher magnification**.** Stainings were performed in the 12 months old female mice in 6 µm cryosections three times. Here is shown the representative image of each section. Blue staining represents nuclei, red staining represents transgenic hHtrA2 and green staining

represents neuron specific staining. Merged picture represents colocalisation of NeuN and transgenic HtrA2. Scale bar=10µm.

3.1.2 BEHAVIORAL CHARACTERISATION OF HTRA2 TRANSGENIC MOUSE LINES

The aim of this set of experiments was to investigate the potential effects of overexpression of human WT HtrA2 and human G399S HtrA2 on the behavior of transgenic mice compared to non-transgenic littermates. To assess the role of overexpressed human WT HtrA2 and G399S mutant HtrA2 in mice, various behavioral studies were conducted on each mouse line, Non-TG, TG HtrA2 WT and TG HtrA2 G399S, respectively, at different ages. For each study 12 female mice from each line was used. The following behavioural studies were chosen:

- Rotarod
- Challenging Beam Walk
- Openfield Test

Animal experiments were performed according to the following schedule:

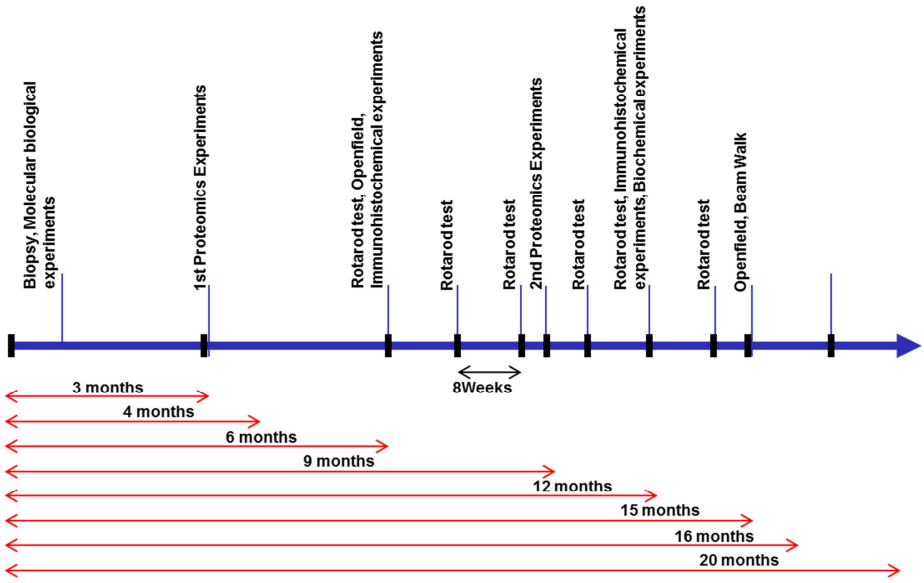

Figure 3.7 Schedule for behavioral experiments in mice

3.1.2.1 ROTAROD

The rotarod test is an efficient and well recognized test to investigate both learning and motor defects in rodents (Jones and Roberts, 1968). Rotarod was performed on the three mouse lines every 8 weeks from the age of 6 months until the age of 14 months. Within each experiment the mice ability on the rotarod was tested for 4 days continuously (three trials each day).

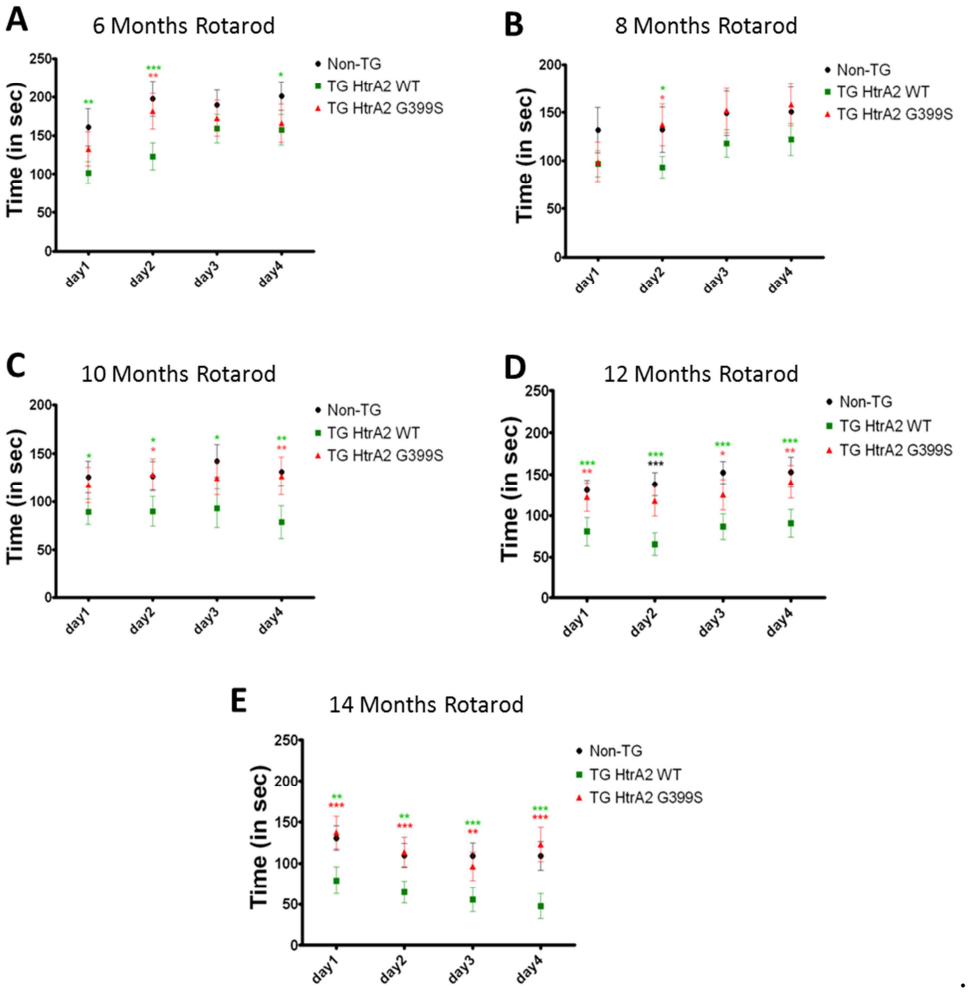

Figure 3.8 Behavioral Characterisation of TG HtrA2 lines on Rotarod (over a four day assessment period). (A) Rotarod 6 months **(B)** Rotarod 8 months **(C)** Rotarod 10 months **(D)** Rotarod 12 months **(E)** Rotarod 14 months**.** Overexpression of HtrA2 WT in mice leads to motor impairments. (A-F) At each time point the rotarod test was performed 4 days continuously and each day 3 trials per mice were done. Here the mean values of 3 trials for each day at 6, 8, 10, 12 and 14 months are indicated for each line. TG HtrA2 WT line showed continuous motor deficits and a weak learning impairment over the 4 days at each time point of experiment. Data is presented as the mean +/- SD, n=12 where n denotes the number of mice from each mouse line; *p<0.05, **p<0.01 and ***p< 0.001, two-way ANOVA, Statistical significance was determined by a following "Tukey's Multiple

Comparison Test". Significance level was achieved comparing Non TG and TG HtrA2 WT (green * stars) and TG HtrA2 WT and TG HtrA2 G399S (red * stars). There was no significant difference between Non-TG and TG HtrA2 G399S.

According to the protocol the mice were kept on the accelerating rotating wheel (4-40 rpm) and the riding time for each mouse was noted at each trial. Figure 3.8 shows the rotarod data over the training period of four days at each age tested.

It is expected that the riding time of each mice would increase over the four days of rotarod test and the difference in the riding time over these four days for each set of mouse lines could define the learning. As seen in figure 3.8 A the Non-TG line and TG HtrA2 G399S mice showed a learning trend over the 4 days of experiment, while TG HtrA2 WT mice were not able to ride on the rotarod as the acceleration increased and over the four days they showed only a weak learning trend i.e. there was not much difference in the riding time of this mouse line between first day and the last day of rotarod. The latency to fall from the rotarod was less for TG HtrA2 mice compared to Non-TG and TG HtrA2 G399S mice. A similar trend for latency and learning was observed over the four days at the age of 8 months, while after 8 months, Non-TG and TG HtrA2 G399S mice showed a weak learning trend while TG HtrA2 WT line were devoid of any learning trend as there was no difference in the riding time between each day of the four days rotarod schedule (Fig 3.8 B-D). At the age of 14 months Non-TG and TG HtrA2 G399S showed no learning while TG HtrA2 WT showed a weak trend of depletion in learning ability as each day the riding time of this set of mice became less over the four days on the rotarod (Fig 3.8 E).

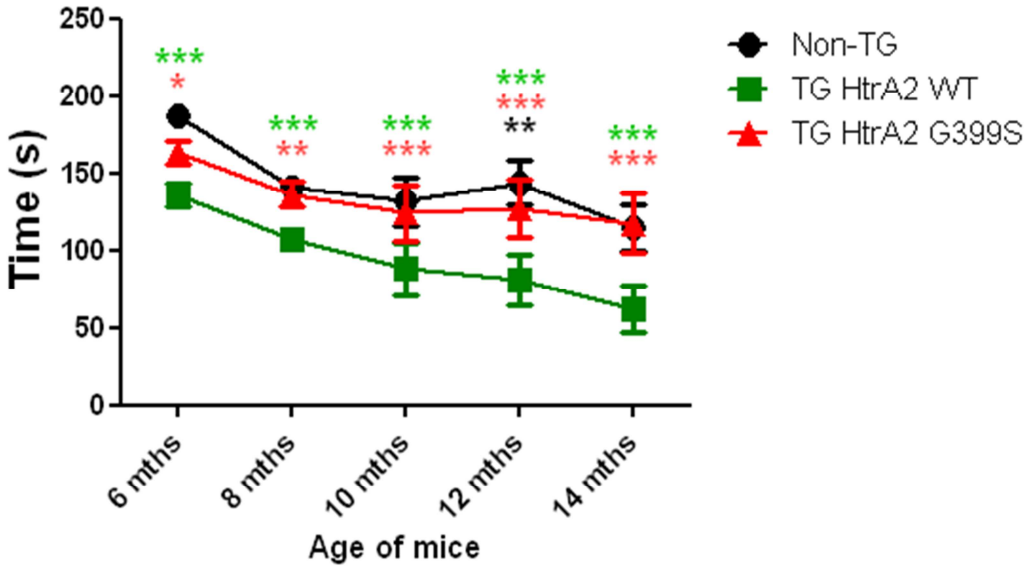

Figure 3.9 Rotarod over-all. Rotarod was followed every 8 weeks, each time 4 days, 3 trials a day with each mouse. Here the mean of all the trials at each time point is represented. TG HtrA2 WT line showed continuous motor impairments over the different time points. Data is presented as the mean +/- SD, n=12 where n denotes the number of mice from each lines; *p<0.05, **p<0.01 and ***p< 0.001, Statistical significance was determined by a two-way ANOVA following "Tukey's Multiple Comparison Test". Significant differences were observed between Non TG and TG HtrA2 WT (green * stars) and TG HtrA2 WT and TG HtrA2 G399S (red * stars).

Figure 3.9 shows that over a 14 month period, NT mice are able to stay on the rotarod for less time and can be considered due to normal ageing. The TG HtrA2 G399S mice behaved in a similar way to the non-TG mice. However, TG HtrA2 WT mice performed worse on the rotarod test after 6 month and continued to exhibit a decline with age in their ability to stay on the rotarod. This data suggests that there are motor defects in mice which overexpress human WT HtrA2 independent of initial learning deficits.

In order to check that the rotarod results observed are not the effect of constitutional differences, the mice were weighed at every experimental time point.

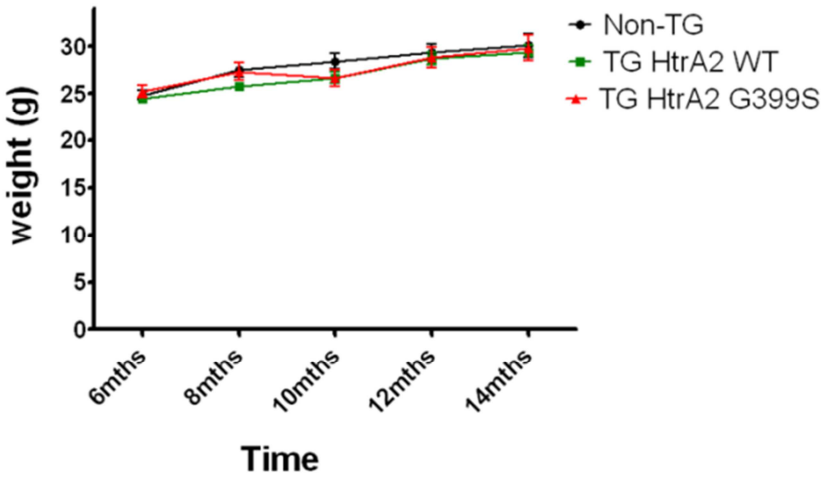

Figure 3.10 Weight over-all. Mice were weighed at each time point of the experiment. There was no difference in the average weights of different mouse lines over time.

Figure 3.10 show that there were no significant differences in the average weight of animals between the different mouse lines over time. These data add support to the rotarod results and confirm a behavioral phenotype is not an artifact of changes in weight.

3.1.2.2 CHALLENGING BEAM WALK

The challenging beam walk is a motor balance and coordination test which was performed with the behavioral set of 12 mice from each group (Non-TG, TG HtrA2 WT and TG HtrA2 G399S) at the age of 15 months. Mice were made to walk along a wire mesh beam consisting of 4 sections (25 cm each, 1 m total length) of different width (3.5 cm to 0.5 cm by 1 cm increments) and leading to the animal's home-cage. The number of times the mouse´s limbs slipped through the wire walkway and the time taken to get to the end point was noted. Mean average values of three trials, for each mouse are expressed.

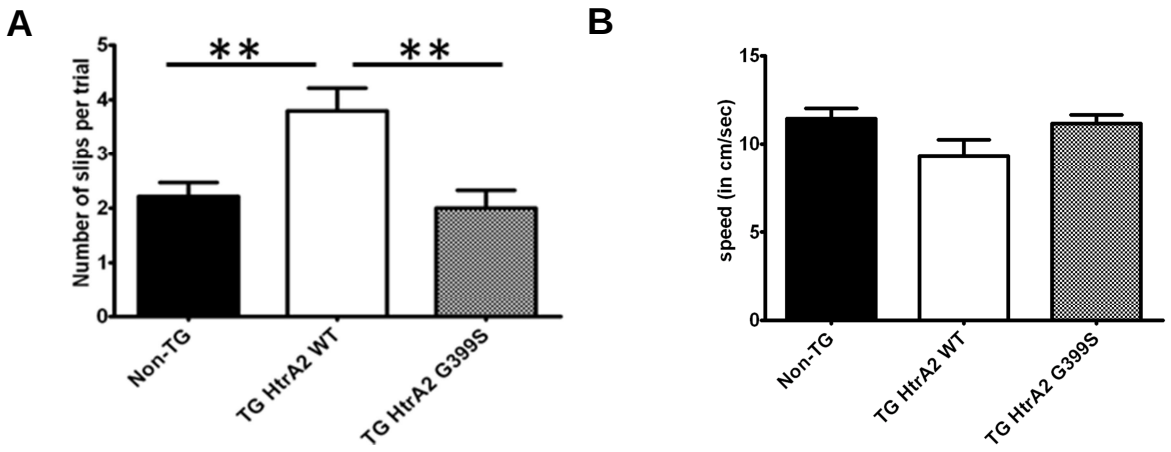

Figure 3.11 Behavioral Characterisation of TG HtrA2 lines by challenging beam walk test for motor balance and coordination. Mice were made to walk on a 1 meter long mesh beam and the number of slips through the plexiglas beam and the time taken to traverse the plexiglas beam were noted for each mouse. Three trials were made by each mouse at the age of 15 months**. (A)** Number of slips made by each mouse at each trial by TG HtrA2 WT mice was increased, compared to Non-TG and TG HtrA2 G399S mice. **(B)** From the distance traversed by mice and time taken, the average speed was calculated per trial. No significant difference was found between the speed of two transgenic mouse lines. Data are presented as the mean +SD n=12 where n is the number of mice used for each mouse line; *p<0.05, **p<0.01 and ***p< 0.001, one-way ANOVA, Statistical significance was determined by a following the "Tukey's Multiple Comparison Test".

The results show that the TG HtrA2 WT mice made significantly more (˜40%) slips compared to Non-TG and TG HtrA2 G399S mice (Fig. 3.11A). The TG HtrA2 WT mice were slightly slower to traverse the wire walkway compared to Non-TG controls but the difference was not statistically significant. This implies that the TG HtrA2 WT mouse line was impaired in motor balance and coordination but not the Non-TG and TG HtrA2 G399S mouse line compared to NT controls.

3.1.2.3 OPENFIELD (OF)

The OF Test was performed with a set of 12 mice from each of the different lines (Non-TG, TG HtrA2 WT and TG HtrA2 G399S) at the age of 6 months to investigate the general locomotor activity and exploratory behavior of the animals. Additional measures were also included such as time taken to reach the center of the field (latency) in order to assess the anxiety level of the mice.

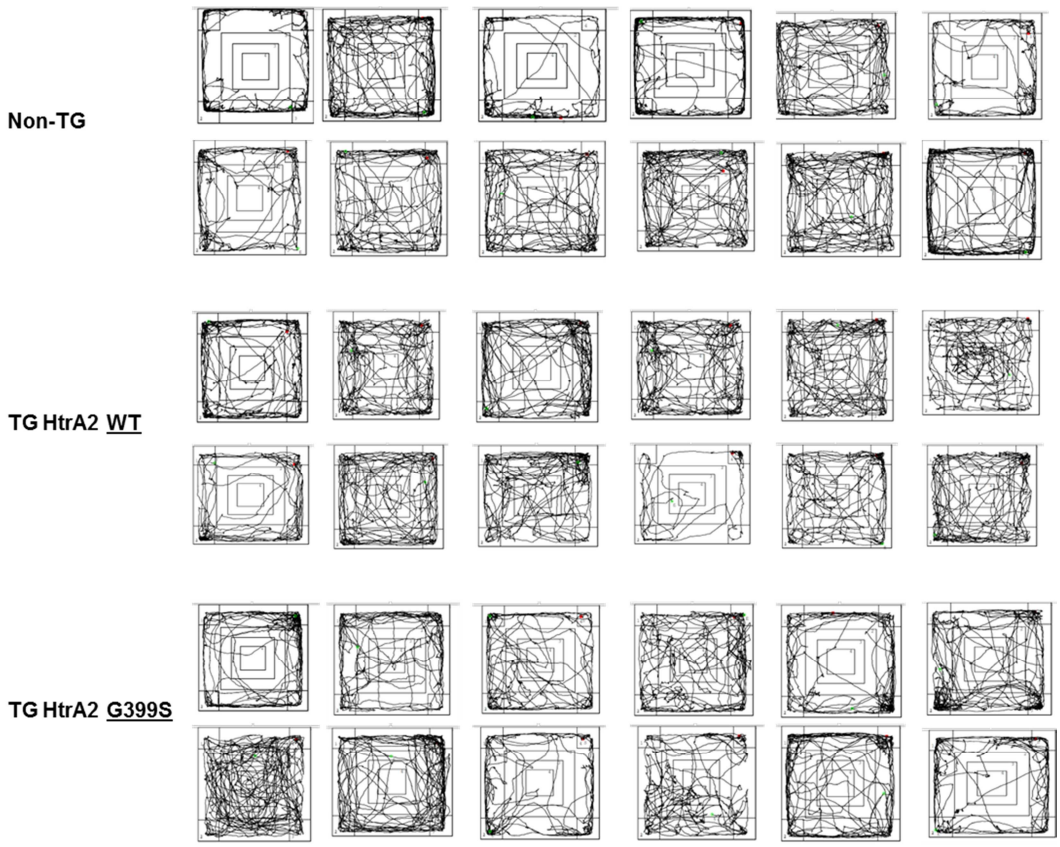

Figure 3.12 Raw data generated by the OF test. The overall movement traces of different mice from TG HtrA2 WT and TG HtrA2 G399S lines in the OF during the 10 minute test.

The data was automatically saved by the OF software connected to the camera tracing the mouse movements. The data obtained was converted to a Microsoft Excel sheet to be analyzed and from this data different parameters were analyzed. The general locomotor activity was assessed by measuring the total time of movement of each mouse in the OF. This was calculated for all the mice from each mouse line and from the average data from the three mouse lines, a graph was generated by plotting the total time of movement against different mouse lines (Fig 3.13 A).

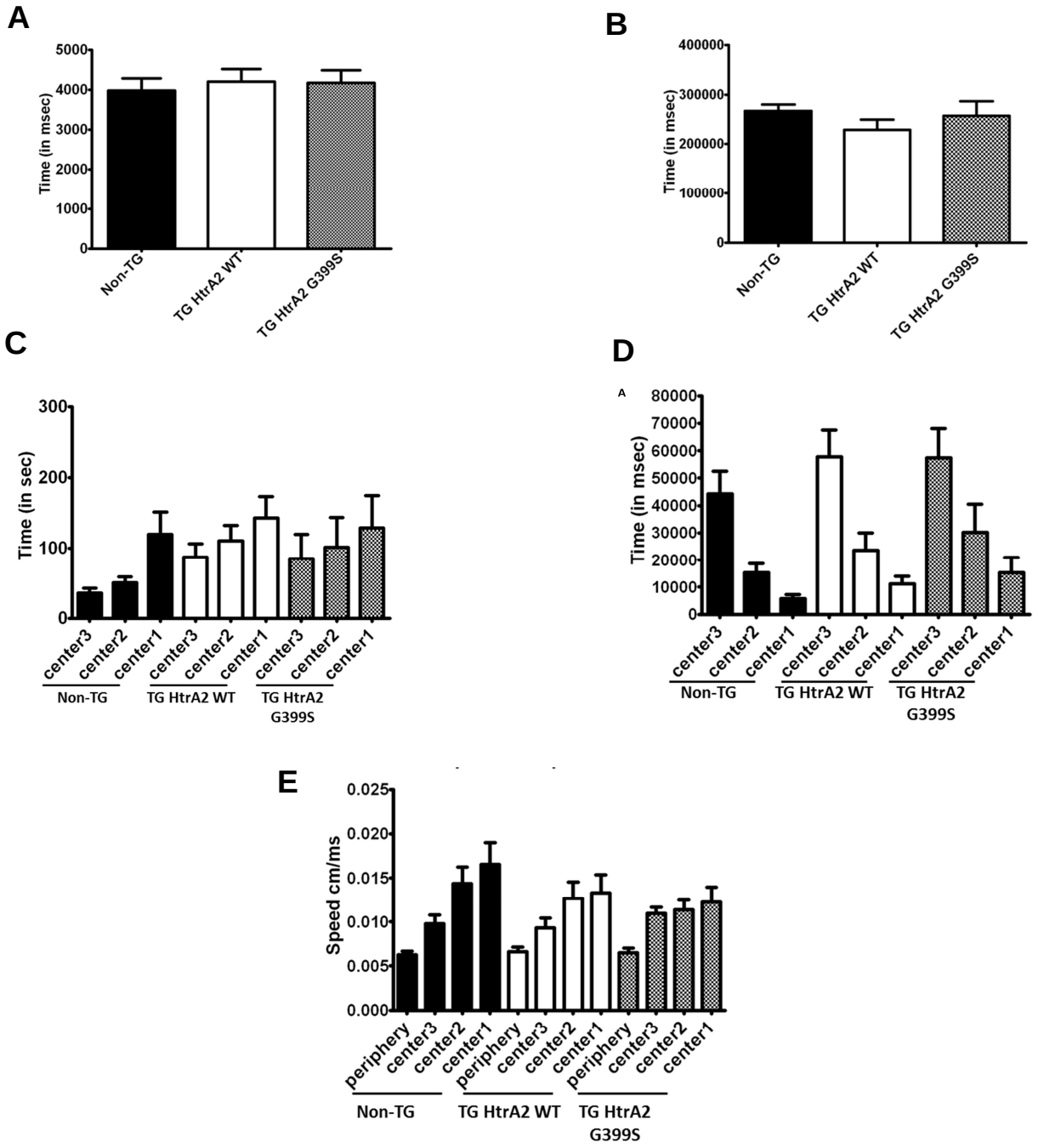

Figure 3.13 Openfield test (OF) for general locomotor activity and anxiety levels. Mice were left at the periphery of the field and different measures such as the total time of movement, the time taken to reach the center (latency), the speed at the center and the amount of time spent in the center by different mouse lines was calculated to check different parameters for example general locomotor activity and anxiety levels. Both transgenic lines took longer time to reach the different centers compared to non-transgenic controls, though the values were not significant. **(A)** Total time of movement **(B)** Time spent in corners **(C)** Latency for the center **(D)** Time spent in the center **(E)** Speed in different regions of OF.

There was no difference in the time of movement of the three different mouse lines which implied no difference in general locomotor activity of the different mouse lines. Graphs were generated for other parameters including anxiety. Anxiety can be assessed by measuring the time the mice spend in the corners (B), latency for the center (C), Time spent in the centers (D), Speed in the different regions of OF (E). From figure 3.13 B it can be seen that individual mice from the TG HtrA2 WT line spent less time at the corners compared to animals of the other two lines, although the difference was not significant. There was a tendency towards more latency (˜10% for center 1, ˜50% for center 2 and 3) for the two transgenic mouse lines compared to Non-TG mouse line. Similarly the speed of transgenic mouse lines (E) in the different centers was less (˜20 % for center 1 and ˜15 % for center 2) compared to Non-TG mouse line. From the figure 3.13 D it can be seen that the two transgenic lines spent more time in the center (˜50% for center 1, ˜40% for center 2 and 25% for center 3) compared to Non-TG mouse lines, but these data were statistically insignificant.

3.1.3 INVESTIGATION OF POTENTIAL MECHANISMS UNDERLYING THE BEHAVIORAL PHENOTYPE OF HTRA2 OVEREXPRESSING MICE

In order to define a potential mechanism underlying the behavioral phenotype of motor impairments in the TG HtrA2 WT mouse was subsequently investigated using various biochemical and immunohistochemical analyses as discussed in the following section.

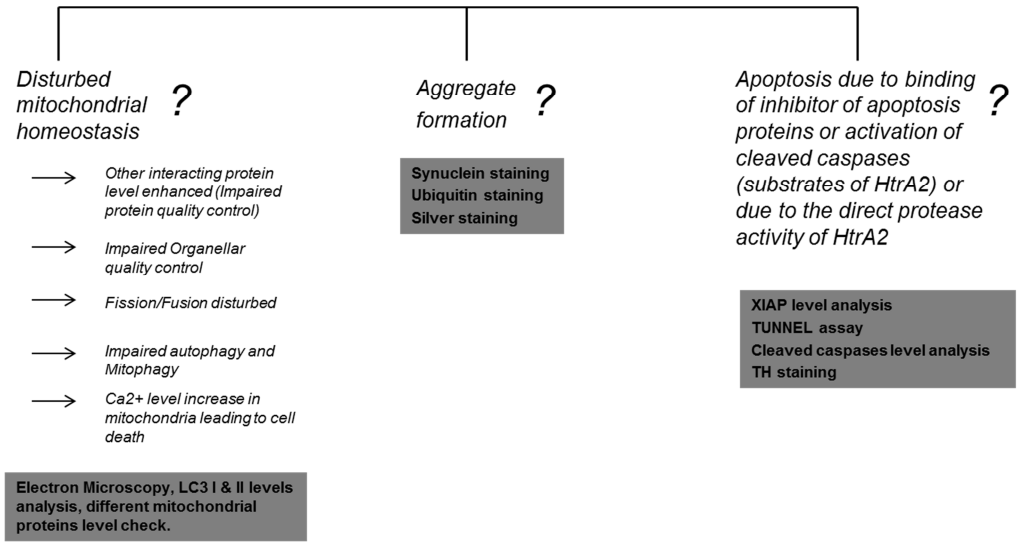

Figure 3.14 Hypotheses. (1). Disturbed mitochondrial homeostasis. Since HtrA2 is involved in mitochondrial homeostasis, one expected reason for motor phenotype in WT HtrA2 overexpressing mice could be mitochondrial dysfunction due to toxic gain of function of HtrA2 protein which can be addressed by assessing the steady-state levels of mitochondrial encoded proteins or by performing Electron microscopy. (**2). Aggregate formation** can be the second hypothesis which lead to behavioral pathology and could be assessed by alpha-synuclein staining, ubiquitin staining or silver staining. **(3). Apoptosis.** The third hypothesis for motor phenotype could be apoptotic cell death which might be investigated by various assays such as the TUNEL assay, expression levels of cleaved caspases and HtrA2 substrates like XIAP (discussed in detail later).

We speculated a motor phenotype in our TG HtrA2 WT mice as result of a toxic gain of function which might be the result of several pathologies. The first expected pathology could be mitochondrial dysfunction, since HtrA2 is a mitochondrial serine protease whose complete knock out in mice leads to PD symptoms and mitochondrial dysfunction (Martins et al., 2004) and so its overexpression might also have effect on mitochondria. Another pathology could be protein aggregation in the brain regions of mice which might lead to motor impairments, for it has already been shown in the literature that widespread accumulation of HtrA2 may occur in Lewy bodies or pathologic alpha-synuclein-containing inclusions in brains with PD, DLB, or MSA and that HtrA2 may be associated with the pathogenesis of alpha-synucleinopathies (Kawamoto et al., 2008). The protease activity of HtrA2 is important not only for mitochondrial quality control but also for promoting to apoptosis once HtrA2 is in the cytosol. Therefore, an additional hypothesis was increased cell death due to a direct increase in protease activity of the overexpressed protein (HtrA2) or binding of HtrA2 to the inhibitor of

apoptotic proteins (IAP´s) like XIAP (X-linked inhibitor of apoptotic proteins, a known substrate of HtrA2) leading to cell death.

3.1.3.1 ANALYSIS OF MITOCHONDRIAL PATHOLOGIES IN BRAINS OF HTRA2 TRANSGENIC MICE

Impairment of mitochondrial function has been long implicated in neurodegeneration in PD (Obeso et al., 2010). Alterations of the electron transport chain enzyme complex I appear to be particularly relevant to PD. In fact mitochondrial dysfunction in relation to PD first came into focus with the discovery of mitochondrial complex I deficiency in the substantia nigra of some PD patients (Schapira et al., 1989). Reduced levels of other mitochondrial proteins have also been reported in PD patients (Arthur et al., 2009). In order to investigate whether our TG HtrA2 mice have dysfunctional mitochondria, mitochondrial encoded complex IV subunit I (MTCO1), steady state levels were measured in the cerebellum, cortex and basal ganglia region of Non-TG, TG HtrA2 WT and TG HtrA2 G399S mouse lines. Anti-MTCO1 antibody is generally used as a mitochondrial marker but is also interesting because this subunit of complex IV is coded for by the mitochondrial genome.

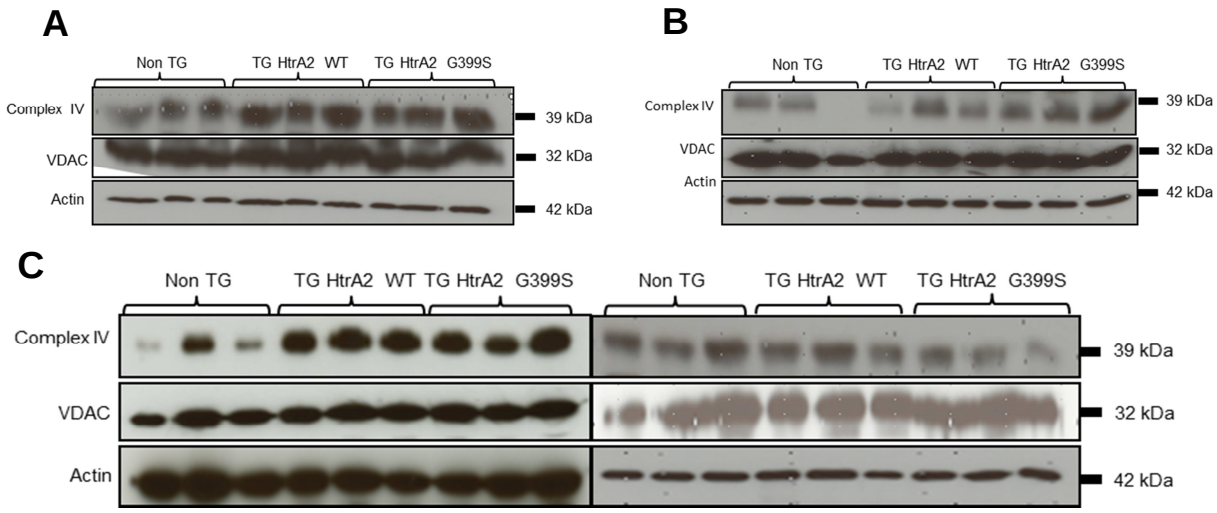

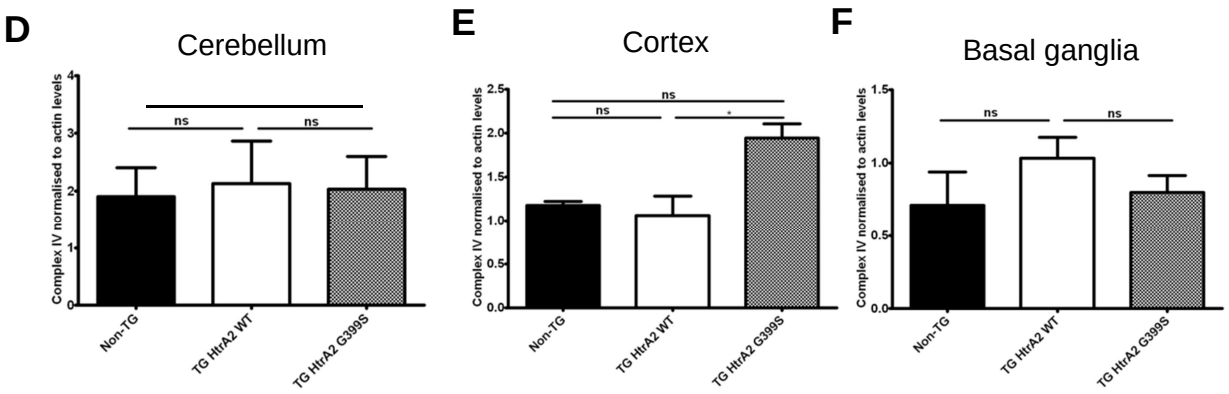

Figure 3.15 Targeted analyses of mitochondria. Complex IV subunit I protein levels in (A) Cerebellum **(B)** Cortex and **(C)** Basal ganglia of Non-TG, TG HtrA2 WT and TG HtrA2 G399S mice. **(D-F)** Densitometry analysis of complex IV subunit I level in different regions of the brain (D) Cerebellum (E) Cortex (F) Basal ganglia. No significant differences observed in the expression of Complex IV subunit I in cerebellum and basal ganglia region although significant increase in Complex IV subunit I was observed in TG HtrA2 G399S mice compared to TG HtrA2 WT mice. Data are presented as the mean +SD of three independent blots from three independent mice from each mouse line for cerebellum and cortex and from six mice for basal ganglia, *p<0.05, **p<0.01 and ***p< 0.001, one-way ANOVA, Statistical significance was determined by following "Tukey's Multiple Comparison Test".

No significant differences were observed in complex IV subunit I (MTCO1) between the different mouse lines in the cerebellum and basal ganglia. Significant upregulation of complex IV subunit I expression was observed in the cortex of TG HtrA2 G399S mice compared to TG HtrA2 WT mice though no significant difference was observed in TG HtrA2 WT mice compared to Non-TG mice. The expression levels of anti-porin (VDAC), a mitochondrial membrane protein, was assessed to correct for the mitochondrial mass in the respective regions of all three mouse lines. ß-actin was used as a loading control.

As a next step to assess mitochondria in these mouse lines, we performed electron microscopy in mouse brain to assess morphology at the organellar level in collaboration with Prof. Dr. Hartwig Wolburg at the Universitätsklinikum Tübingen, Institute for Pathology. Electron microscopy was performed in the cortex, basal ganglia and cerebellum of three different mouse lines – Non-TG, TG HtrA2 WT and TG HtrA2 G399S. The mitochondria were revealed to have a normal shape in each of the mouse lines. If the mitochondrial morphology were affected, they could be swollen, fragmented or elongated for example. But here mitochondrial shape was observed similar in each mouse line. Moreover also other

subcellular structures like nuclei, endoplasmic reticulum and vacuoles appeared normal. So in general no significant ultra-structural differences were observed in any of the investigated regions of brain from three different mouse lines as shown in the figure 3.16A-C.

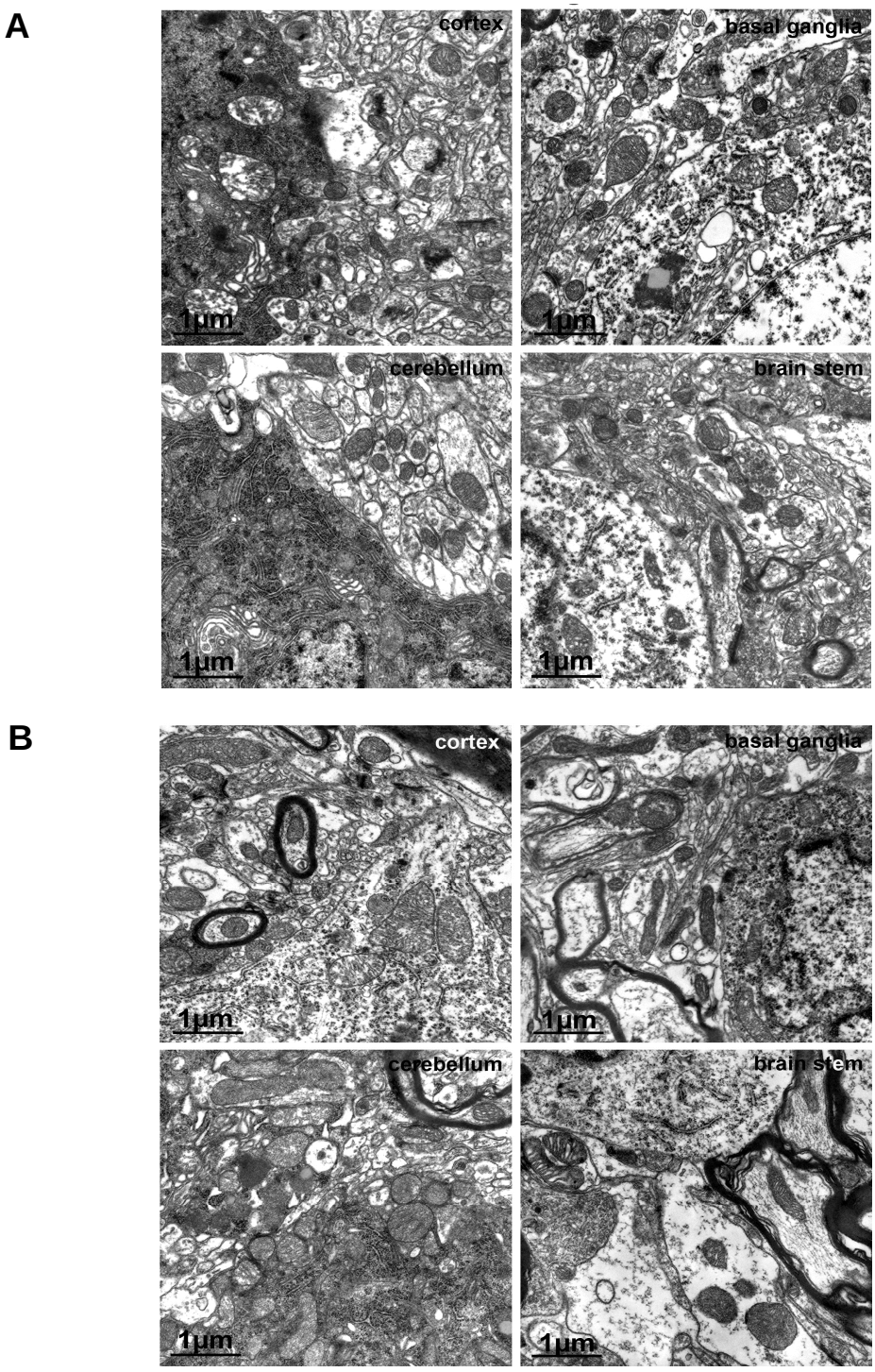

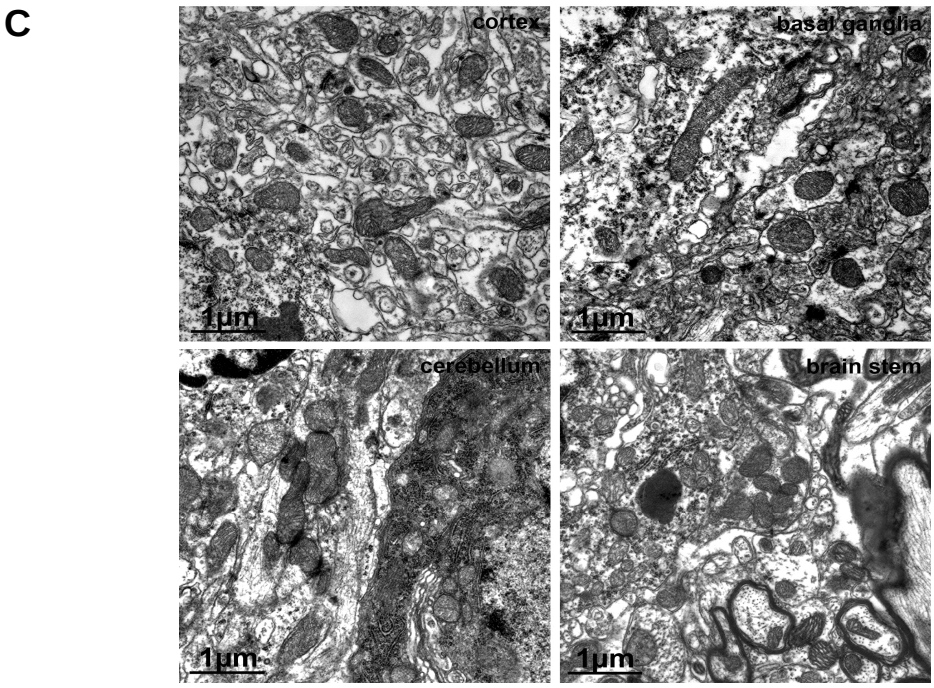

Figure 3.16 Targeted analyses of mitochondria. Electron microscopy (A) Non-TG **(B)** TG HtrA2 WT **(C)** TG HtrA2 G399S **(A-C)** Overexpression of HtrA2 WT and HtrA2 G399S in mice leads to no ultra-structural differences in Electron Microscopy. Electron microscopy was performed in the brain slices of Non-TG **(A),** TG HrA2 WT **(B)** and TG HtrA2 G399S **(C**) mice.

HtrA2 has been reported to be a positive regulator of autophagy and might be important in the quality control mechanisms involved in neurodegenerative diseases (Li et al., 2010). Microtubule-associated protein 1A/1B-light chain 3 (LC3) is well known autophagy marker. It exists in two forms and its cytosolic form LC3-I is conjugated to phosphatidylethanolamine to form LC3-II which is recruited to autophagosomal membranes. These autophagosomes fuse to lysosomes to be degraded. Thus lysosomal turnover of the LC3-II reflects the autophagy status and could be detected by immunoblotting (Tanida et al., 2008). So to check for a potential impairment of autophagy, in mice overexpressing human HtrA2, LC3-II levels were assessed by WB from lysates of the cerebellum, cortex and basal ganglia of the three mouse lines. No significant differences were observed in LC3-II levels normalized to ß-actin, between any of the three mouse lines as shown in figure 3.17.

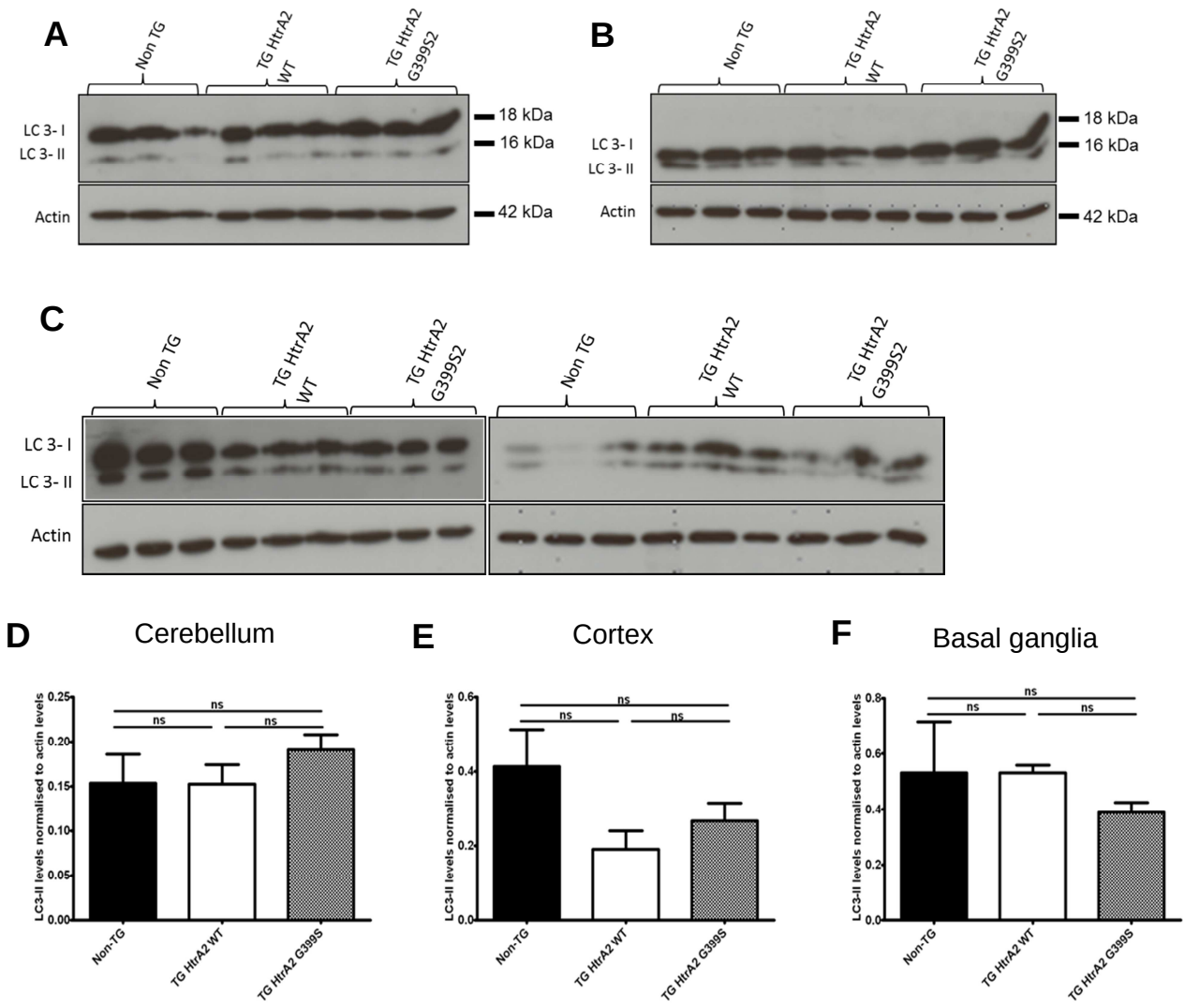

Figure 3.17 Assessment of autophagy markers in transgenic HtrA2 mouse lines by Western blot. LC3-II levels were measured in cerebellum **(A),** cortex **(B)** and basal regions **(C)** of the three different mouse lines**. (D-F)** Densitometry analysis of LC3-II level normalized to ß-actin levels in different regions of the brain **(D)** Cerebellum **(E)** Cortex **(F)** Basal ganglia. . No differences in expression of LC3-II level (normalized to ß-actin level) were observed. Data are presented as the mean +/- SEM; n=6 for basal ganglia, n=3 for cortex and cerebellum where n is the number of mice analysed for each line.

There is a trend of reduced LC3-II levels in cortex and basal ganglia of transgenic mice. But since this difference is not significant further investigations need to be done in this direction by analyzing other autophagy markers such as WIPI or p62 for example to find the autophagy status in our mouse lines.

3.1.3.2 ANALYSIS FOR PATHOLOGICAL PROTEIN AGGREGATES

3.1.3.2.1 SYNUCLEIN STAINING

One of the major hallmarks of PD is the presence of Lewy bodies. Alpha-synuclein is one of the major constituents of Lewy bodies along with ubiquitin and ubiquitinated proteins (Dickson et al., 2009). Therefore to examine whether there are alpha-synuclein aggregates in the respective brain regions - cortex, cerebellum and basal ganglia of each mouse line, stainings were performed in the 6µm brain cryosections of 12 month old mice.

The alpha-synuclein staining was performed using an immunoflourescent method as discussed in section 2.2.5.3. Images were acquired from the three different brain regions of three different mouse lines (three individual mice from each line), on the Zeiss Axio Imager Z1 microscope using two fluorescent channels – blue for nuclei and green for alpha-synuclein staining as shown in figure 3.18 (A-C). Interestingly alpha-synuclein aggregates were found in all the three brain regions of TG HtrA2 WT mice and to a lesser extent were also observed in TG HtrA2 G399S mice, however, no aggregation was found in the Non-TG control mice.

As seen in figures 3.18, compared to the homogenous cytoplasmic alpha-synuclein staining in the Non-TG mice, in the transgenic mice there are bright green cytoplasmic dots that are reminiscent of aggregated alpha-synuclein in all the three regions. The green background in all the alpha-synuclein stainings is due to the fact that mouse brains have been perfused with paraformaldehyde (PFA) which itself gives green autoflourescence.

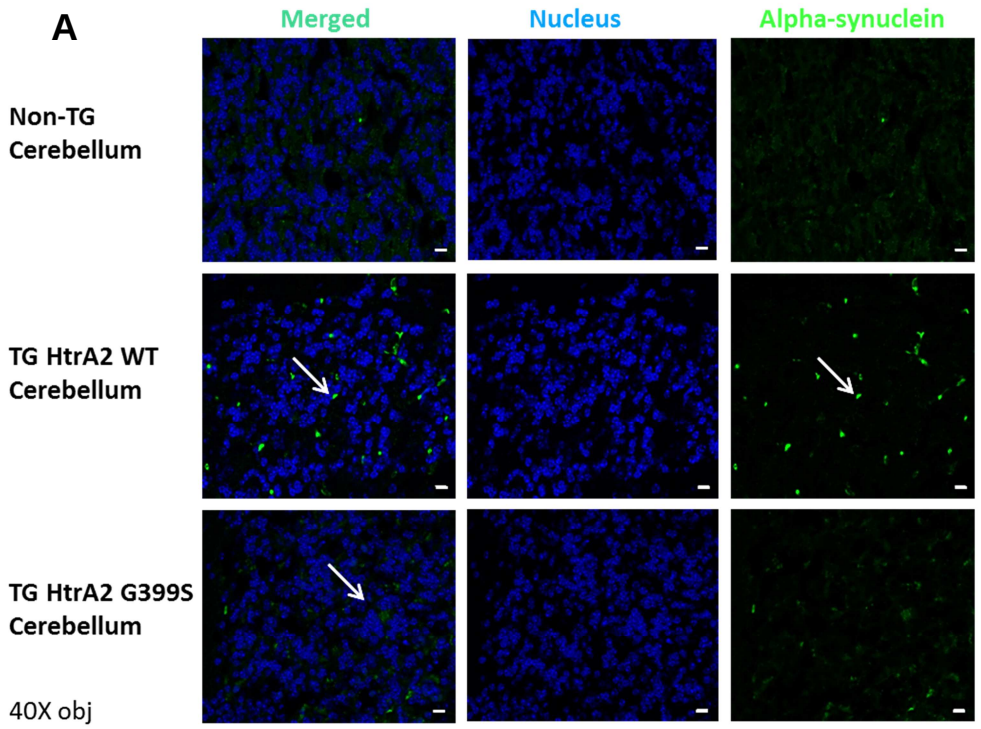
A
Merged
Nucleus
Alpha-synuclein
Non-TG Cerebellum
TG HtrA2 WT Cerebellum
TG HtrA2 G399S Cerebellum
40X obj

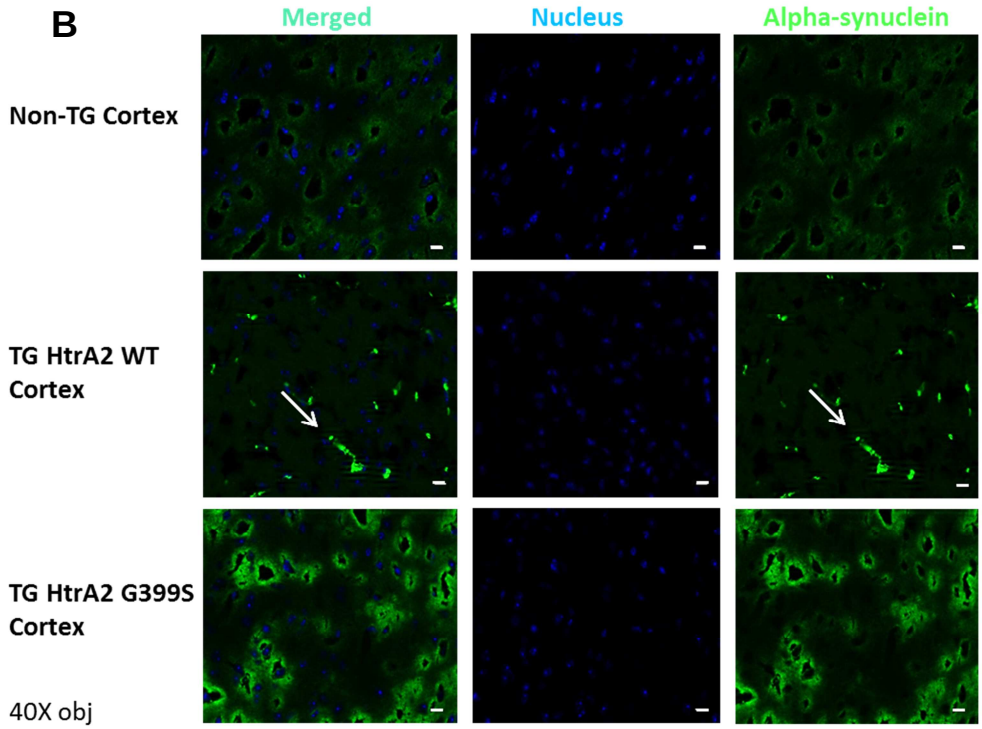
B
Merged
Nucleus
Alpha-synuclein
Non-TG Cortex
TG HtrA2 WT Cortex
TG HtrA2 G399S Cortex
40X obj

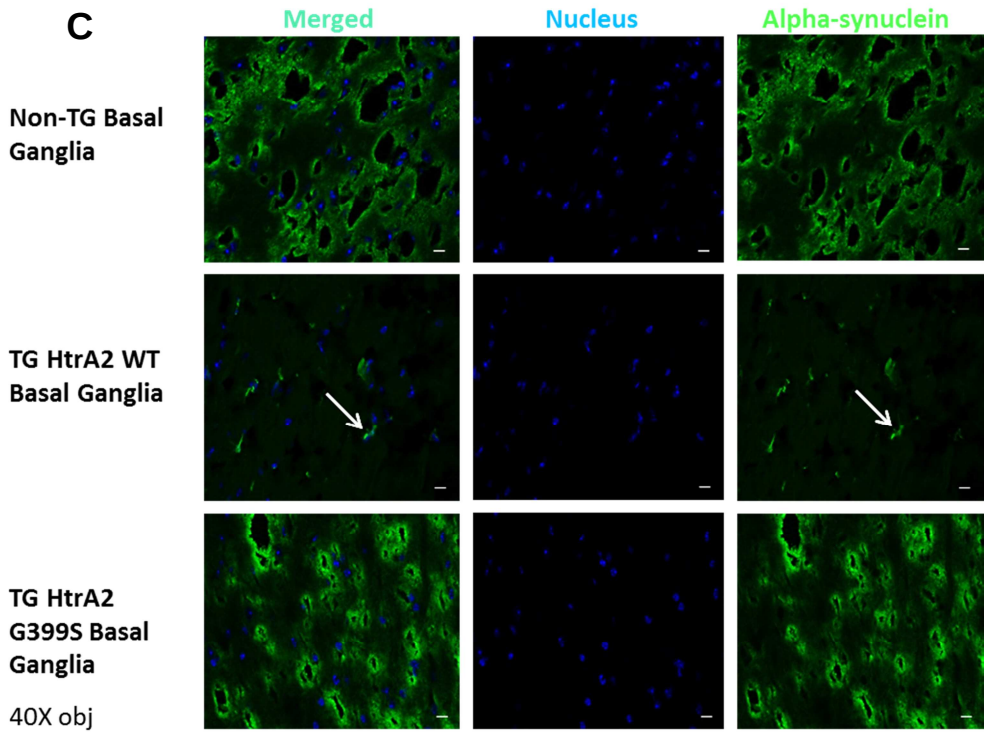

Figure 3.18 Overexpression of human WT HtrA2 in mice leads to alpha-synuclein aggregation. 6 µm cryosections from TG HtrA2 WT, TG HtrA2 G399S and Non-TG mice were stained with an alpha-synuclein antibody**.** Alpha-synuclein aggregates were observed in cerebellum **(A)**, cortex **(B)** and basal ganglia **(C)** region of TG HtrA2 WT mice. Green staining represents alpha-synuclein staining, blue represents nuclei staining and merged picture represents colocalisation of alpha-synuclein and nuclei. White arrows indicate alpha-synuclein aggregates. Scale bar=10µm.

3.1.3.2.2 PROTEINASE K (PK) DIGESTION

To confirm that alpha-synuclein puncta observed in figure. 3.18 correspond to alpha-synuclein aggregates in the TG HtrA2 WT mouse line proteinase K (PK) digestion was performed on the 6µm cryosections on the – Non-TG, TG HtrA2 WT and TG HtrA2 G399S, as discussed in section 2.2.5.4. Proteinase K digests soluble proteins and has been established as a reliable method to define the presence of insoluble aggregates both in vitro and in vivo (Neumann et al., 2002). Following PK digestion, the cryosections were stained with an alpha-synuclein antibody and imaged using the same settings and immunoflourescent method as described previously. Representative images are shown in figure. 3.19 after PK digestion.

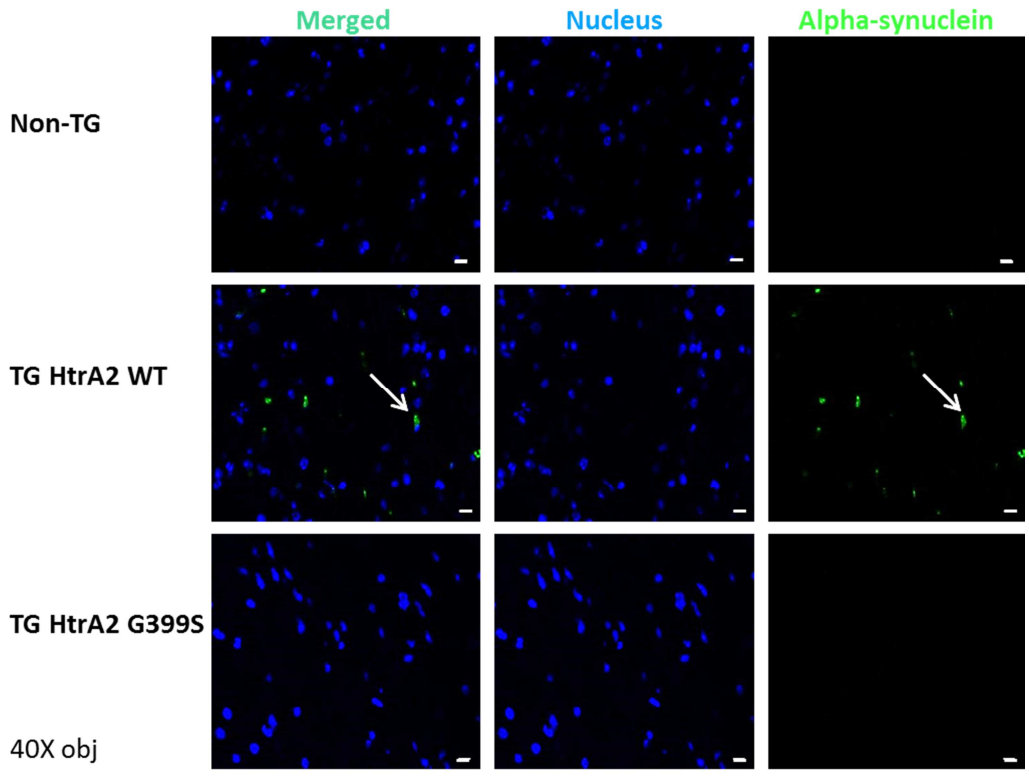

Figure 3.19 Alpha-synuclein staining following PK digestion. Green staining represents alpha-synuclein staining, blue represents nuclei staining and merged picture of alpha-synuclein and nuclei. Scale bar=10µm.

In the case of the TG HtrA2 WT mice, some alpha synuclein aggregates were still observed after PK digestion while no alpha-synuclein staining remained in the TG HtrA2 G399S mice and Non-TG controls. These data indicate the presence of insoluble alpha-synuclein aggregates in TG HtrA2 WT mice, but not in Non-TG or G399S transgenic mice. From the literature there is evidence for alpha-synuclein oligomer toxicity in a mammalian model leads to cell death (Winner et al., 2011). However, we did not assess the oligomer status of alpha-synuclein in our TG HtrA2 models.

3.1.3.2.3 UBIQUITINATION

Ubiquitination is a post translational modification where ubiquitin is attached to a substrate protein. The addition of ubiquitin can affect proteins in many ways: it can signal for their degradation via the proteasome, alter their cellular location, affect their activity and promote or prevent protein interactions (Glickman and Ciechanover, 2002; Schnell and Hicke, 2003).

Ubiquitination plays an important role in aggregate formation and proteins intended for proteasomal degradation and Lewy bodies typically contain ubiquitinated alpha-synuclein (Ubl et al., 2002). So in order to further investigate protein aggregation in the TG HtrA2 lines, unboiled whole lysates from the cerebellum region (chosen for highest expression of the transgenic HtrA2) from each mouse line, were run on an SDS-PAGE gel and after WB probed with a ubiquitin antibody that detects both monomeric and poly-ubiquitin chains. There was more ubiquitination in lysates from the cerebellum of the TG HtrA2 WT mouse line, compared to Non-TG and TG HtrA2 G399S mouse lines. The ubiquitination was observed as a smear or ladder and indicates the presence of proteins with different size (Fig. 3.20). This again points to the fact that there might be accumulation of different proteins in TG HtrA2 WT mice. And since this ubiquitination was also detected more in TG HtrA2 G399S mice compared to Non-TG mice, though less compared to TG HtrA2 WT mice, this shows that there may be also a tendency of protein accumulation in TG HtrA2 G399S mice. This tendency of protein accumulation in TG HtrA2 G399S mice was also observed in alpha-synuclein staining (Fig.3.19A).

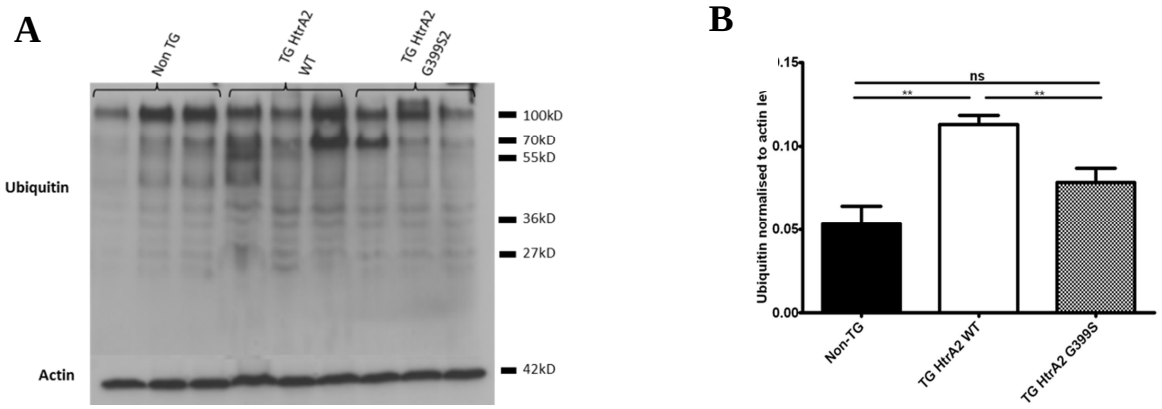

Figure 3.20 Ubiquitin levels. (A) Unboiled whole lysates from cerebellum were loaded on to the gel (50µg in each well). And probed with Ubiquitin antibody (MAB1510 from Millipore) at dilution of 1:4000 in 5% BSA. TG WT mice showed more ubiquitination in the cerebellum region compared to TG G399S and Non-TG mice**. (B)** Densitometric analysis of ubiquitin at a size of around 37 kD. Data are presented as the mean +SD; n=3, where n denotes the number of mice from each mouse line.*p<0.05, **p <0.01 and ***p < 0.001, one-way ANOVA, Statistical significance was determined by following "Tukey's Multiple Comparison Test".

Here in our results we see more ubiquitinated proteins in TG HtrA2 WT line compared to NT controls and TG HtrA2 G399S lines, which suggests that there is an increased amount of

proteins ubiquitinylated for either degradation or other signaling pathways in this line. Further work is required to understand the mechanism and pathways by which HtrA2 modulates ubiquitinylation and how this might relate to the E3 ligase or ubiquitin proteasomal system.

3.1.3.2.4 INVESTIGATION OF ALPHA-SYNUCLEIN AGGREGATES ON WB

In order to further confirm the presence of alpha-synuclein aggregates, the whole lysates (including both soluble and insoluble fractions) from cortex, cerebellum and basal ganglia region were probed on WB. Similar results were observed in each region. Here example Western blots from the cortex region are shown.

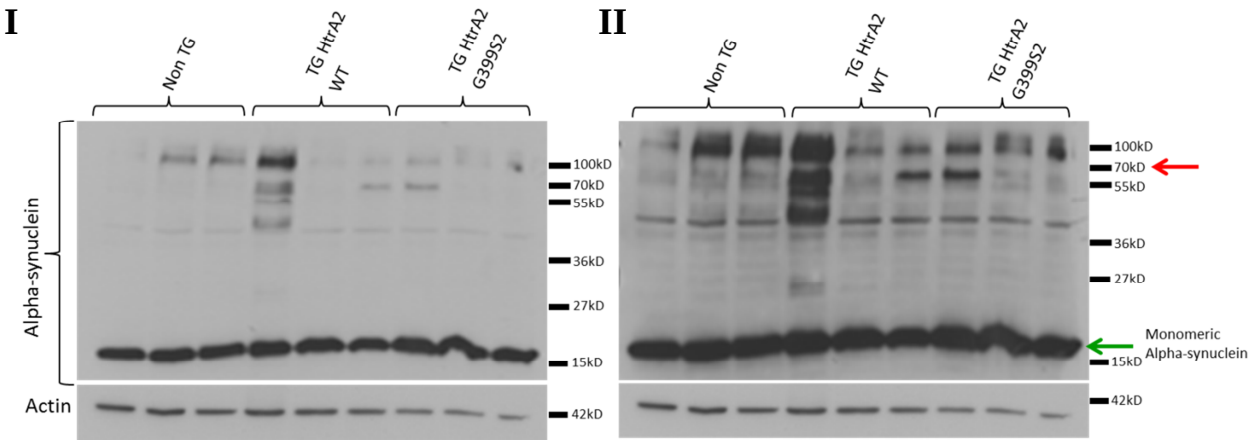

Figure 3.21 Alpha-synuclein aggregation in TG HtrA2 WT and G399S mice. Alpha-synuclein at low exposure (I) and at high exposure (II), investigated on WB by loading whole lysates from the cortex region of TG HtrA2 WT, G399S and Non-TG mice and subsequent staining for alpha-synuclein. The monomeric alpha-synuclein was observed at the band size of 19kD. 3 individual mice were analyzed from each mouse line. ß-actin was used as a loading control. Here S = soluble fraction, I = Insoluble fraction. Green arrow indicates the monomeric alpha-synuclein. Red arrow indicates proposed toxic alpha-synuclein oligomer.

As indicated in figure 3.21 at the size of around 70 kD there are bands which can be seen only in transgenic lines but not in the non-transgenic line. Out of the three mice analyzed from each line, two mice from TG HtrA2 mice while one mice from TG HtrA2 G399S mice showed these bands in cortex, basal ganglia and cerebellum . In the literature bands at similar size have been observed in alpha-synuclein staining which have been referred to as toxic oligomeric species (Arduino et al., 2012). But still it can´t be confirmed with these

results that the oligomers or aggregates which we see in our mouse lines are soluble or insoluble. For assessing this, as a prospective experiment, the TBS soluble and Urea insoluble fractions from the transgenic lines can be analyzed on WB by alpha-synuclein.

3.1.3.3 TARGETED ANALYSIS FOR CELL DEATH

Our next step was to investigate whether overexpression of WT or G399S mutant human HtrA2 results in cell death in the brain and therefore may contribute to the observed behavioral phenotypes. This was achieved using the following methods:

3.1.3.3.1 TUNEL ASSAY

Cleavage of genomic DNA during apoptosis may yield double-stranded, low molecular weight DNA fragments (mono- and oligonucleosomes) as well as single strand breaks (“nicks”) in high molecular weight DNA. These DNA strand breaks can be identified by labeling 3´-OH termini with modified nucleotides in an enzymatic reaction. In TUNEL staining labeling of DNA strand breaks is accomplished by Terminal deoxynucleotidyl transferase (TdT) which catalyzes polymerization of labeled nucleotides to free 3´-OH DNA ends in a template-independent manner. The TUNEL reaction preferentially labels DNA strand breaks generated during apoptosis in comparison to necrosis, therefore discriminating apoptosis from necrosis and from primary DNA strand breaks induced by antitumor drugs or radiation.

TUNEL staining was performed in 6µm cryosections of 12 months old mouse lines as discussed in the material methods section 2.2.5.3. In TUNEL staining red dots represent fragmented, apoptotic nuclei and the amount of apoptotic nuclei allow to assess the amount of apoptotic cell death. Images were acquired from three different regions of the brain, cerebellum, cortex and basal ganglia, respectively, as shown in the figure 3.22 A-C. Microscope images were analyzed manually by counting the total number of nuclei and then counting the number of nuclei which showed red TUNEL staining. Around 700 cells were counted in each region of 3 independent mice from each line. From this the percentage of

apoptotic nuclei was calculated and graphs were made and statistical analysis was performed using prism software (Fig.3.22D-F).

As shown in the figure 3.22 (A-C) the relative amount of apoptotic nuclei was increased in the cerebellum, cortex and basal ganglia region of TG HtrA2 WT mice compared to Non-TG and TG HtrA2 G399S mice. The statistical analysis (Fig.3.22D-F) reveals that there were significantly more apoptotic nuclei in the TG HtrA2 WT mouse line compared to Non-TG and TG HtrA2 G399S mouse lines.

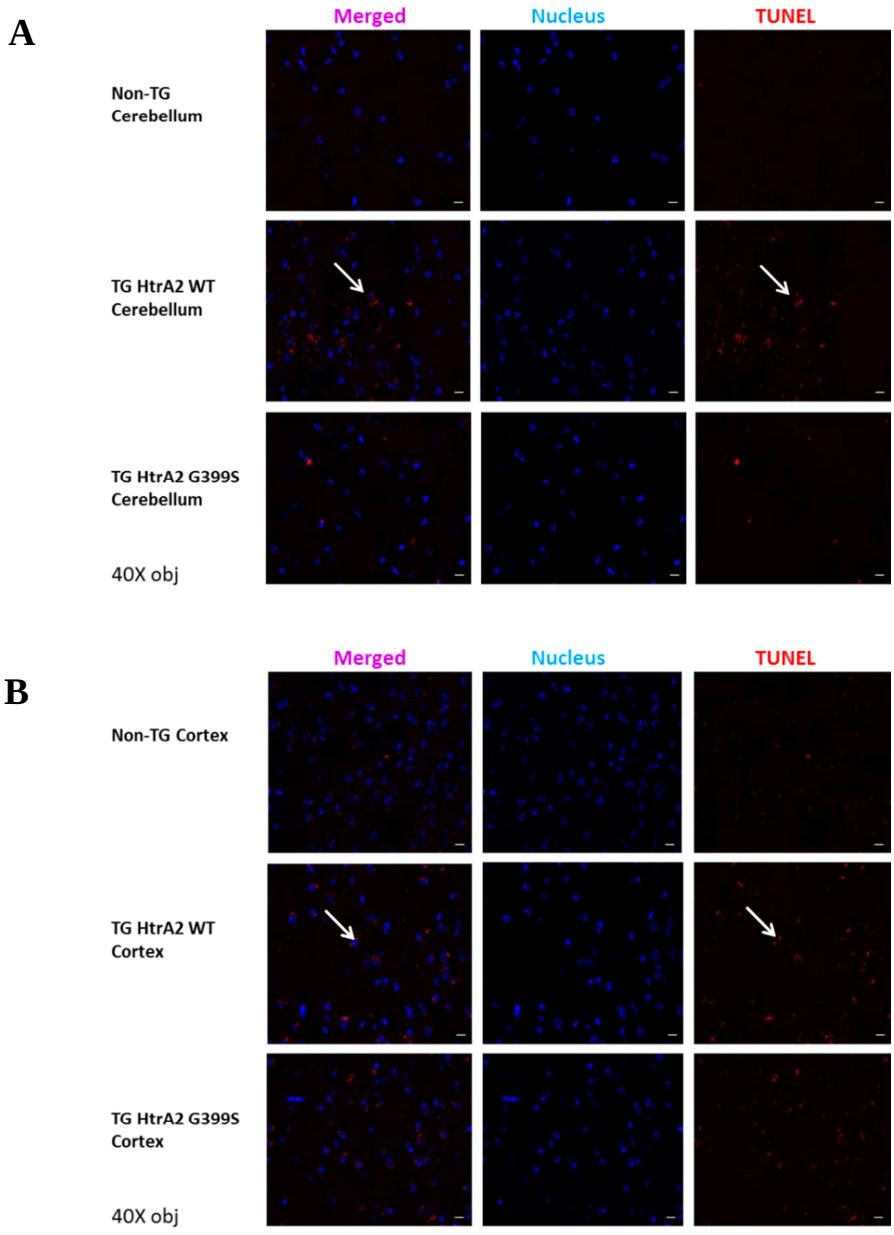

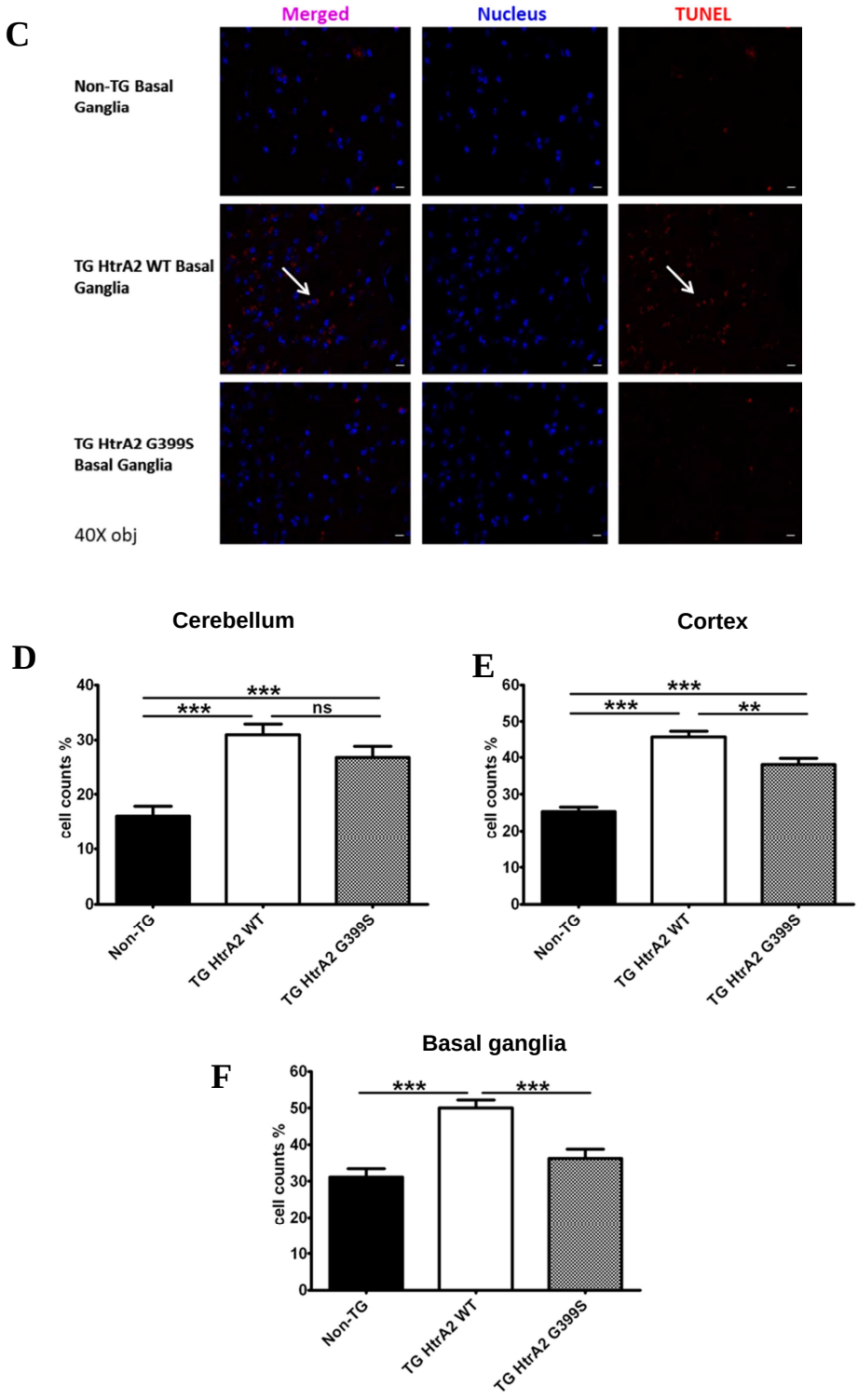

Figure 3.22 Overexpression of WT HtrA2 in mice promotes apoptotic cell death. TUNEL staining revealed apoptosis in the **(A)** cerebellum, **(B)** cortex and **(C)** basal ganglia region of all mice aged 12 months. Scale bar=10µm. **(D-F)** Quantification of TUNEL-positive cells in the **(D)** cerebellum, **(E)** cortex and **(F)** basal ganglia. More TUNEL positive cells were detected in the basal ganglia of age- and sex- matched TG HtrA2 WT mice compared to Non-TG and TG HtrA2 G399S mice. Whereas in the cortex and cerebellum of TG HtrA2 WT and TG HtrA2 G399S mice a significant amount of TUNEL positive cells were found compared to Non-TG mice. 6µm cryosections were used for staining. Data is presented as the mean average +SD; n=3 where n denotes the

number of mice from each mouse line; *p<0.05, **p<0.01 and ***p< 0.001, one-way ANOVA, Statistical significance was determined by following "Tukey's Multiple Comparison Test“.

3.1.3.3.2 MARKERS OF CELL DEATH: CASPASE- EXPRESSION LEVELS AND ACTIVITY

3.1.3.3.2.1 CASPASE 9 EXPRESSION

Well established markers of apoptotic cell death are the activation of caspases such as caspase 3 and 9. The caspases can be activated by two pathways- Intrinsic pathway or extrinsic pathway. Intrinsic pathway is mitochondrial mediated in which permeabilisation of the mitochondria releases cytochrome c into the cytoplasm forming a multi-protein complex known as the apoptosome and initiates activation of the caspase cascade through caspase 9 (Vande Walle et al., 2008). Caspase 3 along with caspase 7 are downstream apoptotic executioners which once activated mark the final, irreversible stages of apoptosis (Perry et al., 1997; Katunuma et al., 2001).

Whereas extrinsic pathway is initiated by death receptors on the plasma membrane such as tumour necrosis factor receptor 1 (TNFR1) and Fas/CD95. When ligands bind to these receptors, the death inducing signaling complex is formed leading to initiation of the caspase cascade through caspase 8 (Taylor et al., 2008).

Based on evidence for increased apoptotic cell death in different brain regions of transgenic mice overexpressing human WT or G399S HtrA2 we assessed the expression of cleaved caspase 9 in the cerebellum, cortex and basal ganglia from the three mouse lines on the WB (Fig. 3.23A-C). Caspase 9 is cleaved for its activation (Guo et al., 2013). Levels of cleaved caspase 9 were increased in all investigated brain regions of TG HtrA2 WT mice compared to Non-TG control mice. The expression of cleaved caspase 9 was also higher in the G399S mouse line in cortex compared to Non-TG mouse lines, which also complies with our TUNEL results.

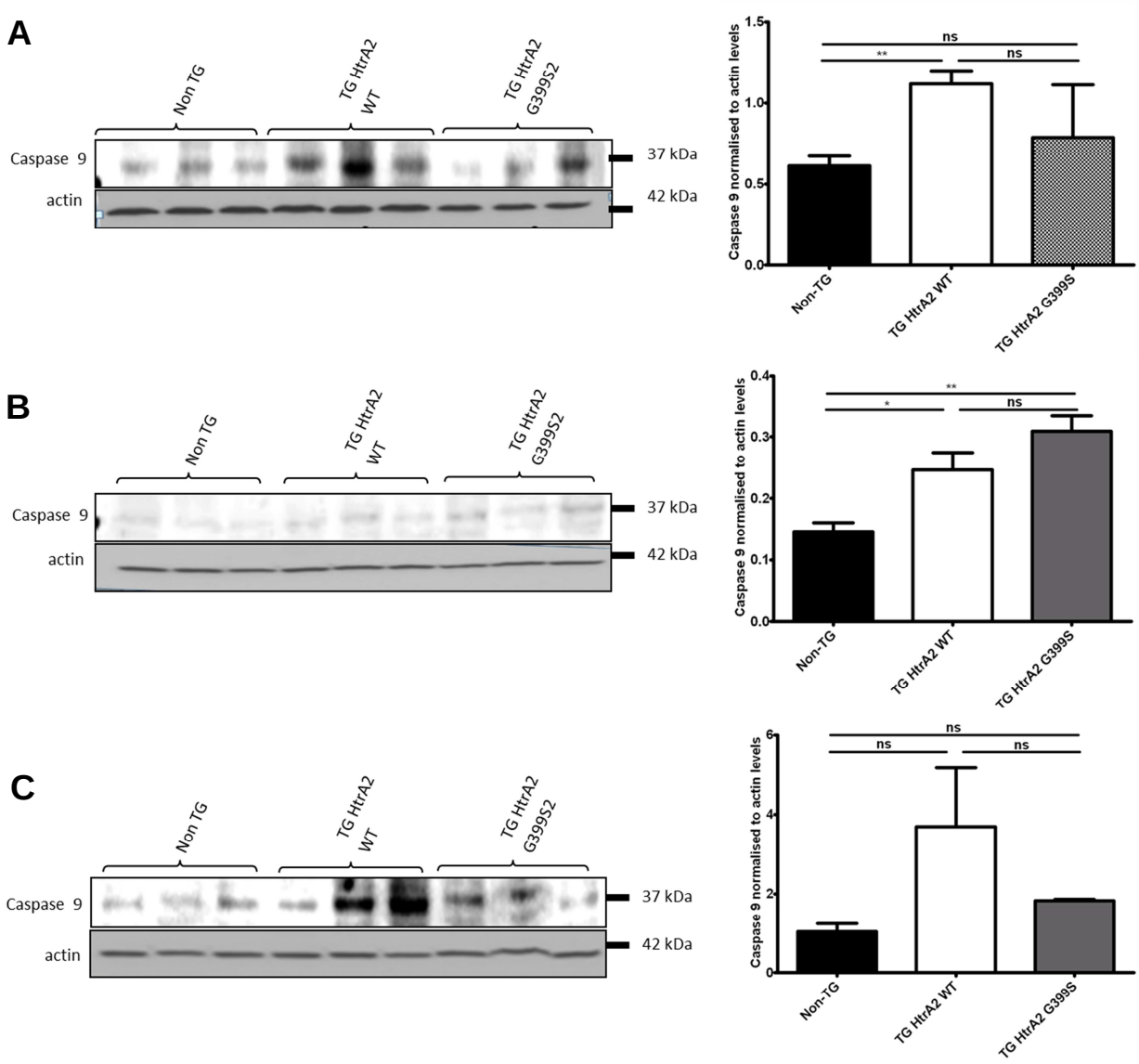

Figure 3.23 Overexpression of HtrA2 WT in mice increases levels of cleaved Caspase 9. The expression of caspase 9 and the amount of cleaved caspase 9 was determined by WB from the protein lysates of 3 independent mice from each line. 50 µg of protein mixed with 5X Laemmli was loaded on to the gel, from cerebellum, cortex and basal ganglia region of brain of three independent mice from Non-TG, TG HtrA2 WT and TG HtrA2 G399S mouse line. The blot was probed for anti-caspase 9 antibody (which detect the cleaved form of caspase-9) followed by incubation with ß-actin as a loading control. Here are shown in the figure the blots from **cerebellum (A)**, **cortex (B)**, and **basal ganglia (C)** region of brain. Densitometric analysis was performed using imagej. ± S.D, where n=3, where n denotes the number of mice from each mouse line. Significance level was checked using the paired t-test, where *p<0.05, **p<0.01 and ***p< 0.001.

3.1.3.3.2.2 CASPASE 3 ACTIVITY

Caspase 3 activity was analysed using the Caspase-3 flourogenic assay as described in section 2.2.3.5 of the material and methods. The caspase 3 activity was assessed in cerebellum, cortex and basal ganglia of each mouse line. Here the results of cortex and cerebellum region of brain are shown. Reliable measurement of caspase 3 activity was not possible in the basal ganglia due to little total protein and therefore low enzyme activities.

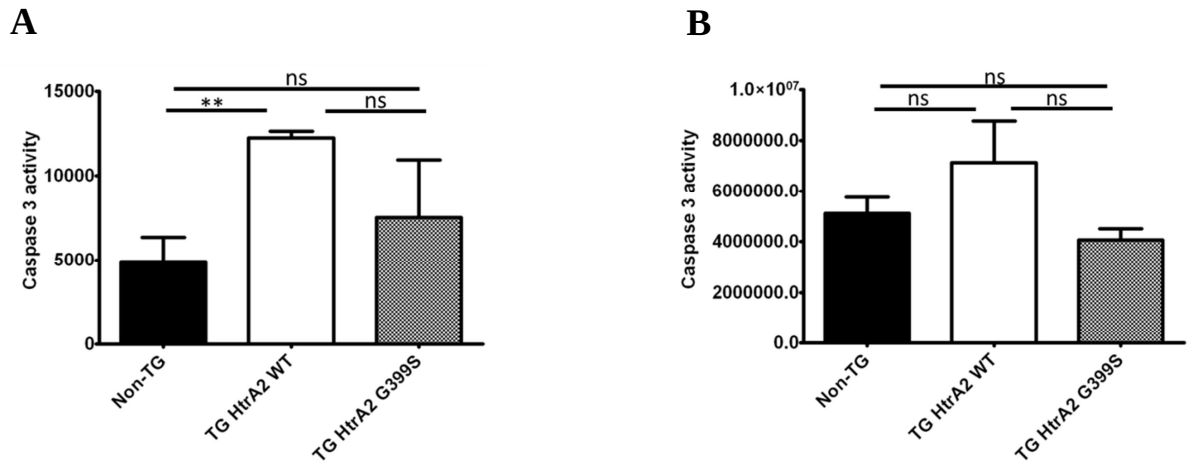

Figure 3.24 Overexpression of HtrA2 WT in mice increases caspase 3 activity. Caspase 3 activity was measured in the lysates of cortex **(A)** and cerebellum **(B)** regions of brain from three different mouse lines - Non-TG, TG HtrA2 WT and TG HtrA2 G399S for 3 h using Acetyl-Asp-Glu-Val-Asp-7-amidomethylcoumarin as a substrate. Four independent mice were analysed from each line. Columns indicate the Caspase 3 activity, which was expressed as mean FU/min/µg protein ± S.D. Significance level was checked using the paired t-test, where *p<0.05, **p<0.01 and ***p< 0.001.

There was a significant increase in the activity of caspase 3 in the cortex region of TG HtrA2 WT mice compared to Non-TG and TG HtrA2 G399S mice. Similarly a trend for an increased activity of caspase 3 was observed in the cerebellum region of the TG-HtrA2 WT mouse line compared to Non-TG and TG HtrA2 G399S mouse lines. This partly corroborates with our results on caspase 9 expressions in cerebellum where we saw more amount of cleaved caspase 9 in TG HtrA2 WT mice compared to the other two lines and in cortex where more amount of caspase 9 was found in TG HtrA2 WT and G399S mice compared to Non-TG mice. This means that there is increased activated caspase 3 in TG HtrA2 WT mice which indicates more apoptotic cell death in these mice.

3.1.3.3.3 EXPRESSION CHECK FOR DOPAMINERGIC NEURONAL MARKER – TYROSINE HYDROXYLASE (TH)

Tyrosine hydroxylase (TH) or tyrosine 3-monooxygenase is an enzyme responsible for catalyzing the conversion of the amino acid L-tyrosine to L-3, 4-dihydroxyphenylalanine (L-DOPA). L-DOPA is a precursor for dopamine, which is a precursor for the important neurotransmitters norepinephrine (noradrenaline) and epinephrine (adrenaline). Tyrosine hydroxylase catalyzes the rate limiting step in this synthesis of catecholamines. Tyrosine hydroxylase is encoded by the *TH* gene and the enzyme is present in the central nervous system (CNS), peripheral sympathetic neurons and the adrenal medulla (Nagatsu, 1995). So TH is an established marker of dopaminergic neurons. And since a consistent abnormality in Parkinson's disease is degeneration of dopaminergic neurons in the substantia nigra, leading to a reduction of striatal dopamine levels, we wanted to address whether the observed apoptotic cell death also refers to dopaminergic neurons in our mice. For this we were checking the TH level in our mouse lines. This was determined in our mouse lines using WB. The whole lysates from three different brain regions, cerebellum, cortex and basal ganglia, respectively, were loaded on a gel and probed for by TH antibody followed by ß-actin as a control.

As we can see in figure 3.25A there was a significant increase in TH level in the cerebellum region of TG HtrA2 WT mice compared to Non-TG and TG HtrA2 G399S mice. In addition there was a tendency of increased TH levels of TG HtrA2 G399S mice compared to Non-TG mice. Though no significant differences were observed in the TH level in the basal ganglia region between different mouse lines, a decrease ($p=0.09$) in TH level was observed in cortex region of TG HtrA2 WT mice compared to Non-TG mice.

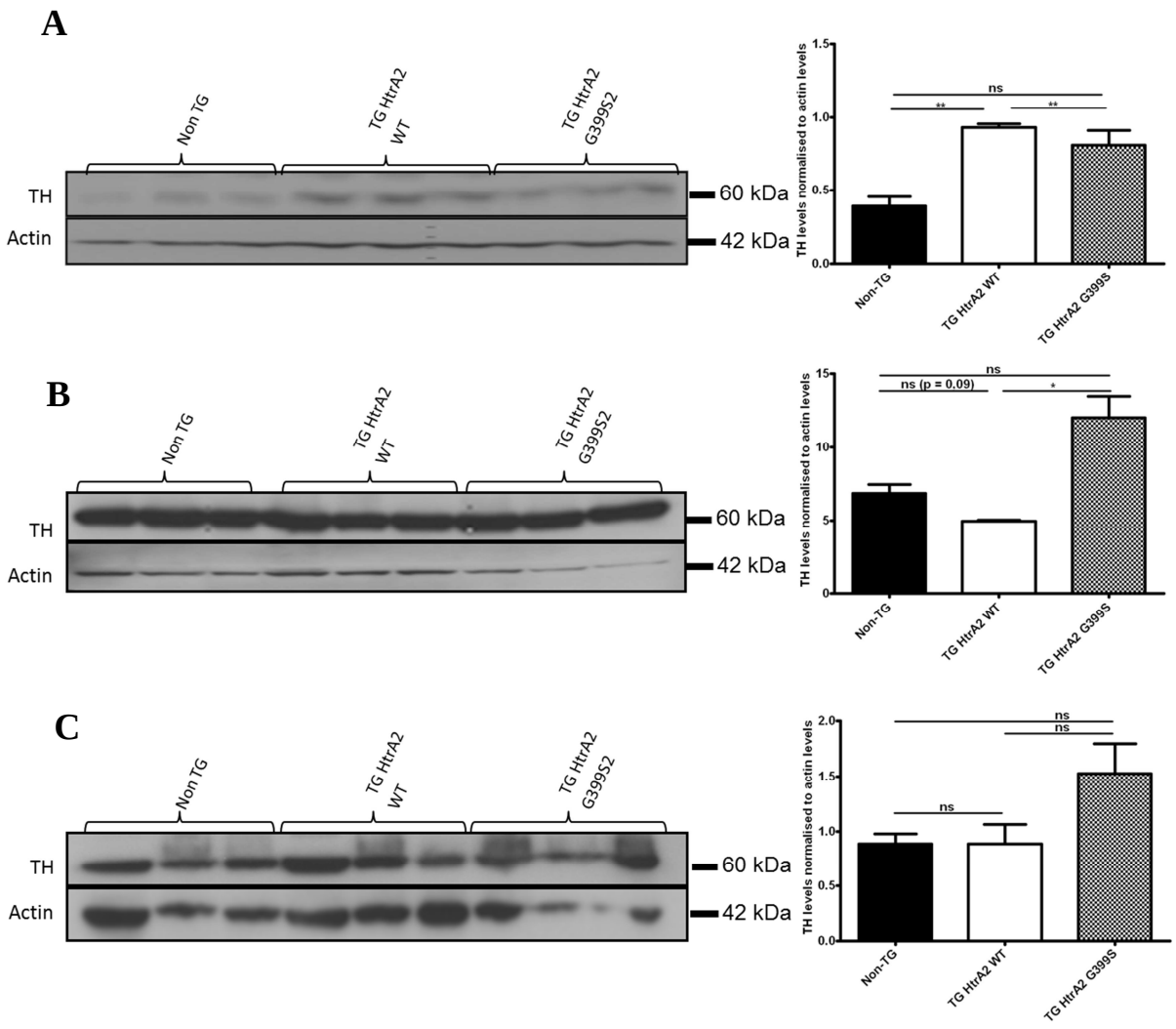

Figure 3.25 TH level expression in (A) Cerebellum (B) Cortex and (C) Basal ganglia region of Non-TG, TG HtrA2 WT and TG HtrA2 G399S mice. 50 µg of protein was loaded on the WB from these regions of brain from the three independent mice from each line. And the blot was probed by TH antibody followed by ß-actin as a control. Densitometric analysis was performed using imagej. ± S.D, Significance level was checked using the paired t-test, where *p<0.05, **p<0.01 and ***p< 0.001.

3.1.3.3.4 EXPRESSION OF THE HTRA2 SUBSTRATE X-LINKED INHIBITOR OF APOPTOTIC PROTEIN (XIAP)

Since we found more apoptotic cell death in TG HtrA2 WT, we speculated which pathways may be influenced via HtrA2 overexpression (explained in detail in introduction part). And one these pathways, is cell death via HtrA2-mediated degradation of inhibitors of apoptosis (IAP´s such as XIAP). To investigate this pathway leading to cell death the protein

expression of the respective substrate was assessed in brain regions where the cell death was previously observed (see Fig. 3.22).

Though several substrates of HtrA2 are known to date, XIAP is one of the best characterized substrates of HtrA2. The expression level of XIAP was assessed in the cerebellum, cortex and basal ganglia region of the TG and control mouse lines.

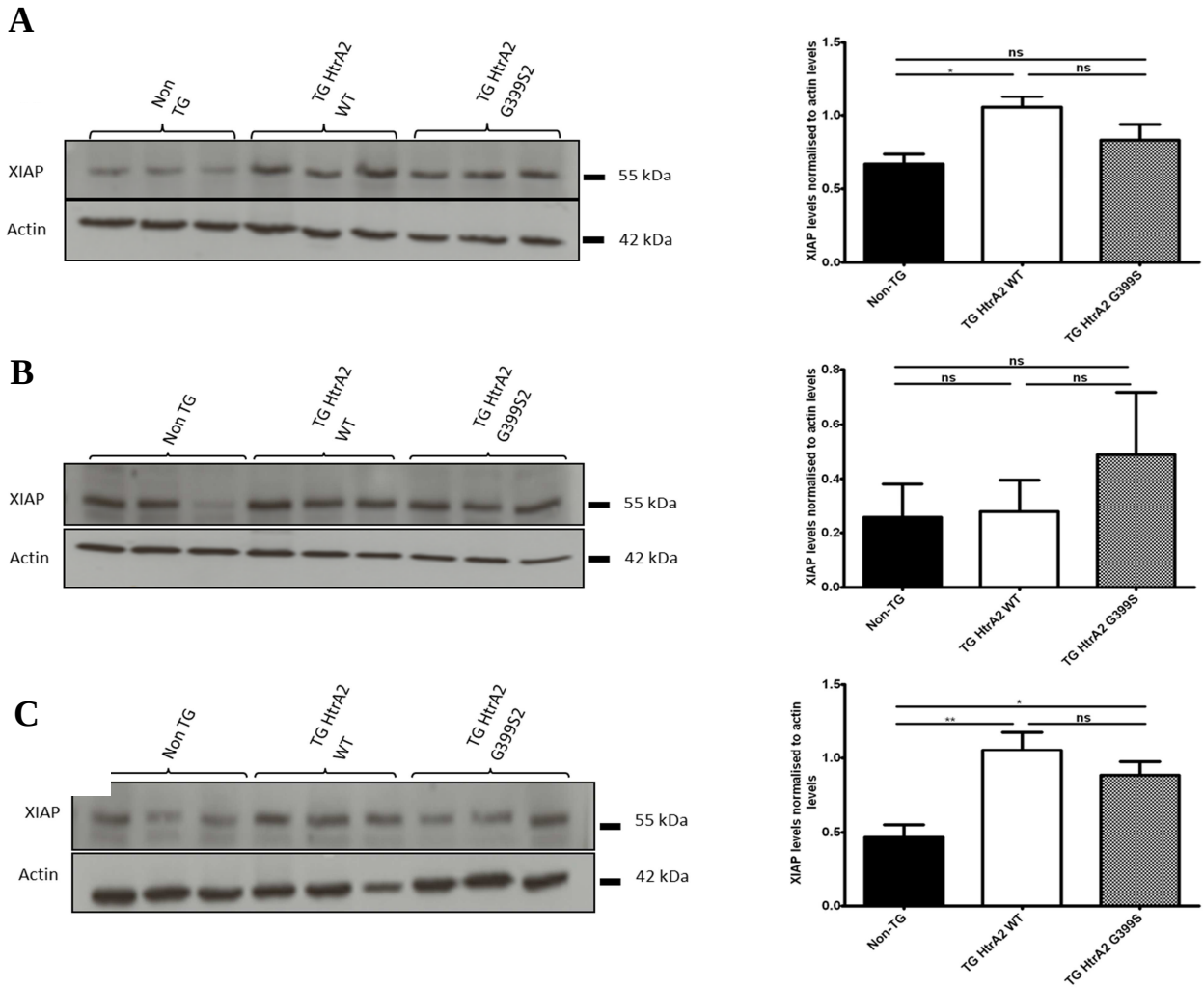

Figure 3.25 XIAP level expression check in (A) Cerebellum **(B)** Cortex and **(C)** Basal ganglia region of Non-TG, TG HtrA2 WT and TG HtrA2 G399S mice. 50 µg of protein was loaded on the WB from these regions of brain from three independent mice from the three different mouse lines. Three technical replicates were performed from the same sets of mice lysates. And the blot was probed by XIAP antibody followed by ß-actin as a control. Densitometric analysis was performed using imagej. ± S.D, where n=3, where n denotes the number of mice from each mouse line. Significance level was checked using the paired t-test, where *p<0.05, **p<0.01 and ***p< 0.001.

As we can see in the figure 3.25A, there was a significant increase in the expression level of XIAP in the cerebellum region of TG HtrA2 WT mice compared to Non-TG and TG-HtrA2 G399S mice. Though this increase was not observed in cortex (Fig.3.25B), there was a significant increase in XIAP levels in the basal ganglia region of TG HtrA2 WT and TG HtrA2 G399S mouse line compared to Non-TG mouse line.

TUNEL and caspase 9 findings showed consistent results in the cerebellum and cortex of TG HtrA2 WT mice while in TG HtrA2 G399S mice findings were consistent in the cortex region. Interestingly there was upregulation of XIAP in the cerebellum and basal ganglia of TG HtrA2 WT mice while in cortex XIAP showed no difference in both the transgenic mouse lines compared to controls. So to conclude, TG HtrA2 WT mice showed consistent findings in cerebellum region and TG HtrA2 G399S mice exhibited consistent findings in cortex region in terms of cell death (TUNEL and caspase 9 markers) even though XIAP levels in these regions do not correlate with these results in each mouse line.

3.1.3.4 TARGETED ANALYSIS FOR PHOSPHOSERINE 400 HTRA2 COLOCALISATION IN NUCLEUS

Serine 400 HtrA2 is one of the three characterized phosphorylation sites of HtrA2 and is located adjacent to G399, which is mutated in some PD patients (Fitzgerald et al. 2012). In fact, two important phosphorylation sites on HtrA2, are thought to be involved in the regulation of its protease activity (Plun-Favreau et al. 2007, Lin et al. , Fitzgerald et al. 2012) and are located adjacent to mutation or polymorphism sites described in PD patients A141S (Strauss et al., 2005), P143A (Lin et al., 2011), G399S (Strauss et al., 2005). As an effort to define the relevance of Phosphoserine 400 HtrA2, one of our collaborators Prof. Katrin Marcus, Proteome Center, Ruhr.University Bochum, found that there is colocalisation of phosphoserine 400 HtrA2 with the nuclei of SHSY-5Y cells overexpressing FLAG-HtrA2 (Fig. 3.26).

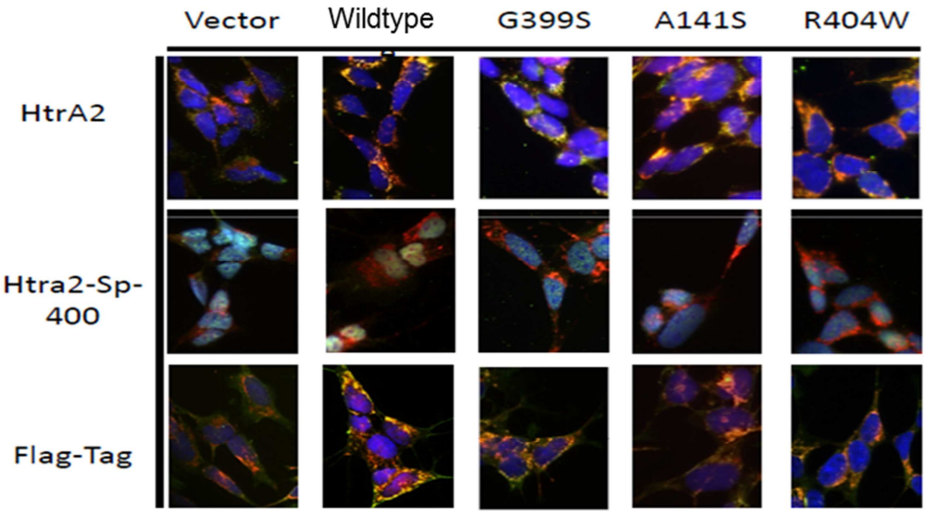

Figure 3.26 Phospho-HtrA2 S400 and FLAG co-staining in SHSY-5Y cells. Blue signal represents nuclear staining, the red signal is for the Phospho-HtrA2 S400 HtrA2 staining, green signal is for the FLAG staining. Where Vector= SH-SY5Y cells transfected with empty vector, Wildtype= wild type HtrA2 transfected SH-SY5Y cells, G399S, A141S and R404W represent SH-SY5Y cells transfected with different HtrA2 mutants. *Performed by Katrin Marcus, Proteom center, Ruhr.University Bochum.*

In order to investigate if this could be confirmed in vivo, phosphoserine 400 HtrA2 stainings were performed on 6µm brain sections of 12 months old mice, using immunoflourescent protocol. Images were acquired from the cerebellum, cortex and basal ganglia regions of Non-TG, TG HtrA2 WT and TG HtrA2 G399S mice at 40X using blue (for nucleus) and red filters (for phospho- S400 staining) as is shown in the figure 3.27 (A-C).

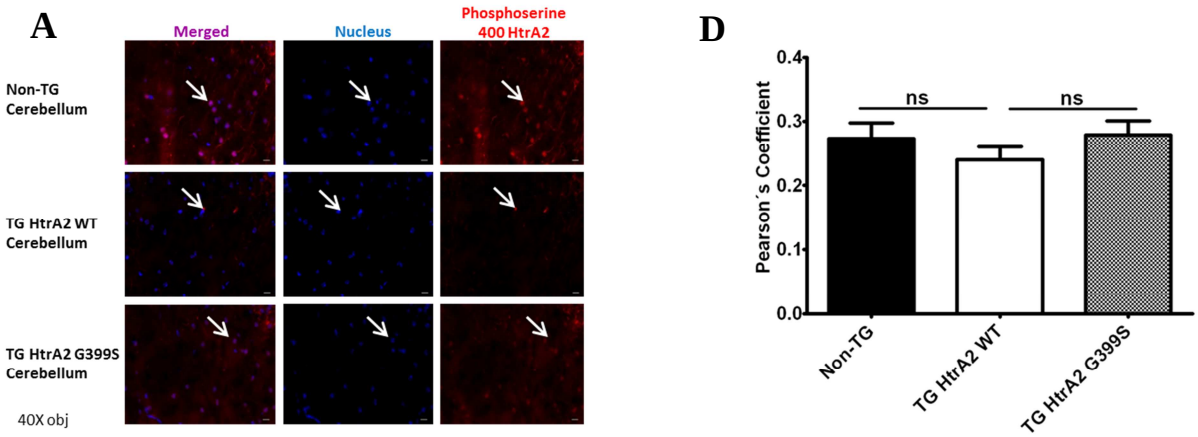

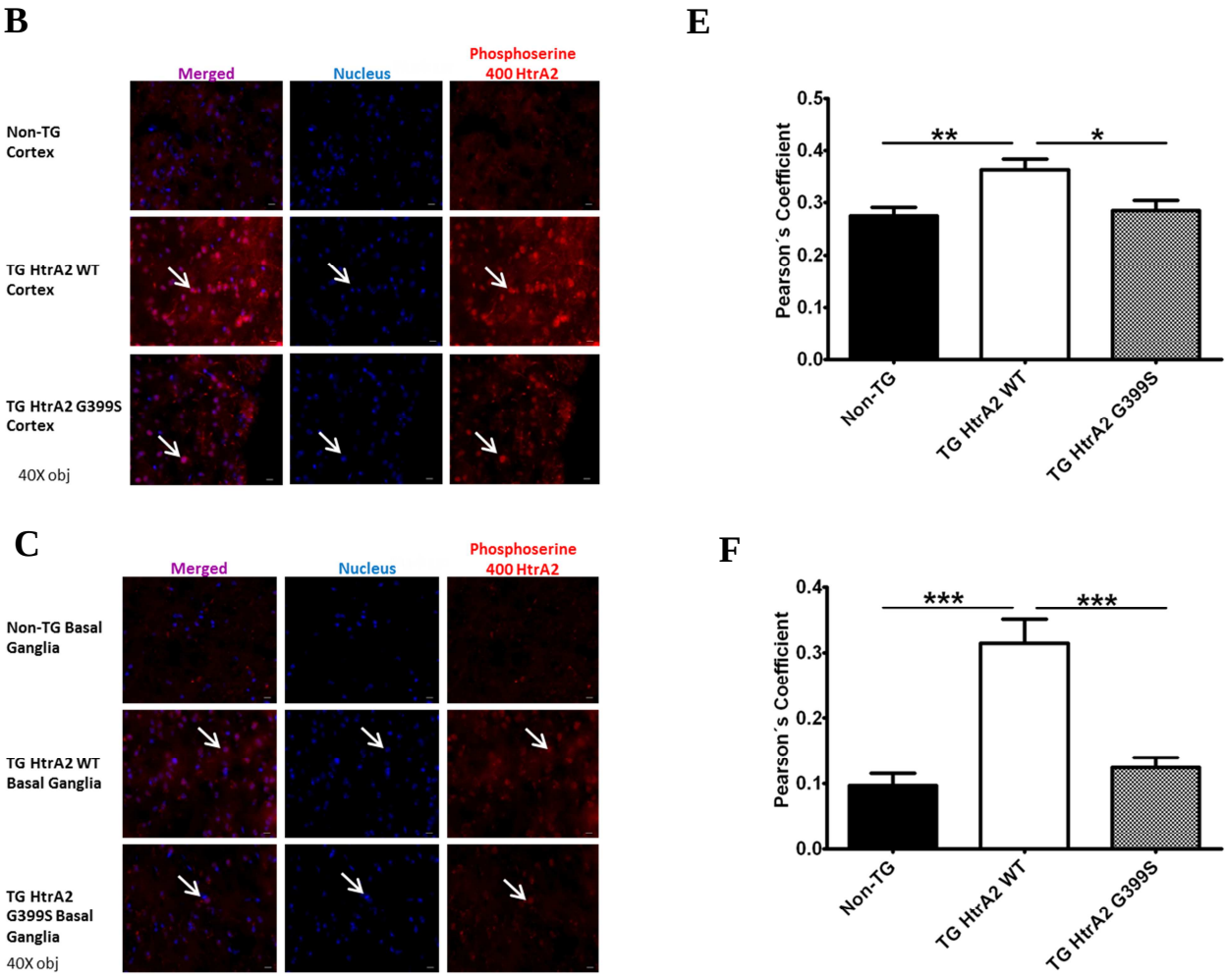

Figure 3.27 Nuclear colocalisation of Phospho-HtrA2 S400 in TG HtrA2 WT mice. Microscope images were acquired at 40X magnification from the immunohistochemical stainings of phosoho-HtrA2 S400 HtrA2 on 6 µm cryosections of 12 month old mice in the cerebellum **(A)**, cortex **(B)** and basal ganglia **(C)** region of TG HtrA2 WT, TG HtrA2 G399s and Non-TG mouse lines. Phospho-HtrA2 S400 HtrA2 Staining (red) were analyzed for colocalisation with nuclei (blue) by ImageJ program in the cerebellum, cortex and basal ganglia region of different mouse lines. Scale bar=10µm. **(D-F)** Quantification of colocalisation of phospho-HtrA2 S400 HtrA2 and nuclei showed significantly more colocalisation in the basal ganglia and cortex regions of TG HtrA2 WT mice as compared to Non-TG and TG HtrA2 G399S mice. Though there was a tendency of less colocalisation in cerebellum region of TG HtrA2 WT mice as compared to Non-TG and TG HtrA2 G399S mouse lines. Data are presented as the mean ±SD; n=3 where n is number of mice used for each line; *p<0.05, **p<0.01 and ***p< 0.001, one-way ANOVA, Statistical significance was determined by following "Tukey's Multiple Comparison Test“.

Quantification of nuclear colocalisation of Phosphoserine 400 HtrA2 was performed using Image J software using Pearson´s coefficient and then later densitometric analysis was performed on 10 images from the cerebellum, cortex and basal ganglia regions of the three different mice from each mouse line. There was a significant colocalisation of phosphoserine 400 HtrA2 with the nucleus in the cortex and basal ganglia regions of TG HtrA2 WT line

compared to Non-TG and TG HtrA2 G399S lines. No difference was observed in the cerebellum region in all the three mouse lines (Fig 3.27.A). So here in the group of 12 months old mice we observed that most of the Phosphoserine 400 HtrA2 is colocalised in the nucleus.

To check if the observed nuclear localization of the phosphoserine 400 HtrA2 staining was not an artifact due to the FLAG-tagged overexpressed human HtrA2, and to confirm the specificity of the antibody, phosphoserine 400 HtrA2 staining was additionally performed in SHSY-5Y cells that were transfected with WT HtrA2 without a FLAG-tag and WT HtrA2 with a FLAG-tag. Here we observed nuclear colocalisation of Phosphoserine 400 HtrA2 also in cells overexpressing WT HtrA2 without FLAG-tag.

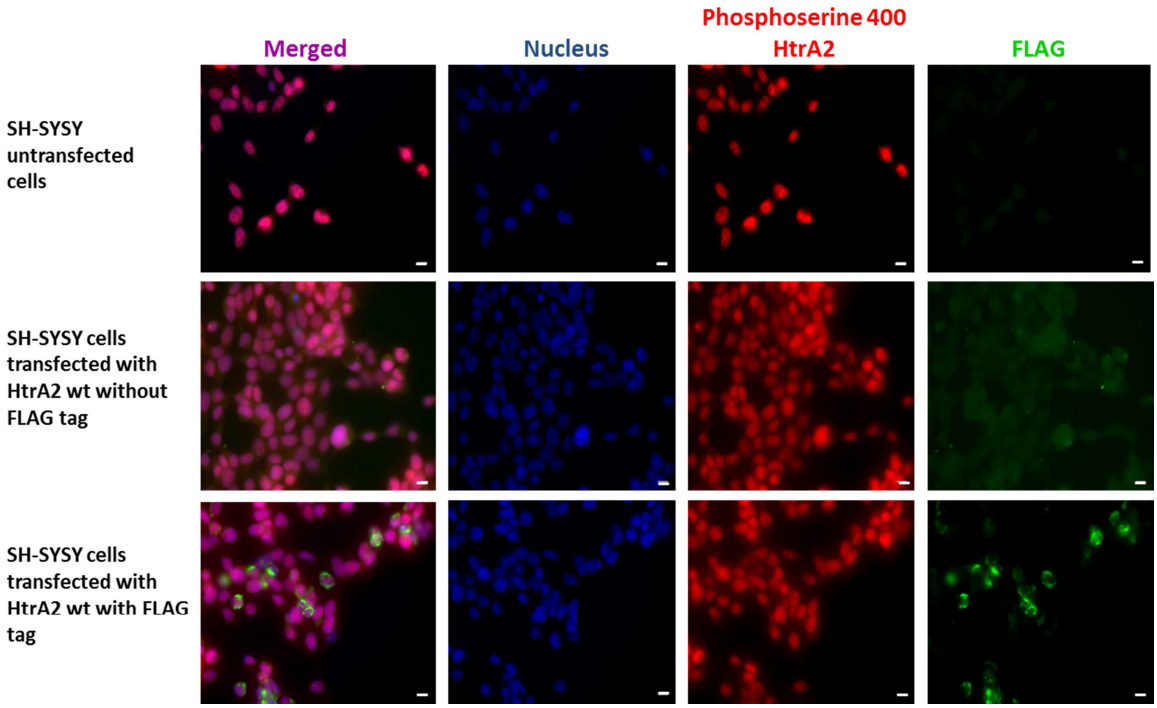

Figure 3.28 Phospho-HtrA2 S400 and FLAG co-staining in SHSY-5Y cells. Blue represents nuclear staining, the red signal is for the Phospho-HtrA2 S400 HtrA2 staining, green signal is for the FLAG staining. Scale bar=5µm.

As we can see in the above figure that there is no difference in the Phosphoserine 400 HtrA2 colocalisation in all the three group of cells which also confirms that FLAG-tag does not influence Phosphoserine 400 HtrA2 staining in terms of its colocalisation with nuclei.

3.2 CELL CULTURE EXPERIMENTS

3.2.1 ROLE OF HTRA2 IN MITOCHONDRIAL MORPHOLOGY REGULATION AND MITOCHONDRIAL DEGRADATION

3.2.1.1 HTRA2 INFLUENCE ON MITOCHONDRIAL AND LYSOSOMAL COLOCALISATION

Additional cellular models were employed in order to characterize the physiological role of the protein. In order to study the effect of HtrA2 on the mitochondrial and lysosomal colocalisation live cell imaging experiments were performed in mouse HtrA2 WT knockout embryonic fibroblasts (MEFs), overexpressing HtrA2 WT, HtrA2 mutant S306A (protease dead) and an empty vector (EV). This was achieved by staining with mitotracker red (for staining mitochondria) and lysotracker green (for staining lysosomes) and taking live cell images. The experiment was repeated three times using the same conditions. With the live cell images mitochondrial and lysosomal colocalisation study was performed using axiovision software (Krebiehl et al., 2010). 5 to 6 images were used for each kind of cells for statistics. Here are shown the example pictures from the live cell imaging and graphical representation of colocalisation data in figure 3.29. There is more yellow signal, which represents overlap of green (lysosomes) and red signals (mitochondria) in EV and HtrA2 mutant expressing cells compared to HtrA2 WT expressing cells which means more number of mitochondria are degraded by lysosomes in these cell lines. Quantification of the data showed a significant increase in lysosomal and mitochondrial colocalisation in HtrA2 KO cells overexpressing HtrA2 mutant or empty vector compared to cells overexpressing HtrA2 WT, which means that there are more mitochondria reaching the lysosomes for degradation in the absence of HtrA2.

As a control experiment, HtrA2 expression was analyzed on the WB in the HtrA2 KO MEFs expressing EV, HtrA2 WT and HtrA2 mutant. There was no HtrA2 expression observed in the

HtrA2 KO MEFs expressing EV while WT HtrA2 and Mutant HtrA2 were equally expressed in the HtrA2 KO MEFs expressing HtrA2 WT and HtrA2 mutant respectively.

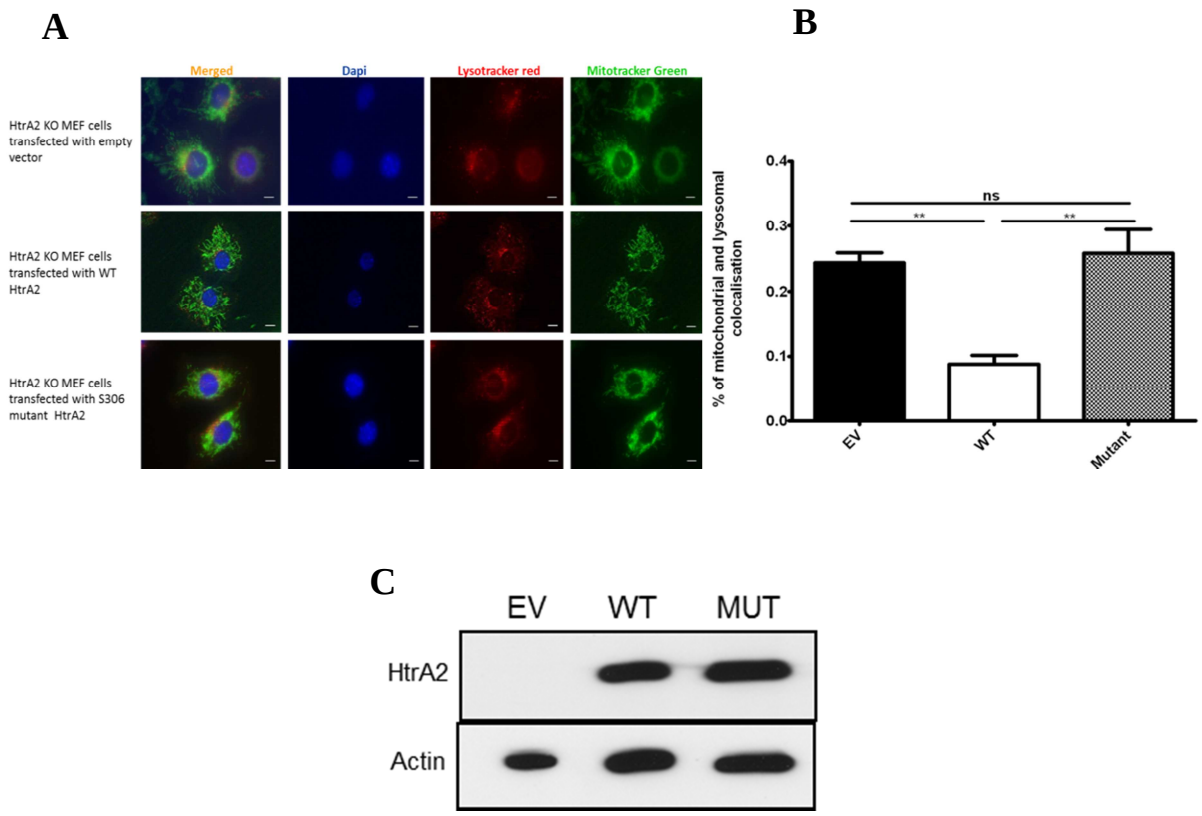

Figure 3.29 HtrA2 influence on Mitochondrial and lysosomal colocalisation. (A) Live cell images from the cells stained with lysotracker red, mitotracker green and DAPI. Merged images (yellow signal) represent mitochondrial and lysosomal colocalisation. Scale bar=10µm. **(B)** Quantification of mitochondrial and lysosomal colocalisation by Axiovision software. **(C)** Expression analysis of HtrA2 in HtrA2 KO MEF´s expressing EV, HtrA2 WT and HtrA2 mutant on WB. Data are presented as the mean ±SD; n=3; *p<0.05, **p<0.01 and ***p< 0.001, one-way ANOVA, Statistical significance was determined by following "Tukey's Multiple Comparison Test". Where EV=Mouse HtrA2 WT knock out embryonic fibroblasts (MEFs) overexpressing empty vector, WT=Mouse HtrA2 WT knock out embryonic fibroblasts (MEFs) overexpressing HtrA2 WT, and Mut=Mouse HtrA2 WT knock out embryonic fibroblasts (MEFs) overexpressing S306 mutant HtrA2.

3.2.1.2 HTRA2 INFLUENCE ON AUTOPHAGIC ACTIVITY

A marker of autophagy was measured in the HtrA2 MEFs with HtrA2 KO background, overexpressing HtrA2 WT, HtrA2 S306A mutant (protease dead) and an empty vector by expressing LC3-GFP (for visualisation of autophagosomes) in these cells. Later from the images of fixed cells, puncta were counted from at least 10 individual cells from each line and later the average number of puncta in each cell per line was calculated. The experiment

was repeated three times using same conditions. Here are shown the example images for LC3-GFP puncta and graph showing their quantification.

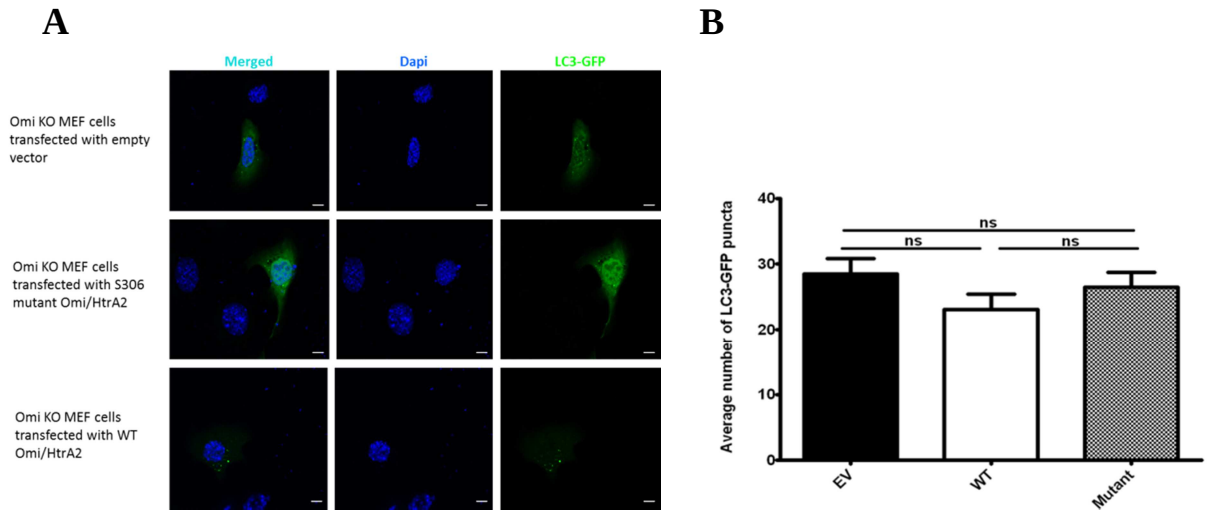

Figure 3.30 HtrA2 influence on autophagosome formation (A) Microscopic images from the fixed cells transfected with LC3-GFP. Blue signal represents nucleus and green signal represent LC3-GFP puncta. Scale bar=10µm. **(B)** Quantification of LC3-GFP puncta. Data is presented as the mean ±SD; n=3 where n represents the number of technical repeats; *p<0.05, **p<0.01 and ***p< 0.001, one-way ANOVA, Statistical significance was determined by following "Tukey's Multiple Comparison Test".

No differences in LC3-GFP puncta were observed between the different cell lines. Since the LC3-GFP punctas are the representative of the number of autophagosomes, these results show that there are more number autophagosomes in the absence of HtrA2.

3.2.1.3 HTRA2 INFLUENCE ON MITOCHONDRIAL MASS

Mitochondrial mass was checked by fluorescence activated cell sorting (FACS) using mitotracker green which stains mitochondria and provides a read-out for mitochondrial mass (Krebiehl et al., 2010). The data is shown here in graphical form and represents the mean of three independent experiments and 50,000 cells were assessed for each line per experiment. As can be seen from the graph the mitochondrial mass was significantly reduced in the complete absence of HtrA2 (HtrA2 KO cells expressing EV) and in the absence of functional HtrA2 (HtrA2 KO cells expressing HtrA2 mutant).

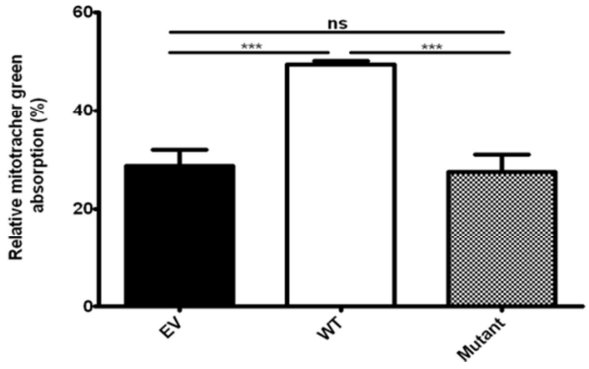

Figure 3.31 HtrA2 influence on mitotracker staining measure by FACS. This was performed by staining HtrA2 KO MEF´s expressing EV, HtrA2 WT and HtrA2 mutant with mitotracker green and then analyzing them with FACS based on the difference in their fluorescent intensity as mitotracker green stains all the mitochondria present in the cells. Here is shown the quantification of three independent experiments on FACS analysis. Data are presented as the mean ±SD; n=3 where n represents the number of independent experiments,*p<0.05, **p<0.01 and ***p< 0.001, one-way ANOVA, Statistical significance was determined by following "Tukey's Multiple Comparison Test".

This data suggest that HtrA2 protease activity is important for normal mitochondrial function and its absence leads to less mitochondrial mass. Absence of HtrA2 enhances dysfunctional mitochondria which are removed by the cells as a protective mechanism against cell death (Kieper et al., 2010).

3.2.1.4 HTRA2 INFLUENCE ON MITOCHONDRIAL CHAPERONE- TRAP1

It was found that the chaperone TRAP1 is a novel HtrA2 interacting partner by MALDI-TOF analysis and later confirmed using co-immunoprecipitation method by colleagues in our laboratory (unpublished work). In order to follow this interaction we investigated the endogenous levels of TRAP1 in the HtrA2 KO MEF cells expressing (empty vector) EV, HtrA2 WT and HtrA2 mutant. TRAP1 levels were assessed by WB in these cells.

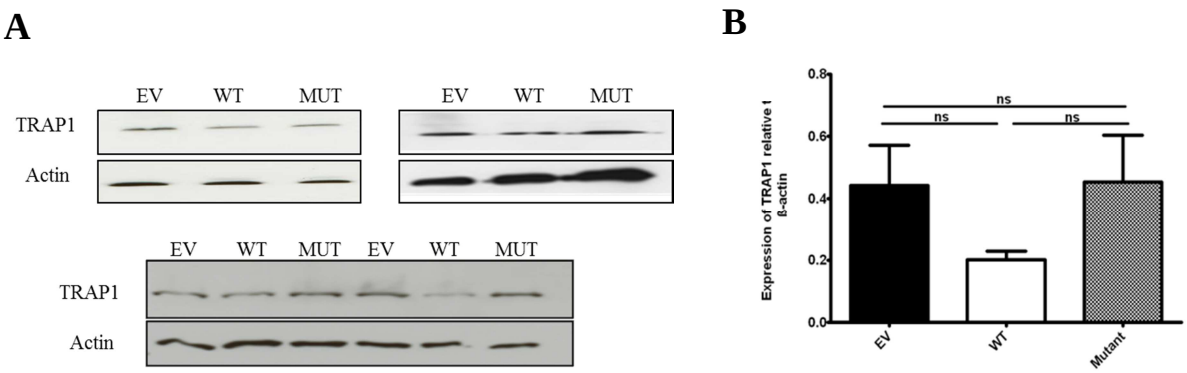

Figure 3.32 HtrA2 influence on TRAP1 (A) Expression analyses of endogenous TRAP1 in HtrA2 KO MEFs overexpressing EV, HtrA2 WT and HtrA2 mutant on WB in four independent experiments. 50µg of protein was loaded in each well and probed for TRAP1 followed by ß-actin as a loading control. **(B)** Quantification of TRAP1 levels. Data is presented as the mean ±SD; n=4 where n is the number of independent experiments; *p<0.05, **p<0.01 and ***p < 0.001, one-way ANOVA, Statistical significance was determined by following "Tukey's Multiple Comparison Test".

As we can see in the figure 3.32, reintroduction of HtrA2 reduces the levels of TRAP1 compared to the knockout situation (EV) and reintroduction of protease dead HtrA2.

So from the above results it could be deduced that the Trap1 levels may be increased in HtrA2KO situation (EV) and that expressing the protease-dead mutant HtrA2 has no effect but HtrA2 WT levels of HtrA2 reduce Trap1 suggesting that TRAP1 might be a substrate of HtrA2 inside mitochondria.

4. DISCUSSION

These results provide the first evidence *in vivo*, linking overexpression of HtrA2 to neurodegeneration. Here we show that the overexpression of human HtrA2 in mice leads to motor deficits, proposed to be caused by apoptosis in cerebellum, cortex and basal ganglia region of brain and paralleled by aggregation of alpha-synuclein. In addition, the G399S mutation in HtrA2 was not found to have a toxic gain of function since the mice overexpressing human G399S HtrA2 do not manifest a significant motor phenotype or neuronal apoptosis. However, low expression levels of transgenic G399S HtrA2 compared to WT HtrA2 in the cerebellum, coupled with a mild pathological and behavioral phenotype means that the toxic effect of the mutation cannot be ruled out completely.

4.1 BIOCHEMICAL & IMMUNOHISTOCHEMICAL CHARACTERISATION OF THE HUMAN HTRA2 MOUSE LINES

Biochemical investigation of our transgenic human HtrA2 mouse models showed similar levels of overexpression of the transgene between HtrA2 G399S and WT mice in the majority of the brain regions investigated with the exception of the cerebellum, where the overexpression of WT HtrA2 protein is higher than that of G399S HtrA2. Using the Prp promotor we expected similar levels of overexpression in both lines. However, the expression of WT and G399S HtrA2 at the DNA (Fig. 3.2) and mRNA level (Fig.3.1), detected by PCR and RT-quantitative PCR respectively is equal. These data suggest that there might be some post-transcriptional or post-translational effects occurring due to the G399S mutation in HtrA2 which leads to less expression in different brain regions of TG HtrA2 G399S mice. So we speculate that G399S mutation in HtrA2 might lead to RNA-instability and hence less protein expression. Another reason for low expression levels of

HtrA2 in TG G399S mice could be that this mutation might lead to protein misfolding and hence promoting its degradation, although the above effects were not assessed in our mouse lines. Yet other important facts that might affect the expression level of protein are the transgene integration site and the transgene copy number. There are evidences which suggest that the randomly integrated transgene is susceptible to “position effect variegation (PEV)” that often causes impaired transgene expression and in some cases might lead to complete gene silencing (Eissenberg, 1989; Allshire et al., 1994). Though increased copy number of transgenes sometimes leads to increased expression, but there are some incidences in literature where low or silenced transgene expression is reported in transgenic mice with high-copy-number arrays of transgene, and a reduction in the copy number in these mice resulted in a significant increase in transgene expression (Garrick et al., 1998). The PCR data from our HtrA2 mouse lines suggested that expression at mRNA level was similar in both TG HtrA2 WT and TG HtrA2 G399S mouse lines (Fig. 3.2).

Our immunohistochemical data also showed expression of transgenic HtrA2 using HtrA2 and FLAG antibody in all brain regions (Fig.3.5A-C) which complements our biochemical investigations. However, HtrA2 has a complex tertiary and quaternary structure and is difficult to stain immunohistochemically and perhaps hidden epitopes. However, Immunohistochemical analyses confirmed HtrA2 overexpression in the brains of transgenic animals and that the expression is ubiquitous in all brain regions and the different body organs tested. This is in accordance with the PD pathology since it is evident from the literature that PD is a multisystem disorder, affecting many brain regions and peripheral nervous system (Braak et al., 2003). Studies have identified early gastrointestinal, olfactory, autonomic, and sleep disorders even before the manifestation of motor symptoms. So these models which are based on a broadly expressed promotor are advantageous because they are likely to reproduce the wide range of abnormal changes associated with PD. In one of the first studies conducted on HtrA2 in vivo, a neuroprotective role of HtrA2 was demonstrated in a mouse model with complete HtrA2 KO. The motor phenotype in these mice was

reminiscent of PD and relevant loss of neurons in the striatum was observed (Martins et al., 2004). In fact HtrA2 came into focus in relation to PD, when mnd2 (motor neuron degeneration 2) mutation found in mouse was identified as a homozygous missense mutation (Ser276Cys) in the protease domain. The earliest symptoms observed in these mice were altered gait and cessation of normal weight gain, followed by ataxia, repetitive movements and akinesis. Striatal neurons were most susceptible in these mice, but other neurons in the central nervous system, brain stem and spinal cord, including motor neurons were affected at later stages (Rathke-Hartlieb et al., 2002). Both the features of necrosis and apoptosis were observed in these mice. More recently mnd2 mice – a mouse model with ubiquitous expression of HtrA2, were used to investigate the rescue potential from the neurodegenerative phenotype by reintroduction of WT HtrA2 in these mice. Therefore mnd2 mice were crossed with a mouse model with transgenic expression of human HtrA2 in the central nervous system (Kang et al., 2013). The transgenic expression of human HtrA2 in the central nervous system of mnd2 mice rescues them from neurodegeneration and prevents their premature death. This study proved very useful as it not only confirmed the neuroprotective role of HtrA2 but also revealed the role of HtrA2 in ageing. Adult transgenic mnd2 mice were reported to develop ageing phenotypes, such as weight loss, hair loss, reduced fertility, curvature of the spine and death by 12-17 months of age. These mice also have elevated levels of clonally expanded mitochondrial DNA deletions in their tissues linking mitochondrial protein quality control to mitochondrial DNA deletions and ageing in mammals (Kang et al., 2013). As our HtrA2 mouse models also express the transgenes in all brain regions they more closely reflect the pathological pattern observed in PD and may be advantageous compared to models based on very restricted expression under brain region specific promoters such as Thy-1 promoter (Kemshead et al., 1982).

4.2 OVEREXPRESSION OF HUMAN HTRA2 WT AND G399S MUTANT IN MICE- BEHAVIORAL IMPLICATIONS

It has already been shown that mice lacking HtrA2 expression or function display a neurodegenerative phenotype resembling PD and mitochondrial dysfunction also observed as one possible pathway involved in molecular pathologies underlying PD (Jones et al., 2003; Martins et al., 2004). Later several studies found an association of different genetic HtrA2 variants with PD (Strauss et al, 2005; Bogaerts et al, 2008; Lin et al, 2007). Additionally, recent reports described, that the G at position 399 and P at 143 is highly conserved in different species compared to other HtrA2 mutations which again points at the importance of these mutation and its further investigation in relation to PD. In a study on German PD patients, the G399S mutation was identified in sporadic PD patients based on the reported absence of other affected family members. In these carriers, the age at disease onset ranged from 49 to 77 years (mean 57.3±SEM 13.3 years). Clinical symptoms included the typical features of idiopathic PD including bradykinesia, tremor and muscular rigidity without any signs of atypical Parkinsonism (Strauss et al., 2005). We speculated on a dominant negative effect of the G399S mutation in relation to PD. Therefore the model of G399S HtrA2 overexpression was chosen to demonstrate its pathogenic role *in vivo* compared to overexpression of WT HtrA2 which was expected not to be harmful according to this concept. So to investigate the possible implications of overexpression of WT HtrA2 and G399S HtrA2 human mutation for PD, behavioral studies were conducted with our HtrA2 transgenic mouse lines overexpressing WT HtrA2 and G399S HtrA2.

Motor impairment test – rotarod – was performed in our mice from the age of 6 months until the age of 14 months every 8 weeks in order to determine progressive potential motor and learning impairment. The advantage of this test is that it creates a discretely measurable continuous variable (length of time) that can be used for statistical purposes to quantify the

effects of different drugs, overexpressed proteins, conditions and procedures (Rustay et al., 2003).Testing of genetic mouse models on rotarod may help to determine the role of particular mutations in genes or the role of mutated proteins for maintaining balance and coordination (Braak et al., 2003; Kalaitzakis et al., 2008).

TG HtrA2 WT mice showed a motor impairment from the first test at 6 months compared to Non-TG and TG HtrA2 G399S animals (Fig.3.8A). These findings persisted over all test time points and gradually worsened (Fig.3.8B-E). While Non-TG and TG HtrA2 G399S animals showed stable results. Moreover, TG HtrA2 WT showed evidence for a mild depletion in learning ability. These results are summarized in figure 3.9. The results for a progressive motor impairment were subsequently confirmed on and independent paradigm, the challenging beam walk (Fig.3.11). In the literature motor performance alterations were described for HtrA2 KO mice on the inclined-platform test (Martins et al., 2004). Inclined-platform test is also a measure of deficiencies in motor coordination like rotarod and beam walk. Poor performance of mice in these tests implies impairments in motor coordination. Our findings on HtrA2 Overexpressing mice and the results of HtrA2 KO mouse suggest that HtrA2 is a double edged sword which in both the cases, either complete loss or overexpression, leads to a PD like phenotype. Rathke-Hartlieb *et al.* observed symptoms of altered gait and cessation of normal weight gain, followed by ataxia, repetitive movements and akinesis in a spontaneous recessive inherited mutation of mnd2 in 2002 and this essentially is the same phenotype as in the HtrA2 KO mice. Our HtrA2 WT overexpressing mice also showed a motor phenotype even though not severe as KO mice. This gives the impression that the HtrA2 gene can lead to similar phenotypes through different pathways.

The question arising from these motor behavioral results is why the overexpression of HtrA2 leads to motor defects in mice as does the knockout of the same protein?

As only TG HtrA2 WT mice showed a PD like phenotype in the rotarod and challenging beam walk test, our results point towards a toxic gain of function for overexpression of WT HtrA2.

The lack of dominant effect of mutation on motor phenotype in TG HtrA2 G399S mice rather argues in favor of haploinsufficieny as a mechanism in humans or could be due to dose effect (since the transgene G399S HtrA2 is less expressed in the cerebellum of this line compared to TG HtrA2 WT line). Indeed it has been shown that G399S mutant HtrA2 displays a reduced serine protease activity *in vitro* following activating stimuli (Strauss et al., 2005). This supports the notion that the loss of HtrA2 function due to the G399S mutation is present, but may not lead to a dominant effect in heterozygous patients. In mice having an endogenous background of WT mouse HtrA2 therefore the loss of function variant G399S may be without an effect on proper HtrA2 function.

In another behavioral test – Open Field (OF) – both mouse lines investigated did not show significant differences in the pattern of movement in a novel environment compared to NT controls (Fig.3.12). The amount of time spent in motion by each mouse line was similar (Fig.3.13A) signifying that there is no difference in the general locomotor activity of the TG HtrA2 WT mice, TG HtrA2 G399S mice and Non-TG mice. However, there was a tendency of increase in the latency for the center for both transgenic lines compared to Non-TG mice, giving an impression of anxiety like behavior or hypersensitivity in these transgenic lines, yet without statistical significance. Moreover the data showed that the mice from TG HtrA2 WT mouse line once reached, spent more time at the center and the tracing pattern at the center as observed from the raw data (Fig. 3.12) was comparable to Thy1-aSyn mice in OF at the age of 4-5 months (Chesselet and Richter, 2011), yet in a lower intensity. 10 of 12 TG HtrA2 WT mice and 8 of 12 TG HtrA2 G399S mice showed this representative pattern of anxiety like behavior or hypersensitivity in contrast to only 6 of 12 mice of the control group. Thus, the phenotype is not displayed in every individual of the group, but frequency and thus might be anxiety level varies between the three groups. Thy1-Syn mice also showed alpha-synuclein aggregates in SN and motor defect on challenging beam (Chesselet et al., 2012). These parallels between Thy1-aSyn mice and HtrA2 mice points to the fact that the two

models may show similarity in terms of anxiety. Although to date, anxiety levels in HtrA2 G399S mutation carrier PD patients have not been investigated. .

According to OF data we suggest that there is no general locomotor defect in any of our mouse lines in a novel environment. However, there might be some anxiety in the transgenic mouse lines, yet these results have to be confirmed by further and alternative experiments to confirm any significance.

Altogether from the behavioral results on HtrA2 overexpressing mice, it can be concluded that the overexpression of WT HtrA2 in mice leads to motor and coordination impairments with mild effect on anxiety levels. Though overexpression of mutant G399S HtrA2 in mice had no implicit effects on motor behavior of the mice, there is tendency of increased anxiety in these mice compared to Non-TG mice.

4.3 MECHANISM UNDERLYING MOTOR PHENOTYPE

4.3.1 IMPAIRED MITOCHONDRIAL QUALITY CONTROL IN TG HTRA2 WT MICE

To find the mechanism underlying the motor phenotype in our TG HtrA2 WT mice, various causes were considered. Since most of the earlier HtrA2 mouse models showed mitochondrial dysfunction or mitochondria dependent apoptosis, we investigated mitochondrial dysfunction including mitochondrial and nuclear encoded mitochondrial proteins expression levels (Fig.3.15). As HtrA2 is a mitochondrial protein we expected that the toxic gain of function in TG HtrA2 WT mice could be the result of disturbed mitochondrial quality control due to overload of protein. And one way to address quality control disturbances is to assess the expression levels of mitochondrial proteins. This method of assessing the mitochondrial protein expression levels was also applied to decipher mitochondrial defects by Moisoi at al., 2009. Complex IV subunit I which is a mitochondrial encoded protein showed no significant differences in expression level in the cerebellum and

basal ganglia of three different mouse lines though in cortex the Complex IV subunit I showed significant higher expression level in TG HtrA2 G399S mice compared to TG HtrA2 WT mice. There was no difference in VDAC (porin) levels, a nuclear encoded mitochondrial protein. Similar results were also described in the HtrA2 KO model with no significant differences in the function of any of the mitochondrial enzymes including complex IV compared to control mice (Martins et al., 2004). The significant upregulation of Complex IV subunit I in cortex of TG HtrA2 G399S mice compared to TG HtrA2 WT mice might be a compensatory, protective or even toxic gain of function of mutant HtrA2 in this region, even though less expressed compared to TG HtrA2 WT mice. There is evidence in the literature that the loss of HtrA2 in mice results in mitochondrial unfolded protein response with insoluble mitochondrial protein aggregation in KO mouse brains (Moisoi et al., 2009). This might further lead to mitochondrial unfolded protein response (mtUPR) with insoluble mitochondrial protein aggregation as shown in HtrA2 KO mouse brains (Moisoi et al., 2009) paralleled by upregulation of several mitochondrial proteins including complex IV subunit I as a result mitochondrial stress response.

From our findings we speculate that HtrA2 G399S overexpression might result in disturbed chaperone network and ROS production in these mice. Increased ROS production has been described in *in vitro* HtrA2 KO condition (Strauss et al., 2005) which can be rescued by reintroduction of WT HtrA2 (Kieper et al., 2010). ROS production might damage respiratory complexes and other mitochondrial proteins (Kang et al., 2013) resulting in the loss of mitochondrial respiratory competence and reduced intracellular ATP levels. This could lead to rupture of the plasma membrane and necrotic cell death (Leist et al., 1997). Hence assessment of ROS production levels in fibroblasts would have been interesting in our mouse lines, but unfortunately the Prp promoter does not result in expression of transgene in fibroblasts.

4.3.2 IMPAIRED AUTOPHAGY IN TG HTRA2 WT MICE

It has been described in the literature that HtrA2 is involved in autophagy (Li et al., 2010) by digestion of proteins such as Hax-1 which is involved in repression of autophagy. HtrA2-induced autophagy also facilitates the degradation of neurodegenerative proteins such as pathogenic A53T alpha-synuclein and endogenous autophagy substrate p62 (Li et al., 2010). We obtained non-significant results for LC3-II, a marker for autophagy. So, further investigation is needed in this direction. Disturbances in autophagy might lead to diminished mitochondrial and organellar quality control in these animals (Li et al., 2010).

4.3.3 AGGREGATE FORMATION IN TG HTRA2 WT MICE

Alpha-synuclein is the main constituent of Lewy bodies in PD patients. Interestingly, we found alpha-synuclein aggregates (Fig.3.18) in cerebellum, cortex and basal ganglia regions of brain of TG HtrA2 WT mice, though no aggregates were found in Non-TG mice and a tendency to form aggregates was observed in TG HtrA2 G399S mice. The tendency to form aggregates in TG HtrA2 G399S mice points to a pathological process that involves alpha-synuclein accumulation and therefore might involve similar mechanisms as in PD. There are findings in literature which suggest a direct relation between alpha-synuclein gene dosage and PD disease progression. Genomic triplication of the alpha-synuclein gene has been reported to cause hereditary early-onset Parkinsonism with dementia (Singleton et al., 2003) On the contrary the clinical phenotype of alpha-synuclein duplication patients closely resembles idiopathic PD with neither cognitive decline nor dementia (Chartier-Harlin et al., 2004). Moreover accumulation of HtrA2 in neuronal and glial inclusions in brains with alpha-synucleinopathies has been reported (Kawamoto et al., 2008) which shows co-existence of HtrA2 and alpha-synuclein pathology and hence support our findings.

PK digestion in brain slices before staining with alpha-synuclein, confirmed the presence of insoluble, PK-resistant alpha-synuclein aggregates in TG HtrA2 WT mice (Fig.3.19).

Proteinase K digests soluble proteins and has been established as a reliable method to define the presence of insoluble aggregates both in vitro and in vivo (Neumann et al., 2002). Alpha-synuclein aggregation in our disease model might be the result of diminished autophagy (Dexter et al., 1989a), dysfunction of cellular machinery that includes chaperone networks (that regulate protein folding and refolding) (Hartl et al., 2011) or impairment of the ubiquitin-proteasomal system (UPS) and autophagy-lysosomal pathway (ALP) which are responsible for elimination of harmful proteins (Tyedmers et al., 2010). Similar abnormal aggregates observed in the mnd2 mice were linked to decreased basal autophagy in these mice (Li et al., 2010). However here in mnd2 mice there is loss of HtrA2 function mechanism involved while in our HtrA2 overexpressing mouse lines it might be the result of interference of human HtrA2 with mouse HtrA2. Disturbed protein quality control and more defective proteins might be the reason for the observed increase in ubiquitinated proteins in TG HtrA2 WT mice (Fig.3.20). Presence of more ubiquitinated proteins can lead to overload and further disturbance in UPS and ALP pathway. The addition of ubiquitin can affect proteins in many ways: it can signal for their degradation via the proteasome, alter their cellular location, affect their activity and promote or prevent protein interactions (Glickman and Ciechanover, 2002; Schnell and Hicke, 2003) Ubiquitination plays an important role in aggregate formation and proteins intended for proteasomal degradation and Lewy bodies typically contain ubiquitinated alpha-synuclein (Ubl et al., 2002)

According to the literature, the human genetic data strongly support a causal role for alpha-synuclein in PD. Whether Lewy bodies are causal or consequential is less clear, but they do support the idea that alpha-synuclein represents an important link between sporadic and inherited PD (Cookson, 2009). The various lines of evidence identify alpha-synuclein as a potentially toxic protein, fulfilling the requirements of a causative agent in PD (Cookson, 2009). There is evidence from the literature for endogenous alpha-synuclein aggregates and oligomers in brain extracts from rodent models (Mazzulli et al., 2011; Winner et al., 2011) as observed in our disease model. Unfolded proteins and aggregates were also observed in

HtrA2 deficient neuronal cells (Moisoi et al., 2009). Since HtrA2 has been proposed to be a mitochondrial chaperone (Gray et al., 2000), overexpression of this protein in mice might lead to dysfunction of the chaperone network resulting in alpha-synuclein aggregation. And we propose that alpha-synuclein mediated toxicity causes cell death leading to motor phenotype in our TG HtrA2 WT mice.

4.3.4 APOPTOSIS IN TG HTRA2 WT MICE

In order to check whether alpha-synuclein toxicity leads to cell death in our TG HtrA2 WT mouse line various cell death assays were conducted in our mouse lines including TUNEL assay which has been used in mouse models and is claimed as a reliable method for finding apoptotic cell death in mice (Hubener et al., 2011). Significantly higher numbers of apoptotic nuclei were observed in TUNEL assay in cerebellum, basal ganglia and cortex region of TG HtrA2 WT mice compared to Non-TG and TG HtrA2 G399S confirming more cell death in this line (Fig.3.22A-F). The number of apoptotic nuclei was also significantly higher in the cerebellum and cortex region of TG HtrA2 G399S mice (Fig.3.22 D, F) compared to Non-TG mice but significantly less than TG HtrA2 WT mice, although the number of apoptotic nuclei in the basal ganglia region of TG HtrA2 G399S mice was almost similar to Non-TG mice (Fig.3.22 E). These results provide an explanation for the motor phenotype observed in TG HtrA2 WT mice in contrast to TG HtrA2 G399S mice, which only show increased cell death in the cortex and cerebellum region. HtrA2 KO mice (Martins et al., 2004) again show similar results with cell death specifically in the striatum, a region in basal ganglia. These findings suggest that motor phenotype specifically is related to cell death in basal ganglia region of brain.

Higher amounts of cleaved caspase 9 (Fig.3.23A-B) in TG HtrA2 WT mice compared to the Non-TG and TG HtrA2 G399S mice confirmed increased apoptotic cell death in cerebellum of this line (Fahn and Cohen, 1992; Perry et al., 1997; Katunuma et al., 2001). Again TG HtrA2 G399S mice showed more cell death in cortex region compared to Non-TG mice and

TG HtrA2 WT, yet TG HtrA2 WT mice showed more cell death than Non-TG mice. The findings in the basal ganglia also confirmed the TUNEL assay with increased cell death only being observed in TG HtrA2 WT animals, though not at significant level. Caspase 9 is the initiator of apoptotic cell death pathway and hence higher amount of cleaved caspase 9 is the marker of cell death (Vande Walle et al., 2008). Similarly caspase 3 which is the marker of the execution phase of apoptosis showed results in line with the findings of caspase 9 in activity assay (Fig.3.23). HtrA2 has already been linked to caspase activity in germ cell death in Drosophila (Yacobi-Sharon et al., 2013). Further we propose as reported in the literature, that induction of mitochondrial permeability pore opening resulting from misfolded and aggregated proteins, might lead to release of mitochondrial pro-apoptosis proteins that activate the caspase-dependent and independent cell death cascades in our disease model (Yacobi-Sharon et al., 2013). Previously, both necrosis and apoptosis were observed in mnd2 mice. Early degeneration of mitochondria was also noted (Rathke-Hartlieb et al., 2002). To investigate specifically the dopaminergic cell death, TH level was also checked in three different regions of brain – cerebellum, basal ganglia and cortex - from the three different mouse lines (Fig. 3.24 A, B and C respectively). In the cerebellum region TH levels are significantly upregulated in both the transgenic mouse lines compared to Non-TG mice. There are some Purkinje cells and some neurons in the deep cerebellar nuclei in which TH is present (Yew et al., 1995). Similarly there was a trend for an increase in TH levels in the basal ganglia of both the transgenic lines, though this tendency was not significant, pointing at disturbed protein quality control in both the transgenic mouse lines in dopaminergic neurons. It has already been shown that TH is upregulated for example in the case of intermittent hypoxia followed by increase in TH activity involving ROS mediated sustained increase in TH phosphorylation via downregulation of protein phosphatase 2A and upregulation of protein kinases (Raghuraman et al., 2009). As there is also evidence from the literature that HtrA2 knock down leads to mitochondrial uncoupling accompanied by altered breathing pattern and, on a cellular level, ATP depletion and vulnerability to chemical

ischaemia (Plun-Favreau et al., 2012), it could be speculated that the overexpression of HtrA2 WT and HtrA2 G399S protein in mice might also have some effect in breathing pattern and lead to intermittent hypoxia followed by ROS production and upregulation of TH. Yet no experiments to confirm this hypothesis have been conducted in our animal lines. Having confirmed increased cell death in TG HtrA2 WT mouse line and to some level also in TG HtrA2 G399S mice, we asked which of the two ways to cell death having been described for HtrA2 in the literature (Papa and Germain, 2011) (Suzuki et al., 2004) was prevalent in our model,

- Inhibiting inhibitor of apoptotic proteins (IAP´s) or
- Direct protease activity.

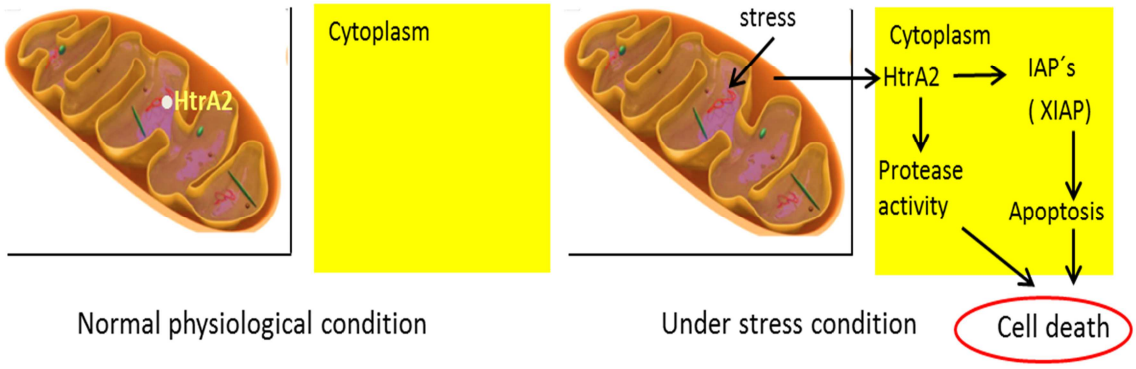

Figure 4.1 HtrA2 mediated cell death

The levels of XIAP (X chromosome-linked inhibitor of apoptosis protein), one of the well-known substrate of HtrA2 (Suzuki et al., 2001), were analyzed in the cerebellum, cortex and basal ganglia region of HtrA2 mouse lines. Surprisingly, the levels of XIAP were increased rather than decreased in TG HtrA2 WT mice compared to Non-TG controls suggesting that increased protein expression of WT HtrA2 does not result in direct degradation of the substrate XIAP. Moreover XIAP showed significant upregulation in the basal ganglia of TG HtrA2 G399S mice compared to Non-TG mice and also a similar tendency in cortex and cerebellum. The increased levels of XIAP could be a compensatory response against apoptotic stimuli triggered due to the catalytic activity of HtrA2 by XIAP, but further work on

the protease activity of HtrA2 in our models needs to be undertaken. The other possibility is that there might be some another substrate than XIAP which is involved in HtrA2 mediated cell death in TG HtrA2 WT mice or there could be cross talk between different cell death pathways involved in the process.

4.4 NUCLEAR COLOCALISATION OF PHOSPHOSERINE 400 HTRA2 IN TG HTRA2 WT MICE

From the literature it is known that two confirmed phosphorylation sites of HtrA2 are adjacent to two of the mutation sites of HtrA2 in PD patients. Serine 400 HtrA2 is adjacent to the site of the conserved amino acid G399, which has been found to be mutated in some PD patients (Strauss et al., 2005). It was found that HtrA2 was phosphorylated upon activation of the p38 pathway in a Pink1-dependent manner, and there was an increase in phosphorylated HtrA2 in the brains of sporadic PD patients and decreased in Pink1 mutated patients (Plun-Favreau et al., 2007; Zhang et al., 2007). It is also reported that HtrA2 is phosphorylated at S400 by Cyclin-dependent kinase-5 (Cdk5) in a p38-dependent manner (Fitzgerald et al., 2012). Here it's also reported that phosphorylation of HtrA2 at S400 is involved in maintaining mitochondrial membrane potential under stress conditions and hence important for mitochondrial function. Activation of similar pathway is also involved in the phosphorylation of another site, S142, which is also located adjacent to the site of mutation, found in PD patients and is phosphorylated in a p38 and Pink1-dependent manner (Plun-Favreau et al., 2007). HtrA2 is also reported to be phosphorylated at S212 by Akt which reduces its protease activity (Yang et al., 2007).

As shown in section 3.1.3.4 of results, phosphorylated HtrA2 showed increased colocalisation with nuclei in TG HtrA2 WT mice, the line with PD like phenotype. This could be another quality control phenomenon under stress conditions. There have been contradicting theories in terms of phosphorylation of HtrA2 in the literature, some PD patients show increased phosphorylated HtrA2, while PINK1 mutant PD patients show the opposite

(Plun-Favreau et al., 2007). It has been suggested that phosphorylation of HtrA2 might modulate its proteolytic activity (Plun-Favreau et al., 2007). Our analysis of colocalisation of phoshpo-HtrA2 in nucleus gave varying results in different regions of the brain of the affected line indicating a still unclear role of the protein in quality control mechanisms. The evaluation of Phosphoserine 400 HtrA2 in SHSY-5Y cells confirmed that the effect of nuclear colocalisation of Phosphoserine 400 HtrA2 is not the effect of FLAG-tag, because most of the Phosphoserine 400 HtrA2 was colocalised in nucleus even in untransfected SHSY-5Y cells and cells transfected with normal WT HtrA2 construct without a FLAG-tag. Altogether, the nuclear colocalisation of phosphoserine 400 HtrA2 could be a signal for the caspase activation, markers of execution phase of apoptosis. An alternative explanation could be that the amount of nuclear colocalisation of Phosphoserine 400 HtrA2 in-vivo could be one of the mechanisms involved in quality control mechanism. It could be interesting to investigate the cause for nuclear colocalisation of Phosphoserine 400 HtrA2 as it could be relevant to mechanism involved in PD.

However, the data is mainly obtained from immunohistochemistry and the use of Phosphoserine 400 HtrA2 antibody in immunohistochemistry is not confirmed, no conclusions can be drawn from the above results.

4.5 HTRA2 ROLE IN MITOCHONDRIAL MORPHOLOGY REGULATION AND MITOCHONDRIAL DEGRADATION

It has already been shown that HtrA2 plays an important role in mitochondrial morphology (Kieper et al., 2010). So to further investigate the role of HtrA2 at a functional level we used stable MEF cells with KO background expressing EV, HtrA2 WT and HtrA2 protease dead mutation (S306), respectively. In live cell imaging results (Fig.3.29) it could be clearly seen that in the absence of HtrA2 expression and function (S306 protease dead mutation) there is more colocalisation of mitochondria with lysosomes which implies that there is more mitophagy. Mitophagy is a mechanism which can be used by cells to remove impaired

mitochondria via the lysosomes. It has been already demonstrated that HtrA2 deficiency causes an accumulation of reactive oxygen species and reduced mitochondrial membrane potential (Martins et al., 2004; Kieper et al., 2010). In HtrA2 KO mouse embryonic fibroblasts, as well as in HtrA2 silenced human Hela cells and Drosophila S2R + cells, it has been shown by live cell imaging that mitochondria are elongated and here mitochondrial morphology alterations were also confirmed by Electron microscopy (Kieper et al., 2010).

The presence of more LC3-GFP puncta in the absence of HtrA2 expression and function showed that autophagy is enhanced when HtrA2 is absent. Furthermore the results from FACS analysis showed that there is less mitochondrial mass in the absence of HtrA2 expression or function confirming the results from live cell imaging. Together these results suggest that HtrA2 is indispensible for mitochondrial integrity.

Being a mitochondrial protease, HtrA2 interacts with several other proteins. One of the novel interacting partners of HtrA2 has been found in our lab named as TRAP1 (unpublished work). Furthermore we found that the loss of HtrA2 expression and function increases TRAP1 expression (Fig.3.32) at endogenous level. Since TRAP1 is a mitochondrial chaperone, our findings from the cell culture experiments suggest that absence of HtrA2, which is also a mitochondrial chaperone, might lead to disturbed chaperone network or upregulation of other chaperones such as TRAP1. This might be a compensatory mechanism to cope up for the loss of HtrA2. Similarly, TRAP1 could be a target of HtrA2 protease activity within mitochondria and the levels of TRAP1 regulated by HtrA2 may prove to be an important quality control mechanism within mitochondria to extend cell survival.

5.CONCLUSIONS

In summary, TG mice overexpressing WT but not G399S HtrA2 have a significant motor behavioral phenotype and alpha-synuclein aggregation followed by apoptotic cell death. Even though no motor phenotype was observed in TG HtrA2 G399S mice, we observed a tendency of alpha-synuclein aggregation and cell death in TG HtrA2 G399 mice compared to Non-TG mice though not at the level of TG HtrA2 WT mice.

All our findings in TG HtrA2 WT mice are quite contradictory to the findings by Liu et al., 2007 who showed that neuron specific overexpression of human HtrA2 leads to no phenotype and that HtrA2 plays a role only in the protection of neurons. However this study showed no behavioral or cell death assays and the results were conferred from basic criteria such as weight of different organs and mice, hair phenotype or pregnancy abnormalities etc. On the other hand, here we show that TG HtrA2 WT mice exhibit a significant motor phenotype in rotarod and challenging beam walk test and point towards a toxic gain of function for overexpression of WT HtrA2. The lack of dominant effect of the G399S mutation on motor phenotype argues in favor of haploinsufficieny as a mechanism in humans or potentially a dose effect (since the transgene G399S HtrA2 is less expressed in the cerebellum of this line compared to TG HtrA2 WT line). But at the same time the extra-cerebellar pathologies were more pronounced in TG HtrA2 WT mice compared to G399S, though expression levels of transgene were similar for example in cortex - both alpha-synuclein aggregation, activation of apoptotic markers such as caspase 9 and apoptotic cell death based on TUNEL assay was observed more in TG HtrA2 WT mice compared to TG HtrA2 G399S mice. Indeed it has been shown that G399S mutant HtrA2 displays a reduced serine protease activity *in vitro* following activating stimuli (Strauss et al., 2005). This supports the notion that the loss of HtrA2 function due to the G399S mutation is present, but may not lead to a dominant effect in heterozygous patients. In mice having an endogenous background of WT mouse HtrA2 therefore the loss of function variant G399S may not fully exert its effect on HtrA2 function.

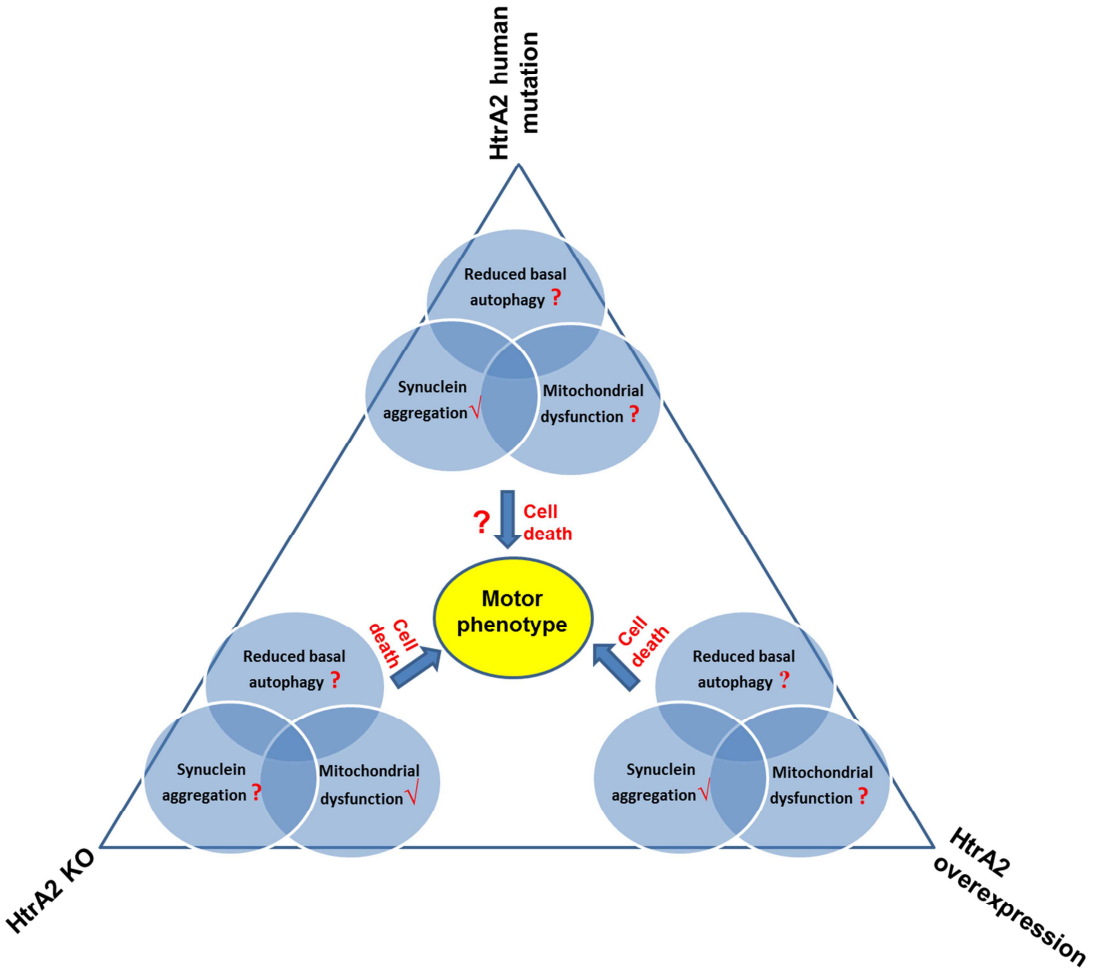

Figure 4.2 Conclusions from HtrA2 mouse models. Our findings on HtrA2 overexpressing models –TG HtrA2 WT and TG HtrA2 G399S mice and findings from the literature on other HtrA2 KO mice suggest that HtrA2 has important and diverse functions inside and outside of mitochondria. Deregulation of HtrA2 can lead to PD like symptoms both in the absence as well as in case of overexpression. The role of the G399S HtrA2 mutation could not be fully deduced by our TG HtrA2 G399S mice due to lack of significant pathologies or phenotype. For example, there was a tendency for alpha-synuclein aggregation in these increased cell death though this was not as significant overall when considering the overall data including behavioral characterization as the TG HtrA2 WT mice compared to Non-TG mice. The exact role of G399S human HtrA2 mutation remains unclear and further work is needed to uncover the effect of this mutation in HtrA2 KO background. Overexpression of WT HtrA2 on the other hand is significantly detrimental in terms of cell death, protein aggregation and motor function of the mice, all phenotypes that are strongly associated with Parkinson's disease in humans.

6.SUMMARY AND OUTLOOK

The mitochondrial protease HtrA2 is localized in the mitochondrial intermembrane space and has a pro-apoptotic function when released into the cytosol. Its role in neuroprotection was initially identified by the demonstration of neurodegeneration and mitochondrial dysfunction in the mice lacking HtrA2 expression or function (Jones et al, 2003; Martins et al, 2004). Furthermore Parkinson's disease (PD)-associated variants of HtrA2 have been described in German, Belgian and Taiwanese patients (Strauss et al, 2005; Bogaerts et al, 2008; Lin et al, 2007). Although several studies have pointed to the importance of a protective role for HtrA2 within the mitochondria, the mechanism of neuroprotection is still not clear. It has been shown that G399S mutant HtrA2 displays a reduced serine protease activity *in vitro* following activating stimuli arguing in favor of a dominant negative effect of the G399S mutation in relation to PD(Strauss et al., 2005). Therefore a mouse model of human G399S HtrA2 overexpression (TG HtrA2 G399S) was chosen to investigate its pathogenic role *in vivo* compared to overexpression of human WT HtrA2 (TG HtrA2 WT).

We assessed the effect of WT HtrA2 and G399S HtrA2 overexpression in mice using behavioral, immunohistochemical and biochemical approaches in order to further define the role of HtrA2 in PD. The TG HtrA2 WT mice showed significant motor impairments compared to Non-TG mice, while TG HtrA2 G399S mice revealed no difference compared to Non-TG mice using rotarod and beam walk test, which was not expected according to our hypothesis. As a potential cause for motor impairments, we found a significant increase of apoptotic nuclei in the cerebellum, cortex and basal ganglia of TG HtrA2 using TUNEL staining. Significant increase in apoptotic nuclei was also found in cerebellum and cortex of TG HtrA2 G399S mice. Alpha-synuclein aggregates were found in cerebellum, cortex and basal ganglia of TG HtrA2 WT mice, which were shown to be PK resistant. Increased amounts of ubiquitinated proteins were observed in cerebellum of the TG HtrA2 WT mice which represents another hint for impairment in degradation mechanisms and aggregation of

insoluble alpha-synculein in this mouse line. Although no obvious change in expression pattern of mitochondrial proteins was observed in cerebellum, cortex and basal ganglia, but significant upregulation of HtrA2 substrate XIAP in basal ganglia, and cleaved caspases in cerebellum and cortex of TG HtrA2 WT and cortex of TG HtrA2 G399S mice were detected. Upregulation of XIAP in basal ganglia might be a compensatory mechanism, but also pointing to the fact that there might be another substrate involved in the cell death caused by HtrA2. Since TG G399S HtrA2 mice do not present with a gain of toxic function, this rather argues against a dominant loss of function mechanism of the G399S mutation according to the behavioral assays. But if results from the biochemical and immunohistochemical assays are taken together we see some non-significant trends in TG HtrA2 G399S mice compared to Non-TG mice, which could be a result of unequal expression of the transgene in the cerebellum in TG HtrA2 G399S mice compared to TG HtrA2 WT mice. Although, the differences in transgene expression cannot completely rule out the differences in phenotype, the conclusion remains that the G399S HtrA2 mutation represents a dominant loss of function and further experiments in a HtrA2 KO background are required.

It is well known that human HtrA2 executes essential roles in the mitochondria and contributes to apoptosis through its protease activity (Plun-Favreau et al., 2007). Indeed protease activity of HtrA2 was previously found to depend on S400 phosphorylation and we found a redistribution of phosphoS400 HtrA2 from the cytosol to the nucleus in basal ganglia and cortex region of TG HtrA2 WT mice compared to the other two lines. It could be interesting to investigate the cause for nuclear colocalization of Phosphoserine 400 HtrA2 as it could be relevant to mechanism involved in PD as nuclear colocalization of phosphoserine 400 HtrA2 could be a signal for the caspase activation, markers of execution phase of apoptosis.

To further investigate the role of HtrA2 in PD the levels of other HtrA2 substrates, such as Hax-1, can be checked in our mouse models as recently HtrA2 has also been implicated as a positive regulator of autophagy facilitating the degradation of mutant proteins involved in

neurodegenerative diseases (Li et al., 2010). Here it has been reported that HtrA2 activates autophagy through digestion of Hax-1, which suppresses autophagy in a Beclin-1-dependent pathway.

The bacterial homologue HtrA is known to act as a molecular chaperone participating in protein re-folding at low temperatures (Faccio et al., 2000). Whether Omi/HtrA2 exerts similar functions in humans is not known, however, together with the known serine protease function Omi/HtrA2 may be involved in the control of protein stability (via its chaperone function) and turnover (via its protease function) and therefore participate in proteolytic stress response. Hence from our findings we speculate that HtrA2 WT and G399S overexpression might result in disturbed chaperone network, and the activity of mitochondrial complexes and ROS level can be assessed to see mitochondrial dysfunction in these models. Reduced Mitochondrial Citrate synthase activity was observed in HtrA2 KO model even though other complexes showed normal activity (Martins et al., 2004). Moreover our HtrA2 model has formation of endogenous alpha-synuclein aggregates and can be a model to study the pathways leading to the formation of alpha-synuclein aggregates, which represent the hallmark of PD as the major component of Lewy bodies in humans.

The lack of dominant effect of mutation on motor phenotype in TG HtrA2 G399S mice rather argues in favor of haploinsufficieny as a mechanism in humans. To confirm the implications of the G399S mutation in PD, the transgenic mouse line TG HtrA2 G399S could be cross bred to HtrA2 KO mice to investigate the effect of the HtrA2 G399S mutation and this experiment would confirm the loss of function by failing in rescue experiments.

Considering the HtrA2 connection with neurodegenerative disorders such as Alzheimer´s, Huntington´s and Parkinson´s disease (PD), HtrA2 has gained much importance in recent years. And these emerging roles of HtrA2 signify the importance of further research on this protein and extending potential findings in PD models to other diseases.

6.ZUSAMMENFASSUNG UND AUSBLICK

Die mitochondriale Protease HtrA2 ist im Intermembranraum lokalisiert und hat eine pro-apoptotische Wirkung, wenn sie in das Zytosol entlassen wird. Ihre neuroprotektive Rolle wurde ursprünglich durch Neurodegeneration und mitochondriale Dysfunktion in Mäusen mit gestörter Expression bzw. Funktion von HtrA2 gezeigt (Martins et al, 2004 Jones et al, 2003) . Darüber hinaus wurden in deutschen, belgischen und taiwanesischen Patienten Varianten von HtrA2 beschrieben, die mit der Parkinson-Krankheit assoziiert sind (Bogaerts et al , 2008; Lin et al , 2007, Strauss et al , 2005). Obwohl mehrere Studien die Bedeutung einer protektiven Wirkung von HtrA2 innerhalb der Mitochondrien gezeigt haben, ist der Mechanismus der Neuroprotektion noch unklar. Es hat sich gezeigt, dass die G399S-Mutation auf aktivierende Reize zu einer reduzierten Aktivität der Serin-Protease *in vitro* führt. Dies würde auf einen dominant negativen Effekt der G399S-Mutation in Bezug auf die PD hindeuten (Strauss et al. , 2005). Um die Rolle von HtrA2 besser zu verstehen haben wir Mäuse, die Wildtyp-HtrA2 und G399S- HtrA2 überexprimieren, mit immunhistochemischen und biochemischen Ansätzen sowie Verhaltenstests untersucht. Die transgene HtrA2-Maus, die Wildtyp-HtrA2 überexprimiert, zeigte signifikante motorische Defizte im Vergleich zu der nicht transgenen Maus, während die transgene Maus die G229S-HtrA2 überexprimiert keinen Unterschied zu der nicht-transgenen Maus im Rotarod-Test und *„beam walk test“* zeigte. Als möglichen Grund für die motorischen Beeinträchtigungen der transgenen HtrA2-Maus, fanden wir einen signifikanten Anstieg von apoptotischen Kernen im Cerebellum und den Basalganglien mittels TUNES-Färbung. Einen signifikanten Anstieg der Zahl an apoptotischen Kernen konnte auch im Cerebellum und Cortex der transgenen G229S-HtrA2 Maus nachgewiesen werden. Aggregate aus α-Synuklein wurden im Cerebellum, den Basalgalien und Kortex der transgenen Wildtyp-HtrA2-Maus gefunden, von denen gezeigt wurde, daß sie Proteinkinase-resistent sind. Im Kleinhirn der transgenen Wildtyp-HtrA2-Maus

wurde eine erhöhte Menge an ubiquitiertem Protein beobachtet, was einen Hinweis auf eine gestörte Aggregation und beeinträchtigtem Abbau von unlöslichem α-Synuklein ist. Obwohl keine offensichtlichen Veränderungen im Expressionsmuster von mitochondrialen Proteinen im Cerebellum, Kortex und Basalganglien beobachtet werden konnte, wurde eine signifikante Hochregulation von dem HtrA2-Substrat XIAP und gespaltene Caspasen im Cerebellum und im Kortex der transgenen Wildtyp-HtrA2-Maus sowie der transgene G399S-HtrA2 festgestellt. Die Hochregulation von XIAP in den Basalganglien könnte ein kompensatorischer Mechanismus sein, der darauf hindeutet, daß noch ein anderes Substrat bei dem Zelltod, der durch HtrA2 verursacht, eine Rolle spielen könnte. Weil die G299S-HtrA2-Maus keine Zunahme einer pathologischen Funktionsweise in den Verhaltenstest zeigt, spricht dies eher spricht dies eher gegen einen dominanten *„loss of function“* Mechanismus der G399S Mutation. Aber wenn man die Ergebnisse der biochemischen und immunhistochemischen Assays zusammennimmt, dann sieht man einige nicht-signifikante Trends im Vergleich der transgegen HtrA2-G399-Maus im Vergleich zu der nicht-transgenen Maus. Obwohl die Unterschiede in der Transgenexpression nicht die Unterschiede im Phenotyp ausschließen können, es bleibt die Vermutung, daß die G399S-HtrA2-Mutation einen dominanten „loss of function“ darstellt und weitere Experimente mit einem HtrA2-Knockout-Hintergrund benötigt werden. Es ist bekannt daß HtrA2 eine wichtige Rolle in den Mitochondrien und eine wichtige Rolle bei der Apoptose spielt (Plun-Favreau et al., 2007). Es konnte bereits gezeigt werden, daß die Proteaseaktivität von HtrA2 in der Tat von der S400-Phosphorylierung abhängt. In der transgenen Wildtyp-HtrA2-Maus konnten wir –im Vergleich zu zwei anderen Linien - eine Umverteilung in den Basalganglien und Kortex von phosphoryliertem S400-HtrA2 vom Zytosol in den Kern beochbachten. Es wäre interessant, die Gründe für die nukleäre Kolokalisation von Phosphoserine 400 HtrA2 näher zu untersuchen, da es ein wichtiger Mechanismus bei Parkinson sein könnte, so könnte Phosphoserine 400 HtrA2 ein Signal für die Aktivierung der Caspasen sein. Um die Rolle von HtrA2 bei Parkinson weiter zu untersuchen könnten in unserem Mausmodell auch die

Level von anderen HtrA2-Substraten wie Hax-1, das als positiver Regulator von Autophagozytose bei neurodegenerativen Erkrankungen den Abbau von mutierten Proteinen erleichtert. (Li et al., 2010). Es wurde berichtet, daß HtrA2 Auophagpzytose durch Verdau von Hax-1, das Autophagozytose über einen Beclin-1-abhängige Pathway unterdrückt.

Vom dem bakterielle Homolog von HtrA2 ist bekannt, daß es als molekulares Chaperon ist, das insbesondere die Faltung von Proteinen bei niedrigen Temperaturen ermöglicht. (Faccio et al., 2000). Ob Omi/HtrA2 eine ähnliche Funktion beim Menschen ausübt ist nicht bekannt. Wie dem auch sei, zusammen mit der bekannten Funktion als Serinprotease könnte Omi/HtrA2 an der Kontrolle (als Chaperon) und am Umsatz (als Proteinkinase) an der Stabilität von Proteinen und damit an der proteolytischen Stressantwort beteiligt sein. Aufgrund unserer Ergebnisse spekulieren wir, daß die Überexpression von Wildtyp-HtrA2 und G399S-HtrA2 zu einem gestörten Chaperon-Netzwerk führt. Die Aktivität des mitochondrialen Komplexes und ROS-Level könnten näher untersucht werden in diesem Modellen. Eine reduzierte Aktivität der Citrat-Synthase wurde in einem HtrA2-Knockout-Modell beobachtet, während alle anderen Komplexe ein normale Aktivität zeigten (Martins et a., 2004). Unser HtrA2-Modell zeigt die Bildung von Aggregaten aus α-Synuklein, was eine Hauptkomponente der Lewy-Körper bei M. Parkinson sind. Das HtrA2-Modell könnte so dazu beitragen, die Signaltransduktion, die zu der Bildung von α-Synuklein führt, besser zu verstehen.

Das Fehlen eines dominanten Effektes der Mutation auf den motorischen Phenotyp in der transgenen G399S-HtrA2-Maus spricht als Mechanismus für eine Haploinsuffizienz beim Menschen. Um die Bedeutung der G399S-Mutation für Parkinson zu bestätigen könnte die transgene Maus Linie G3993-HtrA2 zu einer HtrA2-Knockout-Maus kreuzgezüchtet werden um den Effekt der HtrA2 Mutation zu untersuchen. Zudem könnte dieses Experiment den Effekt des „loss of function“ nach ergebnislosen Rettungsexperimenten bestätigen.

Wenn man die Verbindungen von HtrA2 zu neurodegenerativen Erkrankungen wie Alzheimer und Parkinson betrachtet, hat HtrA2 in den letzten Jahren an Bedeutung gewonnen. Die

herausragende Rolle von HtrA2 erfordert deshalb weitere Forschung in über dieses Protein mit der Möglichkeit, daß sich diese Ergebnisse auch von Parkinson auf andere Erkrankungen übertragen lassen.

ABBREVIATIONS

Ab	Antibody
Ac-DEVD-AMC	Asp-Glu-Val-Asp7-amido4-Methylcoumarin
ANOVA	Analysis of Variance
BG	Basal ganglia
BS	Brain stem
BSA	Bovine serum albumin
C57BL/6	Black 6 wild type mice
CBM	Cerebellum
CNS	Central nervous system
CTX	Cortex
DNA	Deoxyribonucleic acid
dNTP´s	deoxy nucleotide triphosphates
ECL	Enhanced chemiluminescence
EV	Empty vector
FACS	Flourescence activated cell sorting
GAPDH	Glyceraldehyde 3-phosphate dehydrogenase
IAP	Inhibitor of apoptotic proteins
IMM	Inner mitochondrial membrane
IMS	Inter mitochondrial space
KO	Knock out
LB	Lysogeny broth
L-DOPA	L-3,4,-dihydroxyphenylalanine
MALDI-TOF	Matrix-assisted laser desorption/ionization time of flight Mass spectrometry
MEF	Mouse embryonic fibroblasts

Non-TG	Non transgenic mice
OB	Olfactory bulb
OD	Optical density
OF	Openfield
OMM	Outer mitochondrial membrane
PAGE	Polyacrylamide gel electrophoresis
PVDF	Polyvinylidenflourid
PBS	Phosphate buffered saline
PCR	Polymerase chain reaction
PD	Parkinson´s Disease
PFA	Paraformaldehyde
PINK1	PTEN induced putative kinase 1 Phosphatidylinositol (3,4,5)-trisphosphate
qRT-PCR	Quantitative real time polymerase chain reaction
RPM	Revolutions per minute
SD	Standard deviation
SDS	Sodium dodecyl sulfate
SEM	Standard error of mean
SNpc	Substantia nigra pars compacta
TBS	Tris buffered saline
TdT	Terminal deoxynucleotidyl transferase
TEMED	Tetramethylethylenediamine
TG HtrA2 G399S	Transgenic human HtrA2/Omi G399S mutant overexpressing
TG HtrA2 WT	Transgenic human HtrA2/Omi wild type overexpressing
TH	Tyrosine Hydroxylase
TRAP1	TNF receptor-associated protein
TUNEL	Terminal deoxynucleotidyl transferase dUTP nick end labeling

VDAC	Voltage dependent anion channel
WB	Western blot
WT	Wild type
XIAP	X-Linked inhibitor of apoptotic proteins

REFERENCES

Allshire RC, Javerzat JP, Redhead NJ, Cranston G (1994) Position effect variegation at fission yeast centromeres. Cell 76:157-169.

Appel-Cresswell S, Vilarino-Guell C, Encarnacion M, Sherman H, Yu I, Shah B, Weir D, Thompson C, Szu-Tu C, Trinh J, Aasly JO, Rajput A, Rajput AH, Jon Stoessl A, Farrer MJ (2013) Alpha-synuclein p.H50Q, a novel pathogenic mutation for Parkinson's disease. Movement disorders : official journal of the Movement Disorder Society 28:811-813.

Arduino DM, Esteves AR, Cortes L, Silva DF, Patel B, Grazina M, Swerdlow RH, Oliveira CR, Cardoso SM (2012) Mitochondrial metabolism in Parkinson's disease impairs quality control autophagy by hampering microtubule-dependent traffic. Human molecular genetics 21:4680-4702.

Arthur CR, Morton SL, Dunham LD, Keeney PM, Bennett JP, Jr. (2009) Parkinson's disease brain mitochondria have impaired respirasome assembly, age-related increases in distribution of oxidative damage to mtDNA and no differences in heteroplasmic mtDNA mutation abundance. Molecular neurodegeneration 4:37.

Barcia C, Sanchez Bahillo A, Fernandez-Villalba E, Bautista V, Poza YPM, Fernandez-Barreiro A, Hirsch EC, Herrero MT (2004) Evidence of active microglia in substantia nigra pars compacta of parkinsonian monkeys 1 year after MPTP exposure. Glia 46:402-409.

Bedford L, Hay D, Devoy A, Paine S, Powe DG, Seth R, Gray T, Topham I, Fone K, Rezvani N, Mee M, Soane T, Layfield R, Sheppard PW, Ebendal T, Usoskin D, Lowe J, Mayer RJ (2008) Depletion of 26S proteasomes in mouse brain neurons causes neurodegeneration and Lewy-like inclusions resembling human pale bodies. The Journal of neuroscience : the official journal of the Society for Neuroscience 28:8189-8198.

Bevan MD, Magill PJ, Terman D, Bolam JP, Wilson CJ (2002) Move to the rhythm: oscillations in the subthalamic nucleus-external globus pallidus network. Trends in neurosciences 25:525-531.

Bhuiyan MS, Fukunaga K (2009) Mitochondrial serine protease HtrA2/Omi as a potential therapeutic target. Current drug targets 10:372-383.

Bogaerts V, Nuytemans K, Reumers J, Pals P, Engelborghs S, Pickut B, Corsmit E, Peeters K, Schymkowitz J, De Deyn PP, Cras P, Rousseau F, Theuns J, Van Broeckhoven C (2008) Genetic variability in the mitochondrial serine protease HTRA2 contributes to risk for Parkinson disease. Human mutation 29:832-840.

Bonifati V, Rizzu P, van Baren MJ, Schaap O, Breedveld GJ, Krieger E, Dekker MC, Squitieri F, Ibanez P, Joosse M, van Dongen JW, Vanacore N, van Swieten JC, Brice A, Meco G, van Duijn CM, Oostra BA, Heutink P (2003) Mutations in the DJ-1 gene associated with autosomal recessive early-onset parkinsonism. Science 299:256-259.

Bowden MA, Drummond AE, Fuller PJ, Salamonsen LA, Findlay JK, Nie G (2010) High-temperature requirement factor A3 (Htra3): a novel serine protease and its potential

role in ovarian function and ovarian cancers. Molecular and cellular endocrinology 327:13-18.

Braak H, de Vos RA, Bohl J, Del Tredici K (2006) Gastric alpha-synuclein immunoreactive inclusions in Meissner's and Auerbach's plexuses in cases staged for Parkinson's disease-related brain pathology. Neuroscience letters 396:67-72.

Braak H, Del Tredici K, Rub U, de Vos RA, Jansen Steur EN, Braak E (2003) Staging of brain pathology related to sporadic Parkinson's disease. Neurobiology of aging 24:197-211.

Burbulla LF, Schelling C, Kato H, Rapaport D, Woitalla D, Schiesling C, Schulte C, Sharma M, Illig T, Bauer P, Jung S, Nordheim A, Schols L, Riess O, Kruger R (2010) Dissecting the role of the mitochondrial chaperone mortalin in Parkinson's disease: functional impact of disease-related variants on mitochondrial homeostasis. Human molecular genetics 19:4437-4452.

Carter RJ, Morton J, Dunnett SB (2001) Motor coordination and balance in rodents. Current protocols in neuroscience / editorial board, Jacqueline N Crawley [et al] Chapter 8:Unit 8 12.

Chartier-Harlin MC, Kachergus J, Roumier C, Mouroux V, Douay X, Lincoln S, Levecque C, Larvor L, Andrieux J, Hulihan M, Waucquier N, Defebvre L, Amouyel P, Farrer M, Destee A (2004) Alpha-synuclein locus duplication as a cause of familial Parkinson's disease. Lancet 364:1167-1169.

Chaudhuri KR, Schapira AH (2009) Non-motor symptoms of Parkinson's disease: dopaminergic pathophysiology and treatment. Lancet neurology 8:464-474.

Chesselet MF, Richter F (2011) Modelling of Parkinson's disease in mice. Lancet neurology 10:1108-1118.

Chesselet MF, Richter F, Zhu C, Magen I, Watson MB, Subramaniam SR (2012) A progressive mouse model of Parkinson's disease: the Thy1-aSyn ("Line 61") mice. Neurotherapeutics : the journal of the American Society for Experimental NeuroTherapeutics 9:297-314.

Chien J, Campioni M, Shridhar V, Baldi A (2009) HtrA serine proteases as potential therapeutic targets in cancer. Current cancer drug targets 9:451-468.

Chu Y, Dodiya H, Aebischer P, Olanow CW, Kordower JH (2009) Alterations in lysosomal and proteasomal markers in Parkinson's disease: relationship to alpha-synuclein inclusions. Neurobiology of disease 35:385-398.

Cilenti L, Soundarapandian MM, Kyriazis GA, Stratico V, Singh S, Gupta S, Bonventre JV, Alnemri ES, Zervos AS (2004) Regulation of HAX-1 anti-apoptotic protein by Omi/HtrA2 protease during cell death. The Journal of biological chemistry 279:50295-50301.

Clark IE, Dodson MW, Jiang C, Cao JH, Huh JR, Seol JH, Yoo SJ, Hay BA, Guo M (2006) Drosophila pink1 is required for mitochondrial function and interacts genetically with parkin. Nature 441:1162-1166.

Clausen T, Southan C, Ehrmann M (2002) The HtrA family of proteases: implications for protein composition and cell fate. Molecular cell 10:443-455.

Clausen T, Kaiser M, Huber R, Ehrmann M (2011) HTRA proteases: regulated proteolysis in protein quality control. Nature reviews Molecular cell biology 12:152-162.

Conway KA, Harper JD, Lansbury PT (1998) Accelerated in vitro fibril formation by a mutant alpha-synuclein linked to early-onset Parkinson disease. Nature medicine 4:1318-1320.

Cookson MR (2009) alpha-Synuclein and neuronal cell death. Molecular neurodegeneration 4:9.

Corti O, Lesage S, Brice A (2011) What genetics tells us about the causes and mechanisms of Parkinson's disease. Physiological reviews 91:1161-1218.

Danzer KM, Ruf WP, Putcha P, Joyner D, Hashimoto T, Glabe C, Hyman BT, McLean PJ (2011) Heat-shock protein 70 modulates toxic extracellular alpha-synuclein oligomers and rescues trans-synaptic toxicity. FASEB journal : official publication of the Federation of American Societies for Experimental Biology 25:326-336.

de Lau LM, Breteler MM (2006) Epidemiology of Parkinson's disease. Lancet neurology 5:525-535.

Deng H, Le WD, Hunter CB, Ondo WG, Guo Y, Xie WJ, Jankovic J (2006) Heterogeneous phenotype in a family with compound heterozygous parkin gene mutations. Archives of neurology 63:273-277.

Dexter DT, Jenner P (2013) Parkinson disease: from pathology to molecular disease mechanisms. Free radical biology & medicine.

Dexter DT, Wells FR, Lees AJ, Agid F, Agid Y, Jenner P, Marsden CD (1989a) Increased nigral iron content and alterations in other metal ions occurring in brain in Parkinson's disease. Journal of neurochemistry 52:1830-1836.

Dexter DT, Carter CJ, Wells FR, Javoy-Agid F, Agid Y, Lees A, Jenner P, Marsden CD (1989b) Basal lipid peroxidation in substantia nigra is increased in Parkinson's disease. Journal of neurochemistry 52:381-389.

Dexter DT, Holley AE, Flitter WD, Slater TF, Wells FR, Daniel SE, Lees AJ, Jenner P, Marsden CD (1994) Increased levels of lipid hydroperoxides in the parkinsonian substantia nigra: an HPLC and ESR study. Movement disorders : official journal of the Movement Disorder Society 9:92-97.

Dickson DW, Braak H, Duda JE, Duyckaerts C, Gasser T, Halliday GM, Hardy J, Leverenz JB, Del Tredici K, Wszolek ZK, Litvan I (2009) Neuropathological assessment of Parkinson's disease: refining the diagnostic criteria. Lancet neurology 8:1150-1157.

Dunning CJ, Reyes JF, Steiner JA, Brundin P (2012) Can Parkinson's disease pathology be propagated from one neuron to another? Progress in neurobiology 97:205-219.

Eissenberg JC (1989) Position effect variegation in Drosophila: towards a genetics of chromatin assembly. BioEssays : news and reviews in molecular, cellular and developmental biology 11:14-17.

Elstner M, Morris CM, Heim K, Bender A, Mehta D, Jaros E, Klopstock T, Meitinger T, Turnbull DM, Prokisch H (2011) Expression analysis of dopaminergic neurons in

Parkinson's disease and aging links transcriptional dysregulation of energy metabolism to cell death. Acta neuropathologica 122:75-86.

Faccio L, Fusco C, Chen A, Martinotti S, Bonventre JV, Zervos AS (2000) Characterization of a novel human serine protease that has extensive homology to bacterial heat shock endoprotease HtrA and is regulated by kidney ischemia. The Journal of biological chemistry 275:2581-2588.

Fahn S, Cohen G (1992) The oxidant stress hypothesis in Parkinson's disease: evidence supporting it. Annals of neurology 32:804-812.

Farrer M, Chan P, Chen R, Tan L, Lincoln S, Hernandez D, Forno L, Gwinn-Hardy K, Petrucelli L, Hussey J, Singleton A, Tanner C, Hardy J, Langston JW (2001) Lewy bodies and parkinsonism in families with parkin mutations. Annals of neurology 50:293-300.

Fauvet B, Mbefo MK, Fares MB, Desobry C, Michael S, Ardah MT, Tsika E, Coune P, Prudent M, Lion N, Eliezer D, Moore DJ, Schneider B, Aebischer P, El-Agnaf OM, Masliah E, Lashuel HA (2012) alpha-Synuclein in central nervous system and from erythrocytes, mammalian cells, and Escherichia coli exists predominantly as disordered monomer. The Journal of biological chemistry 287:15345-15364.

Fearnley JM, Lees AJ (1991) Ageing and Parkinson's disease: substantia nigra regional selectivity. Brain : a journal of neurology 114 (Pt 5):2283-2301.

Fitzgerald JC, Camprubi MD, Dunn L, Wu HC, Ip NY, Kruger R, Martins LM, Wood NW, Plun-Favreau H (2012) Phosphorylation of HtrA2 by cyclin-dependent kinase-5 is important for mitochondrial function. Cell death and differentiation 19:257-266.

Fleming SM, Salcedo J, Fernagut PO, Rockenstein E, Masliah E, Levine MS, Chesselet MF (2004) Early and progressive sensorimotor anomalies in mice overexpressing wild-type human alpha-synuclein. The Journal of neuroscience : the official journal of the Society for Neuroscience 24:9434-9440.

Forno LS (1996) Neuropathology of Parkinson's disease. Journal of neuropathology and experimental neurology 55:259-272.

Fujishiro H, Frigerio R, Burnett M, Klos KJ, Josephs KA, Delledonne A, Parisi JE, Ahlskog JE, Dickson DW (2008) Cardiac sympathetic denervation correlates with clinical and pathologic stages of Parkinson's disease. Movement disorders : official journal of the Movement Disorder Society 23:1085-1092.

Fujiwara H, Hasegawa M, Dohmae N, Kawashima A, Masliah E, Goldberg MS, Shen J, Takio K, Iwatsubo T (2002) alpha-Synuclein is phosphorylated in synucleinopathy lesions. Nature cell biology 4:160-164.

Garrick D, Fiering S, Martin DI, Whitelaw E (1998) Repeat-induced gene silencing in mammals. Nature genetics 18:56-59.

Geisler S, Holmstrom KM, Treis A, Skujat D, Weber SS, Fiesel FC, Kahle PJ, Springer W (2010) The PINK1/Parkin-mediated mitophagy is compromised by PD-associated mutations. Autophagy 6:871-878.

Ghosh SS, Swerdlow RH, Miller SW, Sheeman B, Parker WD, Jr., Davis RE (1999) Use of cytoplasmic hybrid cell lines for elucidating the role of mitochondrial dysfunction in

Alzheimer's disease and Parkinson's disease. Annals of the New York Academy of Sciences 893:176-191.

Giasson BI, Duda JE, Quinn SM, Zhang B, Trojanowski JQ, Lee VM (2002) Neuronal alpha-synucleinopathy with severe movement disorder in mice expressing A53T human alpha-synuclein. Neuron 34:521-533.

Glickman MH, Ciechanover A (2002) The ubiquitin-proteasome proteolytic pathway: destruction for the sake of construction. Physiological reviews 82:373-428.

Golbe LI, Di Iorio G, Bonavita V, Miller DC, Duvoisin RC (1990) A large kindred with autosomal dominant Parkinson's disease. Annals of neurology 27:276-282.

Gong B, Leznik E (2007) The role of ubiquitin C-terminal hydrolase L1 in neurodegenerative disorders. Drug news & perspectives 20:365-370.

Grau S, Baldi A, Bussani R, Tian X, Stefanescu R, Przybylski M, Richards P, Jones SA, Shridhar V, Clausen T, Ehrmann M (2005) Implications of the serine protease HtrA1 in amyloid precursor protein processing. Proceedings of the National Academy of Sciences of the United States of America 102:6021-6026.

Gray CW, Ward RV, Karran E, Turconi S, Rowles A, Viglienghi D, Southan C, Barton A, Fantom KG, West A, Savopoulos J, Hassan NJ, Clinkenbeard H, Hanning C, Amegadzie B, Davis JB, Dingwall C, Livi GP, Creasy CL (2000) Characterization of human HtrA2, a novel serine protease involved in the mammalian cellular stress response. European journal of biochemistry / FEBS 267:5699-5710.

Greenbaum EA, Graves CL, Mishizen-Eberz AJ, Lupoli MA, Lynch DR, Englander SW, Axelsen PH, Giasson BI (2005) The E46K mutation in alpha-synuclein increases amyloid fibril formation. The Journal of biological chemistry 280:7800-7807.

Greene JC, Whitworth AJ, Kuo I, Andrews LA, Feany MB, Pallanck LJ (2003) Mitochondrial pathology and apoptotic muscle degeneration in Drosophila parkin mutants. Proceedings of the National Academy of Sciences of the United States of America 100:4078-4083.

Guo XL, Liang B, Wang XW, Fan FG, Jin J, Lan R, Yang JH, Wang XC, Jin L, Cao Q (2013) Glycyrrhizic acid attenuates CCl4-induced hepatocyte apoptosis in rats via a p53-mediated pathway. World journal of gastroenterology : WJG 19:3781-3791.

Hampe C, Ardila-Osorio H, Fournier M, Brice A, Corti O (2006) Biochemical analysis of Parkinson's disease-causing variants of Parkin, an E3 ubiquitin-protein ligase with monoubiquitylation capacity. Human molecular genetics 15:2059-2075.

Hara K et al. (2009) Association of HTRA1 mutations and familial ischemic cerebral small-vessel disease. The New England journal of medicine 360:1729-1739.

Harlin H, Reffey SB, Duckett CS, Lindsten T, Thompson CB (2001) Characterization of XIAP-deficient mice. Molecular and cellular biology 21:3604-3608.

Hartl FU, Bracher A, Hayer-Hartl M (2011) Molecular chaperones in protein folding and proteostasis. Nature 475:324-332.

Heikkila RE, Cohen G (1973) 6-Hydroxydopamine: evidence for superoxide radical as an oxidative intermediate. Science 181:456-457.

Heikkila RE, Hwang J, Ofori S, Geller HM, Nicklas WJ (1990) Potentiation by the tetraphenylboron anion of the effects of 1-methyl-4-phenyl-1,2,3,6-tetrahydropyridine and its pyridinium metabolite. Journal of neurochemistry 54:743-750.

Hirsch EC, Hunot S (2000) Nitric oxide, glial cells and neuronal degeneration in parkinsonism. Trends in pharmacological sciences 21:163-165.

Hirsch EC, Breidert T, Rousselet E, Hunot S, Hartmann A, Michel PP (2003) The role of glial reaction and inflammation in Parkinson's disease. Annals of the New York Academy of Sciences 991:214-228.

Hoehn MM, Yahr MD (1967) Parkinsonism: onset, progression and mortality. Neurology 17:427-442.

Hsu CY (2013) PARL and HtrA2: another intricate ischemic neuronal apoptotic process starting within mitochondria. Journal of cerebral blood flow and metabolism : official journal of the International Society of Cerebral Blood Flow and Metabolism.

Hua Y, Schallert T, Keep RF, Wu J, Hoff JT, Xi G (2002) Behavioral tests after intracerebral hemorrhage in the rat. Stroke; a journal of cerebral circulation 33:2478-2484.

Hubener J, Vauti F, Funke C, Wolburg H, Ye Y, Schmidt T, Wolburg-Buchholz K, Schmitt I, Gardyan A, Driessen S, Arnold HH, Nguyen HP, Riess O (2011) N-terminal ataxin-3 causes neurological symptoms with inclusions, endoplasmic reticulum stress and ribosomal dislocation. Brain : a journal of neurology 134:1925-1942.

Hunot S, Hirsch EC (2003) Neuroinflammatory processes in Parkinson's disease. Annals of neurology 53 Suppl 3:S49-58; discussion S58-60.

Jakes R, Spillantini MG, Goedert M (1994) Identification of two distinct synucleins from human brain. FEBS letters 345:27-32.

Jankovic J (2008) Parkinson's disease: clinical features and diagnosis. Journal of neurology, neurosurgery, and psychiatry 79:368-376.

Jellinger KA (2012) Neuropathology of sporadic Parkinson's disease: evaluation and changes of concepts. Movement disorders : official journal of the Movement Disorder Society 27:8-30.

Jones BJ, Roberts DJ (1968) The quantiative measurement of motor inco-ordination in naive mice using an acelerating rotarod. The Journal of pharmacy and pharmacology 20:302-304.

Jones JM, Albin RL, Feldman EL, Simin K, Schuster TG, Dunnick WA, Collins JT, Chrisp CE, Taylor BA, Meisler MH (1993) mnd2: a new mouse model of inherited motor neuron disease. Genomics 16:669-677.

Jones JM, Datta P, Srinivasula SM, Ji W, Gupta S, Zhang Z, Davies E, Hajnoczky G, Saunders TL, Van Keuren ML, Fernandes-Alnemri T, Meisler MH, Alnemri ES (2003) Loss of Omi mitochondrial protease activity causes the neuromuscular disorder of mnd2 mutant mice. Nature 425:721-727.

Kalaitzakis ME, Graeber MB, Gentleman SM, Pearce RK (2008) The dorsal motor nucleus of the vagus is not an obligatory trigger site of Parkinson's disease: a critical analysis of alpha-synuclein staging. Neuropathology and applied neurobiology 34:284-295.

Kalia LV, Kalia SK, McLean PJ, Lozano AM, Lang AE (2013) alpha-Synuclein oligomers and clinical implications for Parkinson disease. Annals of neurology 73:155-169.

Kang S, Louboutin JP, Datta P, Landel CP, Martinez D, Zervos AS, Strayer DS, Fernandes-Alnemri T, Alnemri ES (2013) Loss of HtrA2/Omi activity in non-neuronal tissues of adult mice causes premature aging. Cell death and differentiation 20:259-269.

Karpinar DP et al. (2009) Pre-fibrillar alpha-synuclein variants with impaired beta-structure increase neurotoxicity in Parkinson's disease models. The EMBO journal 28:3256-3268.

Katunuma N, Matsui A, Le QT, Utsumi K, Salvesen G, Ohashi A (2001) Novel procaspase-3 activating cascade mediated by lysoapoptases and its biological significances in apoptosis. Advances in enzyme regulation 41:237-250.

Kawamoto Y, Kobayashi Y, Suzuki Y, Inoue H, Tomimoto H, Akiguchi I, Budka H, Martins LM, Downward J, Takahashi R (2008) Accumulation of HtrA2/Omi in neuronal and glial inclusions in brains with alpha-synucleinopathies. Journal of neuropathology and experimental neurology 67:984-993.

Kempster PA, Hurwitz B, Lees AJ (2007) A new look at James Parkinson's Essay on the Shaking Palsy. Neurology 69:482-485.

Kempster PA, O'Sullivan SS, Holton JL, Revesz T, Lees AJ (2010) Relationships between age and late progression of Parkinson's disease: a clinico-pathological study. Brain : a journal of neurology 133:1755-1762.

Kemshead JT, Ritter MA, Cotmore SF, Greaves MF (1982) Human Thy-1: expression on the cell surface of neuronal and glial cells. Brain research 236:451-461.

Kenborg L, Lassen CF, Hansen J, Olsen JH (2012) Parkinson's disease and other neurodegenerative disorders among welders: a Danish cohort study. Movement disorders : official journal of the Movement Disorder Society 27:1283-1289.

Kieper N, Holmstrom KM, Ciceri D, Fiesel FC, Wolburg H, Ziviani E, Whitworth AJ, Martins LM, Kahle PJ, Kruger R (2010) Modulation of mitochondrial function and morphology by interaction of Omi/HtrA2 with the mitochondrial fusion factor OPA1. Experimental cell research 316:1213-1224.

Kitada T, Asakawa S, Hattori N, Matsumine H, Yamamura Y, Minoshima S, Yokochi M, Mizuno Y, Shimizu N (1998) Mutations in the parkin gene cause autosomal recessive juvenile parkinsonism. Nature 392:605-608.

Klein C, Westenberger A (2012) Genetics of Parkinson's disease. Cold Spring Harbor perspectives in medicine 2:a008888.

Kobayashi H, Kruger R, Markopoulou K, Wszolek Z, Chase B, Taka H, Mineki R, Murayama K, Riess O, Mizuno Y, Hattori N (2003) Haploinsufficiency at the alpha-synuclein gene underlies phenotypic severity in familial Parkinson's disease. Brain : a journal of neurology 126:32-42.

Krebiehl G, Ruckerbauer S, Burbulla LF, Kieper N, Maurer B, Waak J, Wolburg H, Gizatullina Z, Gellerich FN, Woitalla D, Riess O, Kahle PJ, Proikas-Cezanne T, Kruger R (2010) Reduced basal autophagy and impaired mitochondrial dynamics due to loss of Parkinson's disease-associated protein DJ-1. PloS one 5:e9367.

Kruger R, Kuhn W, Muller T, Woitalla D, Graeber M, Kosel S, Przuntek H, Epplen JT, Schols L, Riess O (1998) Ala30Pro mutation in the gene encoding alpha-synuclein in Parkinson's disease. Nature genetics 18:106-108.

Kuninaka S, Iida SI, Hara T, Nomura M, Naoe H, Morisaki T, Nitta M, Arima Y, Mimori T, Yonehara S, Saya H (2007) Serine protease Omi/HtrA2 targets WARTS kinase to control cell proliferation. Oncogene 26:2395-2406.

Lang AE, Lozano AM (1998) Parkinson's disease. Second of two parts. The New England journal of medicine 339:1130-1143.

Langston JW (2006) The Parkinson's complex: parkinsonism is just the tip of the iceberg. Annals of neurology 59:591-596.

Langston JW, Ballard P, Tetrud JW, Irwin I (1983) Chronic Parkinsonism in humans due to a product of meperidine-analog synthesis. Science 219:979-980.

Langston JW, Forno LS, Tetrud J, Reeves AG, Kaplan JA, Karluk D (1999) Evidence of active nerve cell degeneration in the substantia nigra of humans years after 1-methyl-4-phenyl-1,2,3,6-tetrahydropyridine exposure. Annals of neurology 46:598-605.

Lee MK, Stirling W, Xu Y, Xu X, Qui D, Mandir AS, Dawson TM, Copeland NG, Jenkins NA, Price DL (2002) Human alpha-synuclein-harboring familial Parkinson's disease-linked Ala-53 --> Thr mutation causes neurodegenerative disease with alpha-synuclein aggregation in transgenic mice. Proceedings of the National Academy of Sciences of the United States of America 99:8968-8973.

Lees AJ, Hardy J, Revesz T (2009) Parkinson's disease. Lancet 373:2055-2066.

Leist M, Single B, Castoldi AF, Kuhnle S, Nicotera P (1997) Intracellular adenosine triphosphate (ATP) concentration: a switch in the decision between apoptosis and necrosis. The Journal of experimental medicine 185:1481-1486.

Lesage S, Anheim M, Letournel F, Bousset L, Honore A, Rozas N, Pieri L, Madiona K, Durr A, Melki R, Verny C, Brice A, for the French Parkinson's Disease Genetics Study G (2013) G51D alpha-synuclein mutation causes a novel parkinsonian-pyramidal syndrome. Annals of neurology.

Li B, Hu Q, Wang H, Man N, Ren H, Wen L, Nukina N, Fei E, Wang G (2010) Omi/HtrA2 is a positive regulator of autophagy that facilitates the degradation of mutant proteins involved in neurodegenerative diseases. Cell death and differentiation 17:1773-1784.

Li X, Fang P, Mai J, Choi ET, Wang H, Yang XF (2013) Targeting mitochondrial reactive oxygen species as novel therapy for inflammatory diseases and cancers. Journal of hematology & oncology 6:19.

Liu M J, Liu MJ, Shen YF, Kim JM, Lee BH, Lee YS, Hong ST (2007) Transgenic mice with neuron-specific overexpression of HtrA2/Omi suggest a neuroprotective role for HtrA2/Omi. Biochem Biophys Res Commun 362:295-300.

Lin CH, Chen ML, Chen GS, Tai CH, Wu RM (2011) Novel variant Pro143Ala in HTRA2 contributes to Parkinson's disease by inducing hyperphosphorylation of HTRA2 protein in mitochondria. Human genetics 130:817-827.

Lohmann E et al. (2003) How much phenotypic variation can be attributed to parkin genotype? Annals of neurology 54:176-185.

Lucking CB, Durr A, Bonifati V, Vaughan J, De Michele G, Gasser T, Harhangi BS, Meco G, Denefle P, Wood NW, Agid Y, Brice A, French Parkinson's Disease Genetics Study G, European Consortium on Genetic Susceptibility in Parkinson's D (2000) Association between early-onset Parkinson's disease and mutations in the parkin gene. The New England journal of medicine 342:1560-1567.

Martins LM, Iaccarino I, Tenev T, Gschmeissner S, Totty NF, Lemoine NR, Savopoulos J, Gray CW, Creasy CL, Dingwall C, Downward J (2002) The serine protease Omi/HtrA2 regulates apoptosis by binding XIAP through a reaper-like motif. The Journal of biological chemistry 277:439-444.

Martins LM, Morrison A, Klupsch K, Fedele V, Moisoi N, Teismann P, Abuin A, Grau E, Geppert M, Livi GP, Creasy CL, Martin A, Hargreaves I, Heales SJ, Okada H, Brandner S, Schulz JB, Mak T, Downward J (2004) Neuroprotective role of the Reaper-related serine protease HtrA2/Omi revealed by targeted deletion in mice. Molecular and cellular biology 24:9848-9862.

Mazzulli JR, Xu YH, Sun Y, Knight AL, McLean PJ, Caldwell GA, Sidransky E, Grabowski GA, Krainc D (2011) Gaucher disease glucocerebrosidase and alpha-synuclein form a bidirectional pathogenic loop in synucleinopathies. Cell 146:37-52.

McGeer PL, Schwab C, Parent A, Doudet D (2003) Presence of reactive microglia in monkey substantia nigra years after 1-methyl-4-phenyl-1,2,3,6-tetrahydropyridine administration. Annals of neurology 54:599-604.

McNaught KS, Olanow CW, Halliwell B, Isacson O, Jenner P (2001) Failure of the ubiquitin-proteasome system in Parkinson's disease. Nature reviews Neuroscience 2:589-594.

McNaught KS, Belizaire R, Jenner P, Olanow CW, Isacson O (2002a) Selective loss of 20S proteasome alpha-subunits in the substantia nigra pars compacta in Parkinson's disease. Neuroscience letters 326:155-158.

McNaught KS, Shashidharan P, Perl DP, Jenner P, Olanow CW (2002b) Aggresome-related biogenesis of Lewy bodies. The European journal of neuroscience 16:2136-2148.

McNaught KS, Belizaire R, Isacson O, Jenner P, Olanow CW (2003) Altered proteasomal function in sporadic Parkinson's disease. Experimental neurology 179:38-46.

Milner JM, Patel A, Rowan AD (2008) Emerging roles of serine proteinases in tissue turnover in arthritis. Arthritis and rheumatism 58:3644-3656.

Mizuno Y, Ohta S, Tanaka M, Takamiya S, Suzuki K, Sato T, Oya H, Ozawa T, Kagawa Y (1989) Deficiencies in complex I subunits of the respiratory chain in Parkinson's disease. Biochemical and biophysical research communications 163:1450-1455.

Moisoi N, Klupsch K, Fedele V, East P, Sharma S, Renton A, Plun-Favreau H, Edwards RE, Teismann P, Esposti MD, Morrison AD, Wood NW, Downward J, Martins LM (2009) Mitochondrial dysfunction triggered by loss of HtrA2 results in the activation of a brain-specific transcriptional stress response. Cell death and differentiation 16:449-464.

Nagatsu T (1995) Tyrosine hydroxylase: human isoforms, structure and regulation in physiology and pathology. Essays in biochemistry 30:15-35.

Narendra D, Tanaka A, Suen DF, Youle RJ (2008) Parkin is recruited selectively to impaired mitochondria and promotes their autophagy. The Journal of cell biology 183:795-803.

Neumann M, Kahle PJ, Giasson BI, Ozmen L, Borroni E, Spooren W, Muller V, Odoy S, Fujiwara H, Hasegawa M, Iwatsubo T, Trojanowski JQ, Kretzschmar HA, Haass C (2002) Misfolded proteinase K-resistant hyperphosphorylated alpha-synuclein in aged transgenic mice with locomotor deterioration and in human alpha-synucleinopathies. The Journal of clinical investigation 110:1429-1439.

Nie GY, Hampton A, Li Y, Findlay JK, Salamonsen LA (2003) Identification and cloning of two isoforms of human high-temperature requirement factor A3 (HtrA3), characterization of its genomic structure and comparison of its tissue distribution with HtrA1 and HtrA2. The Biochemical journal 371:39-48.

Nussbaum RL, Ellis CE (2003) Alzheimer's disease and Parkinson's disease. The New England journal of medicine 348:1356-1364.

Obeso JA, Rodriguez-Oroz MC, Goetz CG, Marin C, Kordower JH, Rodriguez M, Hirsch EC, Farrer M, Schapira AH, Halliday G (2010) Missing pieces in the Parkinson's disease puzzle. Nature medicine 16:653-661.

Outeiro TF, Putcha P, Tetzlaff JE, Spoelgen R, Koker M, Carvalho F, Hyman BT, McLean PJ (2008) Formation of toxic oligomeric alpha-synuclein species in living cells. PloS one 3:e1867.

Paisan-Ruiz C et al. (2004) Cloning of the gene containing mutations that cause PARK8-linked Parkinson's disease. Neuron 44:595-600.

Paleologou KE, Kragh CL, Mann DM, Salem SA, Al-Shami R, Allsop D, Hassan AH, Jensen PH, El-Agnaf OM (2009) Detection of elevated levels of soluble alpha-synuclein oligomers in post-mortem brain extracts from patients with dementia with Lewy bodies. Brain : a journal of neurology 132:1093-1101.

Pallen MJ, Wren BW (1997) The HtrA family of serine proteases. Molecular microbiology 26:209-221.

Papa L, Germain D (2011) Estrogen receptor mediates a distinct mitochondrial unfolded protein response. Journal of cell science 124:1396-1402.

Park HJ, Kim SS, Seong YM, Kim KH, Goo HG, Yoon EJ, Min do S, Kang S, Rhim H (2006a) Beta-amyloid precursor protein is a direct cleavage target of HtrA2 serine protease. Implications for the physiological function of HtrA2 in the mitochondria. The Journal of biological chemistry 281:34277-34287.

Park J, Lee SB, Lee S, Kim Y, Song S, Kim S, Bae E, Kim J, Shong M, Kim JM, Chung J (2006b) Mitochondrial dysfunction in Drosophila PINK1 mutants is complemented by parkin. Nature 441:1157-1161.

Perier C, Tieu K, Guegan C, Caspersen C, Jackson-Lewis V, Carelli V, Martinuzzi A, Hirano M, Przedborski S, Vila M (2005) Complex I deficiency primes Bax-dependent neuronal apoptosis through mitochondrial oxidative damage. Proceedings of the National Academy of Sciences of the United States of America 102:19126-19131.

Perry DK, Smyth MJ, Stennicke HR, Salvesen GS, Duriez P, Poirier GG, Hannun YA (1997) Zinc is a potent inhibitor of the apoptotic protease, caspase-3. A novel target for zinc in the inhibition of apoptosis. The Journal of biological chemistry 272:18530-18533.

Plun-Favreau H, Klupsch K, Moisoi N, Gandhi S, Kjaer S, Frith D, Harvey K, Deas E, Harvey RJ, McDonald N, Wood NW, Martins LM, Downward J (2007) The mitochondrial protease HtrA2 is regulated by Parkinson's disease-associated kinase PINK1. Nature cell biology 9:1243-1252.

Plun-Favreau H, Burchell VS, Holmstrom KM, Yao Z, Deas E, Cain K, Fedele V, Moisoi N, Campanella M, Miguel Martins L, Wood NW, Gourine AV, Abramov AY (2012) HtrA2 deficiency causes mitochondrial uncoupling through the F(1)F(0)-ATP synthase and consequent ATP depletion. Cell death & disease 3:e335.

Polymeropoulos MH, Lavedan C, Leroy E, Ide SE, Dehejia A, Dutra A, Pike B, Root H, Rubenstein J, Boyer R, Stenroos ES, Chandrasekharappa S, Athanassiadou A, Papapetropoulos T, Johnson WG, Lazzarini AM, Duvoisin RC, Di Iorio G, Golbe LI, Nussbaum RL (1997) Mutation in the alpha-synuclein gene identified in families with Parkinson's disease. Science 276:2045-2047.

Popat RA, Van Den Eeden SK, Tanner CM, McGuire V, Bernstein AL, Bloch DA, Leimpeter A, Nelson LM (2005) Effect of reproductive factors and postmenopausal hormone use on the risk of Parkinson disease. Neurology 65:383-390.

Pramstaller PP, Schlossmacher MG, Jacques TS, Scaravilli F, Eskelson C, Pepivani I, Hedrich K, Adel S, Gonzales-McNeal M, Hilker R, Kramer PL, Klein C (2005) Lewy body Parkinson's disease in a large pedigree with 77 Parkin mutation carriers. Annals of neurology 58:411-422.

Proukakis C, Dudzik CG, Brier T, MacKay DS, Cooper JM, Millhauser GL, Houlden H, Schapira AH (2013) A novel alpha-synuclein missense mutation in Parkinson disease. Neurology 80:1062-1064.

Prut L, Belzung C (2003) The open field as a paradigm to measure the effects of drugs on anxiety-like behaviors: a review. European journal of pharmacology 463:3-33.

Raghuraman G, Rai V, Peng YJ, Prabhakar NR, Kumar GK (2009) Pattern-specific sustained activation of tyrosine hydroxylase by intermittent hypoxia: role of reactive oxygen species-dependent downregulation of protein phosphatase 2A and upregulation of protein kinases. Antioxidants & redox signaling 11:1777-1789.

Ragonese P, D'Amelio M, Salemi G, Aridon P, Gammino M, Epifanio A, Morgante L, Savettieri G (2004) Risk of Parkinson disease in women: effect of reproductive characteristics. Neurology 62:2010-2014.

Rathke-Hartlieb S, Schlomann U, Heimann P, Meisler MH, Jockusch H, Bartsch JW (2002) Progressive loss of striatal neurons causes motor dysfunction in MND2 mutant mice and is not prevented by Bcl-2. Experimental neurology 175:87-97.

Rustay NR, Wahlsten D, Crabbe JC (2003) Assessment of genetic susceptibility to ethanol intoxication in mice. Proceedings of the National Academy of Sciences of the United States of America 100:2917-2922.

Saito Y, Ruberu NN, Sawabe M, Arai T, Kazama H, Hosoi T, Yamanouchi H, Murayama S (2004) Lewy body-related alpha-synucleinopathy in aging. Journal of neuropathology and experimental neurology 63:742-749.

Schapira AH (2007) Future directions in the treatment of Parkinson's disease. Movement disorders : official journal of the Movement Disorder Society 22 Suppl 17:S385-391.

Schapira AH (2008) Mitochondria in the aetiology and pathogenesis of Parkinson's disease. Lancet neurology 7:97-109.

Schapira AH (2010) Complex I: inhibitors, inhibition and neurodegeneration. Experimental neurology 224:331-335.

Schapira AH (2011) Mitochondrial pathology in Parkinson's disease. The Mount Sinai journal of medicine, New York 78:872-881.

Schapira AH, Gegg M (2011) Mitochondrial contribution to Parkinson's disease pathogenesis. Parkinson's disease 2011:159160.

Schapira AH, Jenner P (2011) Etiology and pathogenesis of Parkinson's disease. Movement disorders : official journal of the Movement Disorder Society 26:1049-1055.

Schapira AH, Cooper JM, Dexter D, Jenner P, Clark JB, Marsden CD (1989) Mitochondrial complex I deficiency in Parkinson's disease. Lancet 1:1269.

Schnell JD, Hicke L (2003) Non-traditional functions of ubiquitin and ubiquitin-binding proteins. The Journal of biological chemistry 278:35857-35860.

Sharma M et al. (2012) A multi-centre clinico-genetic analysis of the VPS35 gene in Parkinson disease indicates reduced penetrance for disease-associated variants. Journal of medical genetics 49:721-726.

Sharon R, Bar-Joseph I, Frosch MP, Walsh DM, Hamilton JA, Selkoe DJ (2003) The formation of highly soluble oligomers of alpha-synuclein is regulated by fatty acids and enhanced in Parkinson's disease. Neuron 37:583-595.

Shashidharan P, Good PF, Hsu A, Perl DP, Brin MF, Olanow CW (2000) TorsinA accumulation in Lewy bodies in sporadic Parkinson's disease. Brain research 877:379-381.

Shimura H, Hattori N, Kubo S, Mizuno Y, Asakawa S, Minoshima S, Shimizu N, Iwai K, Chiba T, Tanaka K, Suzuki T (2000) Familial Parkinson disease gene product, parkin, is a ubiquitin-protein ligase. Nature genetics 25:302-305.

Shulman JM, De Jager PL, Feany MB (2011) Parkinson's disease: genetics and pathogenesis. Annual review of pathology 6:193-222.

Silvestri L, Caputo V, Bellacchio E, Atorino L, Dallapiccola B, Valente EM, Casari G (2005) Mitochondrial import and enzymatic activity of PINK1 mutants associated to recessive parkinsonism. Human molecular genetics 14:3477-3492.

Simon-Sanchez J, Singleton AB (2008) Sequencing analysis of OMI/HTRA2 shows previously reported pathogenic mutations in neurologically normal controls. Human molecular genetics 17:1988-1993.

Singleton AB et al. (2003) alpha-Synuclein locus triplication causes Parkinson's disease. Science 302:841.

Spillantini MG, Crowther RA, Jakes R, Hasegawa M, Goedert M (1998) alpha-Synuclein in filamentous inclusions of Lewy bodies from Parkinson's disease and dementia with lewy bodies. Proceedings of the National Academy of Sciences of the United States of America 95:6469-6473.

Spillantini MG, Schmidt ML, Lee VM, Trojanowski JQ, Jakes R, Goedert M (1997) Alpha-synuclein in Lewy bodies. Nature 388:839-840.

Spina MB, Cohen G (1989) Dopamine turnover and glutathione oxidation: implications for Parkinson disease. Proceedings of the National Academy of Sciences of the United States of America 86:1398-1400.

Srinivasula SM, Gupta S, Datta P, Zhang Z, Hegde R, Cheong N, Fernandes-Alnemri T, Alnemri ES (2003) Inhibitor of apoptosis proteins are substrates for the mitochondrial serine protease Omi/HtrA2. The Journal of biological chemistry 278:31469-31472.

Stanford SC (2007) The Open Field Test: reinventing the wheel. Journal of psychopharmacology 21:134-135.

Steigerwald F, Potter M, Herzog J, Pinsker M, Kopper F, Mehdorn H, Deuschl G, Volkmann J (2008) Neuronal activity of the human subthalamic nucleus in the parkinsonian and nonparkinsonian state. Journal of neurophysiology 100:2515-2524.

Strauss KM, Martins LM, Plun-Favreau H, Marx FP, Kautzmann S, Berg D, Gasser T, Wszolek Z, Muller T, Bornemann A, Wolburg H, Downward J, Riess O, Schulz JB, Kruger R (2005) Loss of function mutations in the gene encoding Omi/HtrA2 in Parkinson's disease. Human molecular genetics 14:2099-2111.

Suzuki Y, Takahashi-Niki K, Akagi T, Hashikawa T, Takahashi R (2004) Mitochondrial protease Omi/HtrA2 enhances caspase activation through multiple pathways. Cell death and differentiation 11:208-216.

Suzuki Y, Imai Y, Nakayama H, Takahashi K, Takio K, Takahashi R (2001) A serine protease, HtrA2, is released from the mitochondria and interacts with XIAP, inducing cell death. Molecular cell 8:613-621.

Tagliati M, Martin C, Alterman R (2010) Lack of motor symptoms progression in Parkinson's disease patients with long-term bilateral subthalamic deep brain stimulation. The International journal of neuroscience 120:717-723.

Tain LS, Chowdhury RB, Tao RN, Plun-Favreau H, Moisoi N, Martins LM, Downward J, Whitworth AJ, Tapon N (2009) Drosophila HtrA2 is dispensable for apoptosis but acts downstream of PINK1 independently from Parkin. Cell death and differentiation 16:1118-1125.

Tanida I, Ueno T, Kominami E (2008) LC3 and Autophagy. Methods in molecular biology 445:77-88.

Tanner CM, Kamel F, Ross GW, Hoppin JA, Goldman SM, Korell M, Marras C, Bhudhikanok GS, Kasten M, Chade AR, Comyns K, Richards MB, Meng C, Priestley B, Fernandez HH, Cambi F, Umbach DM, Blair A, Sandler DP, Langston JW (2011) Rotenone, paraquat, and Parkinson's disease. Environmental health perspectives 119:866-872.

Taylor RC, Cullen SP, Martin SJ (2008) Apoptosis: controlled demolition at the cellular level. Nature reviews Molecular cell biology 9:231-241.

Tolosa E, Pont-Sunyer C (2011) Progress in defining the premotor phase of Parkinson's disease. Journal of the neurological sciences 310:4-8.

Trencia A, Fiory F, Maitan MA, Vito P, Barbagallo AP, Perfetti A, Miele C, Ungaro P, Oriente F, Cilenti L, Zervos AS, Formisano P, Beguinot F (2004) Omi/HtrA2 promotes cell death by binding and degrading the anti-apoptotic protein ped/pea-15. The Journal of biological chemistry 279:46566-46572.

Tsika E, Moysidou M, Guo J, Cushman M, Gannon P, Sandaltzopoulos R, Giasson BI, Krainc D, Ischiropoulos H, Mazzulli JR (2010) Distinct region-specific alpha-synuclein oligomers in A53T transgenic mice: implications for neurodegeneration. The Journal of neuroscience : the official journal of the Society for Neuroscience 30:3409-3418.

Tyedmers J, Mogk A, Bukau B (2010) Cellular strategies for controlling protein aggregation. Nature reviews Molecular cell biology 11:777-788.

Ubl A, Berg D, Holzmann C, Kruger R, Berger K, Arzberger T, Bornemann A, Riess O (2002) 14-3-3 protein is a component of Lewy bodies in Parkinson's disease-mutation analysis and association studies of 14-3-3 eta. Brain research Molecular brain research 108:33-39.

Ueda K, Fukushima H, Masliah E, Xia Y, Iwai A, Yoshimoto M, Otero DA, Kondo J, Ihara Y, Saitoh T (1993) Molecular cloning of cDNA encoding an unrecognized component of amyloid in Alzheimer disease. Proceedings of the National Academy of Sciences of the United States of America 90:11282-11286.

Valente EM et al. (2004) Hereditary early-onset Parkinson's disease caused by mutations in PINK1. Science 304:1158-1160.

van Loo G, van Gurp M, Depuydt B, Srinivasula SM, Rodriguez I, Alnemri ES, Gevaert K, Vandekerckhove J, Declercq W, Vandenabeele P (2002) The serine protease Omi/HtrA2 is released from mitochondria during apoptosis. Omi interacts with caspase-inhibitor XIAP and induces enhanced caspase activity. Cell death and differentiation 9:20-26.

Vande Walle L, Lamkanfi M, Vandenabeele P (2008) The mitochondrial serine protease HtrA2/Omi: an overview. Cell death and differentiation 15:453-460.

Walsh DM, Lomakin A, Benedek GB, Condron MM, Teplow DB (1997) Amyloid beta-protein fibrillogenesis. Detection of a protofibrillar intermediate. The Journal of biological chemistry 272:22364-22372.

Wang S, Haynes C, Barany F, Ott J (2009) Genome-wide autozygosity mapping in human populations. Genetic epidemiology 33:172-180.

Winner B, Jappelli R, Maji SK, Desplats PA, Boyer L, Aigner S, Hetzer C, Loher T, Vilar M, Campioni S, Tzitzilonis C, Soragni A, Jessberger S, Mira H, Consiglio A, Pham E, Masliah E, Gage FH, Riek R (2011) In vivo demonstration that alpha-synuclein oligomers are toxic. Proceedings of the National Academy of Sciences of the United States of America 108:4194-4199.

Witt M, Bormann K, Gudziol V, Pehlke K, Barth K, Minovi A, Hahner A, Reichmann H, Hummel T (2009) Biopsies of olfactory epithelium in patients with Parkinson's disease. Movement disorders : official journal of the Movement Disorder Society 24:906-914.

Yacobi-Sharon K, Namdar Y, Arama E (2013) Alternative germ cell death pathway in Drosophila involves HtrA2/Omi, lysosomes, and a caspase-9 counterpart. Developmental cell 25:29-42.

Yang L, Sun M, Sun XM, Cheng GZ, Nicosia SV, Cheng JQ (2007) Akt attenuation of the serine protease activity of HtrA2/Omi through phosphorylation of serine 212. The Journal of biological chemistry 282:10981-10987.

Yew DT, Luo CB, Shen WZ, Chow PH, Zheng DR, Yu MC (1995) Tyrosine hydroxylase- and dopamine-beta-hydroxylase-positive neurons and fibres in the developing human cerebellum--an immunohistochemical study. Neuroscience 65:453-461.

Yoshida T, Mizuta T, Shimizu S (2010) Neurodegeneration in mnd2 mutant mice is not prevented by parkin transgene. Biochemical and biophysical research communications 402:676-679.

Yoshioka H, Katsu M, Sakata H, Okami N, Wakai T, Kinouchi H, Chan PH (2013) The role of PARL and HtrA2 in striatal neuronal injury after transient global cerebral ischemia. Journal of cerebral blood flow and metabolism : official journal of the International Society of Cerebral Blood Flow and Metabolism.

Yun J, Cao JH, Dodson MW, Clark IE, Kapahi P, Chowdhury RB, Guo M (2008) Loss-of-function analysis suggests that Omi/HtrA2 is not an essential component of the PINK1/PARKIN pathway in vivo. The Journal of neuroscience : the official journal of the Society for Neuroscience 28:14500-14510.

Zarranz JJ, Alegre J, Gomez-Esteban JC, Lezcano E, Ros R, Ampuero I, Vidal L, Hoenicka J, Rodriguez O, Atares B, Llorens V, Gomez Tortosa E, del Ser T, Munoz DG, de Yebenes JG (2004) The new mutation, E46K, of alpha-synuclein causes Parkinson and Lewy body dementia. Annals of neurology 55:164-173.

Zhang Y, Appleton BA, Wu P, Wiesmann C, Sidhu SS (2007) Structural and functional analysis of the ligand specificity of the HtrA2/Omi PDZ domain. Protein science : a publication of the Protein Society 16:1738-1750.

Zumbrunn J, Trueb B (1996) Primary structure of a putative serine protease specific for IGF-binding proteins. FEBS letters 398:187-192.

ACKNOWLEDGEMENTS

First of all I would like to thank Professor Rejko Krueger for giving me the opportunity to join his lab and entrusting me the animal work of the laboratory of functional neurogenomics. His passion for his work and his scientific suggestions were of good help for the success of my work.

I would also like to thank Professor Olaf Riess and Professor Hartwig Wolburg for accepting my request for being the member of my thesis committee. Their expert opinion and critical reviewing of the results proved very helpful in the development and successful completion of my task. I would also thank Professor Hartwig Wolburg for performing electron microscopy experiments on my mice models.

I also would like to thank PD Dr. Thomas Ott for all his help in coping up with the tasks and formalities related to animal work. .

I would also like to thank Dr. Julia Fitzgerald for her supervision during the last year of my PhD. Her reviewing of my experimental results and thesis writing proved very useful in developing my scientific skills and writing skills.

I would also to take the opportunity to offer my gratitude towards people from several labs including labs in Hertie Institute, though naming each of them here would be difficult, who were helping me by providing equipments and new techniques and also with their valuable suggestions to proceed with my experiments. In this context I would like to specially thank Nicolas Casadei who was explaining me how to analyze my mice behavioral experimental data and was also helping me to learn some of the new scientific techniques. He was also performing DAB staining on my mouse models and as a fact he was always available with his suggestions during my PhD. I would also like to thank Dr. Heinrich Schell for his valuable suggestions about my project. I would also thank Ulrike Obermüller, technical assistant in Professor Mathias Jucker´s lab, who helped me in learning immunohistochemical techniques.

I would like to thank all my lab members specially Andreas Hummel, Brigitte Maurer, Carolin Obermaier, and Carina Mielke for their cooperation and all their help in the experiments and learning of new techniques during my PhD. I would also thank Dr. Daniela Moniz Arduino who became a good friend in short time and was also giving me valuable advices for writing my thesis.

Last but not the least I would like to thank my parents and family, for without their cooperation and prayers this task wouldn´t have fulfilled. And most important I want to thank God for His grace which He bestowed upon me to accomplish my PhD thesis.